THE ROLE OF MEMBRANE CHOLESTEROL CONTENT ON INSULIN-STIMULATED GLUCOSE UPTAKE IN A TISSUE CULTURE MODEL OF SKELETAL MUSCLE MYOFIBERS

A Dissertation
Presented to the
Faculty of the Department of Health and Human Performance
University of Houston

In Partial Fulfillment
of the Requirements for the Degree

Doctor of Philosophy

By Lyle Babcock
August 2018

THE ROLE OF MEMBRANE CHOLESTEROL CONTENT ON INSULIN-STIMULATED GLUCOSE UPTAKE IN A TISSUE CULTURE MODEL OF SKELETAL MUSCLE MYOFIBERS

Lyle Babcock

APPROVED:

Dr. Mark S.F. Clarke, PhD.
Committee Chair

Dr. Melissa M. Markofski, Ph.D.

Dr. Daniel P. O'Connor, Ph.D.

Dr. Tahir Hussain, Ph.D.
Pharmacological and Pharmaceutical Sciences

Dr. Antonio D. Tillis, Ph.D.
Dean College of Liberal Arts and Social Sciences
Department of Hispanic Studies

THE ROLE OF MEMBRANE CHOLESTEROL CONTENT ON INSULIN-STIMULATED GLUCOSE UPTAKE IN A TISSUE CULTURE MODEL OF SKELETAL MUSCLE MYOFIBERS

An Abstract of Dissertation
Presented to the Faculty of the
Department of Health and Human Performance
University of Houston

In Partial Fulfillment
of the Requirements for the Degree of

Doctor of Philosophy

By Lyle Babcock
August 2018

ABSTRACT

Insulin resistance is a condition characterized by the inability of insulin to stimulate glucose uptake in skeletal muscle. This can lead to serious diseases such as metabolic syndrome, diabetes mellitus 2, cancer and blindness. The onset and progression of insulin resistance is correlated with a variety of environmental-related conditions, such as a high fat diet, chronic physical inactivity and sarcopenia, as well as physiological conditions such as obesity, hypercholesterolemia and chronic inflammation. It is clear that insulin resistance in skeletal muscle and the onset of Type 2 diabetes is correlated with a number of conditions that exhibit abnormal regulation of lipid metabolism, such as obesity and hypercholesterolemia. However, it still remains unclear if and how elevated circulating levels of cholesterol impact myofiber function at a cellular level, resulting in the inhibition of insulin signaling and glucose uptake. Mounting evidence suggests that accrual of cholesterol within skeletal muscle myofiber membranes may be causally linked to skeletal muscle insulin resistance and the onset of Type 2 diabetes. Cholesterol is found in both the external sarcolemma/T-tubule and internal sarcoplasmic reticulum membranes of skeletal myofibers. In the case of sarcolemma/T-tubule membranes, cholesterol-enriched micro-domains called caveolae contain insulin receptors and glucose transporter 4 (GLUT4) docking proteins. Cholesterol-rich caveolae are the site of GLUT4 vesicle fusion with the sarcolemma/T-tubule membrane system during insulin-stimulated GLUT-4 mediated myofiber glucose uptake. Cholesterol is also found in sarcoplasmic reticulum membranes, a complex intra- membrane system from which GLUT-4 containing membrane vesicles are derived. The sarcoplasmic reticulum is also the source and storage organelle for the intracellular calcium required for SNARE-mediated GLUT4

vesicle fusion with the external sarcolemma/T-tubule membrane which is the final step in insulin stimulated myofiber glucose uptake. Evidence to suggest that overall myofiber membrane cholesterol content is an important regulator of insulin stimulated glucose uptake comes from *in vivo* and *in vitro* studies where increasing or decreasing myofiber membrane cholesterol content resulted in the inhibition or enhancement of insulin-stimulated glucose uptake. Here we demonstrate a reliable and reproducible tissue culture model of skeletal myofibers consisting of highly differentiated C2C12 myotubes in which to mechanistically investigate the effects of selectively enriching or depleting the sarcolemma/T-tubule and/or sarcoplasmic reticulum membrane alone on insulin-stimulated glucose uptake. Selective enrichment or depletion of C2C12 myotube membranes with native cholesterol was achieved by exposing differentiated C2C12 myotubes to a methyl-β-cyclodextrin/cholesterol complex or methyl-β-cyclodextrin alone, utilizing specific pulse-chase labeling conditions in tissue culture. Confirmation that these defined pulse-chase labeling conditions selectively enriched or depleted specific myotube membranes was confirmed using a fluorescent analog of cholesterol, 23-(dipyrrometheneboron-difluoride)-24-norcholesterol, which in turn was spatially resolved within myotube membranes using scanning confocal microscopy. The effects of selective cholesterol membrane enrichment in differentiated C2C12 myotubes on insulin-stimulated glucose uptake were determined by measuring the uptake of 2-NBDG, a fluorescent analog of glucose. A 5x6-way ANOVA was used to determine any differences in insulin stimulated glucose uptake between membrane enrichment/depletion conditions across a range of insulin concentrations, while one-way ANOVAs were used to determine the effects of insulin concentration within each enrichment condition, as

well as any differences between enrichment conditions for particular insulin concentrations. Using this defined tissue culture model of insulin stimulated glucose uptake in skeletal muscle myotubes, we demonstrate that increased membrane cholesterol content is causally related to disruption of insulin receptor signaling and inhibition of insulin stimulated glucose uptake in C2C12 myotubes. We further demonstrate that this inhibition is greatest when the difference between the relative concentrations of cholesterol in the sarcolemma/T-tubule and the SR membranes is highest, rather than when the total cholesterol content of either membrane system is increased. Our findings provide direct experimental evidence that increased muscle membrane cholesterol content is causally related to inhibition of insulin signaling, insulin stimulated glucose uptake, and by extension GLUT4 translocation in skeletal muscle. These findings have significant physiological implications, especially as they relate to the underlying cellular mechanisms responsible for the development and onset of insulin resistance

Acknowledgements

This dissertation would not have been possible if not for the effort and support of certain individuals. First I would like to thank my graduate advisor, Dr. Mark Clarke, for his patience and guidance. This project was plagued with unforeseen obstacles and I thank him for not giving up on me.

I'd also like to thank Dr. Tahir Hussain for allowing me to using his lab and equipment, and all my committee members for their time in helping me along the way and with finishing this document.

Next I'd like to thank those that supported me in my personal life. First of all, my Mother for unwavering support of my dreams, and Edrina for the encouragement to finish. This was the most trying period of my life, and I could not have finished this without you both.

TABLE OF CONTENTS

LIST OF FIGURES

LIST OF TABLES

Chapter 1 – Introduction

Whole Body Glucose Homeostasis and the Importance of Skeletal Muscle

Skeletal muscle is responsible not only for the generation of force required for musculoskeletal movement but is also one of the most metabolically active tissues in the body. Representing up to 40% of total body mass in humans, skeletal muscle is a primary consumer of circulating glucose and is crucially important for maintaining whole body glucose homeostasis. Over and above the constitutive levels required to maintain basal cellular function, glucose uptake into skeletal muscle is stimulated by both the activation of the insulin signaling pathway in response to increased levels of glucose in the circulation, or by the increased metabolic needs of skeletal muscle during muscle contraction as a consequence of exercise or increased physical activity. As such, skeletal muscle tissue is critical in maintaining circulating levels of glucose within safe, normal levels within the body.

Maintenance of circulating glucose levels are regulated by two major endocrine hormones: insulin and glucagon, both polypeptides produced within the pancreas. Glucagon is released into the circulation in response to decreased levels of circulating glucose and induces gluconeogenesis from glycogen stores in the liver. In contrast, insulin is released into the circulation in response to increased levels of circulating glucose and induces glucose uptake by target cells expressing the insulin receptor. In terms of whole body glucose homeostasis, it is the interplay between the actions of these two endocrine hormones and their target tissues, which result in maintenance of circulating glucose levels within normal ranges.

In healthy individuals, circulating levels of glucose are normally maintained within a physiological concentration range of approximately 60–100 iumilligrams per deciliter (mg/dL) in the fasted state. Food intake results in a rapid increase in the circulating levels of glucose to as much as ~200mg/dL within 1hr. This postprandial hyperglycemia induces the release of insulin into the circulation in order to bring circulating glucose concentrations in circulation back down to normal levels. Disruption of insulin's ability to stimulate glucose uptake by its target tissues, especially in the case of skeletal muscle, results in a range of negative physiological outcomes resulting from bouts of both acute and chronic hyperglycemia.

If left unchecked, chronic hyperglycemia is a dangerous condition that contributes to the development of a variety of diseases such as metabolic syndrome, adult onset Type 2 diabetes mellitus, gout, blindness and many cancers. The latest data from the National Health and Nutrition Examination Surveys found that 33% of adults living in the U.S. have metabolic syndrome, a condition exemplified by chronically high levels of circulating glucose concentrations and increased risk of adult-onset diabetes mellitus (Type 2 diabetes). The condition in which insulin stimulation of target tissues fails to elicit an adequate glucose uptake response is called insulin resistance/glucose intolerance, and further exacerbates the effects of chronic hyperglycemia due to decreased insulin-stimulated uptake of glucose by insulin resistant target tissues, especially skeletal muscle. Insulin resistance can be induced by poor diet [1, 2] and chronic physical inactivity [3-10], both of which unfortunately plague the typical American lifestyle.

Glucose Uptake in Skeletal Muscle

Skeletal muscle is the largest insulin-sensitive tissue in the body and is the primary target for insulin-stimulated glucose uptake. As with all living cells in the body, glucose must pass through specific glucose transporters in the plasma membrane (specifically referred to as the sarcolemma in muscle cells) in order to enter the cell cytoplasm to be metabolized. As with many types of transmembrane signaling which rely on channel proteins that span the lipid bilayer of cell membranes, different cell types express different channel protein isoforms related to the function of the particular cell in which they are expressed. In the case of transmembrane glucose transporters, all cell types express a common isoform of the channel protein known as glucose transporter 1 (GLUT1). GLUT1 is a highly evolutionary-conserved protein constitutively expressed in the plasma membrane of all cell types, including the sarcolemma (SL) of skeletal myofibers, and is responsible for the basal glucose uptake essential for energy production [11]. GLUT1 content in the sarcolemma is not affected by acute exercise or insulin stimulation, however GLUT1 biosynthesis is [12]. Therefore, long-term basal uptake can be affected by daily exercise and insulin-stimulation.

Another major type of glucose transporter is the GLUT4 isoform, found predominantly in skeletal muscle cells, cardiac muscle cells, and adipocytes. Unlike GLUT1, which is primarily localized to the external plasma membrane of adipocytes and SL membranes of muscle cells, GLUT4 is primarily localized to internal membrane domains within these cell types and only translocates to the plasma/SL membrane following insulin stimulation of the target cell, and additionally in the case of skeletal muscle specifically, upon contraction and/or physical activity [13-15].

As a transmembrane protein, GLUT4 is embedded within internal membranes and must be translocated to the external plasma/SL membrane through an exocytosis-like mechanism before it can transport glucose from the interstitial fluid across the plasma/SL membrane into the cell cytoplasm. While the exact sequence of events required for the translocation of GLUT4 from internal to external membranes is as yet not fully understood, experimental evidence suggests that it is under the control of several intracellular signaling pathways and ultimately, a membrane-membrane fusion event modulated by a series of docking proteins. As is the case with adipocytes, insulin stimulation of skeletal muscle myofibers results in translocation of GLUT4 from internal membrane stores (i.e. the sarcoplasmic reticulum – SR - membrane) to the external plasma membrane (i.e. sarcolemma membrane – SL), thereby increasing the rate and amount of glucose taken up by the myofiber. Insulin-stimulated, GLUT4-mediated glucose uptake by skeletal muscle is responsible for removal of 70% to 80% of the increased amounts of circulating glucose observed during postprandial hyperglycemia after food intake. As such, skeletal muscle tissue and its overall sensitivity to circulating insulin levels is a critical factor in maintaining circulating blood glucose levels within safe, normal ranges [16, 17] and preventing the development of chronic hyperglycemia.

In addition to direct insulin stimulation, GLUT4 translocation from the internal SR membrane to the external SL membrane also occurs in response to skeletal muscle contractile activity induced during physical activity/exercise. Skeletal muscle contractile activity, even in the absence of insulin stimulation, results in the translocation of large amounts of GLUT4 from internal SR membrane stores to the SL membrane of the myofiber. Contraction-induced GLUT4 translocation results in a rapid and substantial

increase in glucose uptake from the circulation by the myofiber [14], in order to satisfy the increased metabolic needs of the contracting skeletal muscle tissue. As such, increased GLUT4-mediated uptake of circulating glucose in response to voluntary muscle contraction during physical activity is also a critical factor in maintaining circulating glucose levels within safe, normal ranges and preventing the development of chronic hyperglycemia. While there are many documented health benefits of regular exercise and a physically active lifestyle, such as a reduction in the risk of Type 2 diabetes, obesity, cancer and chronic inflammation, it can be argued that many of the health benefits attributed to regular exercise may be directly related to the role of skeletal muscle GLUT4-mediated glucose uptake in that the maintenance of normal circulating glucose levels and the prevention of chronic hyperglycemia.

The classic model of insulin-stimulated glucose uptake by GLUT4 in individual cells is primarily based on experimental studies carried out in isolated or cultured adipocytes. Many, if not all, of the same signaling molecules that make up the canonical insulin signaling pathway are common to both adipocytes and skeletal myofibers. Both cell types ultimately respond to insulin stimulation in the same manner, namely translocation of GLUT4 from internal membrane stores to the external membrane resulting in increased glucose uptake. In the case of skeletal muscle, insulin-mediated glucose uptake begins with ligand (i.e. insulin) binding of the insulin receptor located on the SL membrane. Insulin receptors (IR) are localized within cholesterol-rich micro-domains or “lipid rafts” located within the SL membrane of the myofiber, specifically a subset of lipid rafts called caveolae [14, 18-23]. These cholesterol-rich membrane micro-domains constitute a considerable portion of the total SL membrane fraction, are less

fluid and more ordered than the surrounding regions of the SL membrane, and harbor a unique set of receptors and membrane proteins involved in a range of other important signal transduction pathways in addition to insulin signaling [19, 22].

Cholesterol and Myofiber Membrane Content

Cholesterol is a small, amphipathic molecule having both polar and non-polar regions that exhibits both hydrophilic and hydrophobic properties. Found in all mammalian membranes, cholesterol's amphipathic properties allow it to pack between the phospholipids of the membrane bilayer were it serves an important structural support role increasing the overall tensile strength of the membrane. Because of its amphipathic nature, cholesterol is also capable of forming a molecular sheath around predominantly hydrophilic transmembrane proteins, such as the insulin receptor (IR) or GLUT channels, allowing the hydrophilic transmembrane proteins to span the hydrophobic regions of the lipid bilayer. Further, in cholesterol-enriched membrane microdomains such as caveolae, increased packing of cholesterol within the bilayer region locally increases membrane order and membrane rigidity, while decreasing membrane permeability [24].

Modulation of membrane cholesterol content has been shown to impact not only the mechanical properties of cell membranes but also the fidelity of a range of transmembrane signaling pathways in a variety of cell types including skeletal muscle [13, 18, 25]. Transmembrane signaling involved in calcium homeostatis, insulin signaling and other cell signaling-related endocytotic events all appear to be related to the cholesterol content of the membrane. These effects have been attributed to the ability or inability of these signaling proteins to undergo conformational changes during ligand

binding/activation related to the relative cholesterol content of the membrane region in which these signaling proteins normally reside. Interestingly, caveolae located in the plasma membrane are also the docking site for internal membrane GLUT4 trafficking vesicles [13, 18] suggesting that the cholesterol content of these membrane microdomains may also play a role in modulating GLUT4 translocation, in addition to the impact of membrane cholesterol content on the fidelity of transmembrane signaling by proteins residing within membrane caveolae.

Cholesterol and Insulin Resistance

Evidence to suggest that membrane cholesterol content is related to the overall glucose uptake process comes from the observation that depletion of plasma membrane cholesterol in adipocytes results in increased GLUT4 translocation and subsequent glucose uptake in this cell type [13, 18]. It is currently unknown if changes in the cholesterol content of skeletal muscle fiber membranes, either in the caveolae of the external SL where IR receptors reside, or the internal SR membrane components where GLUT4 channels reside, results in similar modulation of insulin signaling, GLUT4 translocation events or overall glucose uptake by skeletal muscle tissue. However, whole animal studies utilizing methyl-β-cyclodextrin (MβC) administration to generally deplete cellular membrane cholesterol content resulted in increased GLUT4-dependent glucose uptake and reduced insulin resistance in obese mice [2] suggesting that membrane cholesterol content may be linked to insulin-dependent signaling pathways and glucose uptake in skeletal muscle.

In skeletal muscle, ligand binding of the IR normally results in the phosphorylation of the insulin receptor substrate (IRS), in turn activating the PI3K/Akt signaling pathway inducing GLUT4 translocation to the sarcolemma [13, 18]. In addition, GLUT4 vesicle fusion is also dependent on another insulin-stimulated signaling pathway distinct from the PI3K/Akt pathway. In a separate pool of insulin receptors, ligand binding initiates the assembly of the CrkII-C3G/Exo70 exocytosis complex, which appears to be responsible for the final fusion step of GLUT4 vesicle trafficking [18, 26-30]. Experimental evidence suggests that chronic hyperglycemia leads to insulin resistance through a negative feedback loop involving up-regulation of specific signaling molecules in the PI3K/Akt pathway, namely mTORC1 and SK6, that in turn inhibit IRS phosphorylation [31]. Perversely, chronic over stimulation by insulin (i.e. chronic hyperinsulinemia) can also induce insulin resistance by over-stimulation of IR and by over activation of mTOR and SK6 as part of the PI3K/Akt signaling pathway [31].

While several molecular mechanisms have been identified that may explain chronic hyperglycemia-induced and hyperinsulinemia-induced insulin resistance in skeletal muscle, increases in SL membrane cholesterol due to elevated circulating levels of cholesterol may also contribute. For example, Bonora et al. demonstrated the prevalence of insulin resistance in various metabolic disorders and found insulin resistance to be present in 53% of all hypercholesterolemia patients, 84% of hypertriglyceridemia patients, and 88% of subjects with low circulating levels of high-density lipoprotein (HDL) [32]. Further, diet-induced hypercholesterolemia has been shown to increase membrane cholesterol in the skeletal muscle of obese mice [1, 2], specifically the T-tubule system of the SL membrane [2], and to cause a dysfunction in

GLUT4 vesicle transport due to a reduction in the formation of polymerized F-actin required for vesicle translocation [1]. It has also been demonstrated that lowering membrane cholesterol using methyl-β-cyclodextrin (MβC) increases GLUT4-dependent glucose uptake and reduces insulin resistance in obese mice [2].

Models for Studying Membrane Cholesterol and Insulin-Stimulated Glucose Uptake

The effect of altered plasma membrane cholesterol content on insulin stimulation has been studied extensively *in vitro* using 3T3-L1 adipocytes [13, 18]. For example, large-scale membrane cholesterol depletion using MβC or inhibitors of cholesterol biosynthesis such as chromium has been shown to inhibit IR autophophorylation, IRS-1 phosphorylation, glucose uptake, and activation of the PI3K/Akt pathway in this cell type [33-36]. Counter-intuitively, partial depletion of membrane cholesterol using chromium exposure has been shown to increase GLUT4 translocation and glucose uptake in 3T3-L1 adipocytes [37]. However, to date it is unclear that the effects of artificially modulating membrane cholesterol content previously described in cultured adipocytes accurately mimics *in vivo* cellular responses to hypercholesterolemia in general, or the effects of hypercholesterolemia on insulin signaling, GLUT4 translocation and/or glucose uptake in skeletal muscle tissue specifically.

Considering skeletal muscle is one of the most important tissues in the body as it relates to insulin-stimulated glucose uptake and whole body glucose homeostasis, an *in vitro* model that more closely resembles a functional skeletal muscle fiber may be better suited than the current adipocyte models for investigating the underlying molecular mechanisms involved in insulin-stimulated glucose uptake in skeletal muscle tissue.

There is no doubt that normal insulin signaling and glucose uptake in skeletal myofibers *in vivo* involve the interaction of a complex set of transmembrane and intracellular signaling pathways that rely on specific signaling proteins located in discrete but spatially related membrane systems. Whole animal and *ex vivo* tissue studies have provided significant understanding of these cellular events but still have many confounding variables which are difficult if not impossible to control when studying individual elements of this response. While the use of cultured myocyte cell lines to further study and dissect the underlying cellular mechanisms involved in normal myofiber insulin signaling and glucose uptake *in vivo*, as well as investigating the etiology of a number of pathological conditions such as insulin resistance and glucose tolerance would appear to be a logical approach, the use of such tissue culture models also present several significant experimental challenges.

Experimental Challenges

Cultured myocytes are individual cells that lack the highly organized contractile elements and membrane systems found in fully formed, multi-cellular myofibers. As such, cultured myocytes do not provide an ideal model for studying the complex cascade of events already known to be involved in insulin signaling and glucose uptake by myofibers *in vivo*. In addition, myocyres do not provide an appropriate experimental platform to study the pathological effects of environmental conditions such as chronic hyperglycemia or chronic hypercholesterolemia, or the underlying etiology of diseases states related to these conditions *in vivo*, such as insulin resistance or Type 2 diabetes. To overcome some of these experimental challenges and address the need for a model more

closely resembling myofibers *in vivo*, individual myocyte cells can be induced to fuse together in culture to form multi-cellular myotube structures analogous to myofibers *in vivo*. However, depending on the type of myocytes utilized and the culture conditions under which they are grown, it is still unclear if such myotube models truly exhibit the differentiated characteristics needed to fully mimic the cellular mechanisms involved in insulin signaling and glucose uptake in skeletal muscle tissue *in vivo*.

Both mouse C2C12 and rat L6 skeletal muscle-derived cell lines have been previously used to study insulin signaling and glucose uptake mechanisms *in vitro*[12, 38-45]. While the L6 cell line has been used to investigate insulin-stimulated GLUT4 translocation and glucose uptake [46], L6 myotubes do not form sarcomeres efficiently and lack the potential for contractile activity [47, 48]. This suggests that the membrane systems involved not only in the control of excitation-contraction (EC) coupling, but also insulin signaling, GLUT4 translocation and ultimately insulin-stimulated glucose uptake are missing or have not fully formed in these myotubes. In contrast, the C2C12 myocyte cell line can be used to generate myotubes that form sarcomeres and develop contractile potential [47, 49] in culture. However, the use of the C2C12 mouse myoblast cell line has provided contradictory information regarding insulin-stimulated GLUT4 translocation and glucose uptake. A number of researchers have reported little or no glucose uptake in response to insulin stimulation in either C2C12 myocytes or myotubes [12, 38, 44, 50], while others have observed limited insulin-stimulated glucose uptake [43] and GLUT4 translocation [39] but only in C2C12 myotubes. Further, those who have reported an insulin-stimulated glucose uptake response in C2C12 myotubes describe a blunted insulin response that varies from culture passage to culture passage [43].

The contradictory information reported with regard to insulin signaling and subsequent glucose uptake in cultured myocytes and myotubes may be related to confounding experimental conditions that to date have not been recognized as such. Interestingly, much of the literature investigating insulin stimulated glucose uptake by cultured myocytes or myotubes does not report the precise glucose concentrations under which these cells were propagated or tested [38, 50]. This critical factor may explain the contradictory results previously reported with regard to whether or not cultured myocytes and myotubes respond similarly to myofibers *in vivo* in response to insulin stimulation. For example, several researchers have demonstrated that even short-term incubation in tissue culture medium containing the high levels of glucose normally utilized in standard media preparations (25mM, or physiologically speaking 450mg/dL) appears to cause insulin resistance in a number of cultured cell types including skeletal muscle, while in some studies insulin-stimulated glucose uptake was observed only after pre-incubation in low-glucose media (5.5mM or 100mg/dL glucose) [31, 43].

Additionally, Nedachi et al. also demonstrated that the effects of altering glucose concentration in the tissue culture medium was extremely rapid as exposure to high glucose concentrations of 25mM (450mgd/L) after culture in low glucose concentrations (5.5mM, 100mg/dL) impaired subsequent insulin-stimulated 2-deoxyglucose (2DG) uptake within 5 minutes [43]. Further evidence to suggest the importance of controlling culture conditions as it relates to glucose concentration comes from Leonitieva et al. who demonstrated impaired insulin-stimulated Akt phosphorylation in C2C12 myoblasts and inhibition of glucose uptake in retinal pigment epithelial (RPE) cells when cultured in a standard high glucose (25mM or 450 mg/dL) medium preparations, while exposure to the

same medium preparation containing low glucose (5.5mM, 100mg/dL) restored insulin sensitivity in both these cells types [31]. Taken together, these experimental data suggest that to develop a tissue culture model of insulin-stimulated glucose uptake in skeletal muscle will require not only the use of the appropriate cell type capable exhibiting the structural and molecular organization of skeletal myofibers *in vivo*, but will also require significant control of culture conditions such as glucose medium concentration. Without taking such culture conditions into account, it will be impossible to ensure that any effects related to insulin-stimulated glucose uptake observed *in vitro* accurately reflect cellular responses to pathological conditions such as chronic hyperglycemia or hypercholesetrolremia related to the development of insulin resistance and glucose intolerance of skeletal muscle *in vivo*.

Summary

Hypercholesterolemia and/or physical inactivity has been shown to contribute to insulin resistance and glucose intolerance in the whole animal. Altered cholesterol content in the plasma membrane of adipocytes has been shown to affect various signaling pathways involved in GLUT4 translocation and glucose uptake *in vitro*, while animal and human models suggest a strong association between hypercholesterolemia, increased membrane cholesterol, and insulin resistance. An increasing amount of experimental evidence suggests that these pathological effects may be specifically correlated with an increase in membrane cholesterol content in skeletal muscle fibers. To date, the pathological impact of increased membrane cholesterol content on insulin-stimulated glucose uptake in skeletal muscle myofibers has yet to be directly investigated, either *in*

vivo or *in vitro*. Furthermore, many of the experimental findings regarding the underlying cellular mechanisms involved in insulin-stimulated glucose uptake in cultured muscle cells are confounded by a lack of adequate control of culture conditions, such as glucose media concentrations, making it difficult to discern whether or not these models reflect the normal insulin-stimulated glucose uptake response in skeletal myofibers *in vivo*, or rather, the effects of chronic hyperglycemic culture conditions on this response. Therefore the overall aim of this study is to develop a reliable tissue culture model utilizing differentiated C2C12 myotubes to study insulin-stimulated glucose uptake under physiologically normal glycemic conditions. In turn, this model will then be used to investigate the putative pathological effects of altered membrane cholesterol content on insulin-stimulated glucose uptake and its potential role in the etiology of skeletal muscle insulin resistance as it relates to the development of metabolic syndrome and the onset of Type 2 diabetes *in vivo*.

Problem Statement

Hypercholesterolemia has been identified as a major confounding factor for insulin resistance and type 2 diabetes which may be related to an increase in membrane cholesterol in muscle fibers leading to a decrease in insulin sensitivity and subsequent glucose uptake. While the role of increased membrane cholesterol content in impaired insulin signaling and glucose uptake in skeletal muscle is not well understood, previous experimental evidence is consistent with the concept that such a cholesterol-mediated effect is related to disruption of GLUT4 membrane translocation that relies on membrane-membrane fusion events rather than direct disruption of insulin receptor

activation. Currently, there is no suitable model for studying the complex cascade of events known to be involved in insulin signaling and glucose uptake by myofibers *in vivo*, nor any defined *in vitro* experimental platform to study the pathological effects of increased membrane cholesterol content on insulin-stimulated glucose uptake in skeletal muscle or the role of increased membrane content on the underlying etiology of diseases states such as insulin resistance or Type 2 diabetes.

Therefore, the overall aim of this study is to develop a reliable and reproducible tissue culture model utilizing differentiated C2C12 to study insulin-stimulated glucose uptake under physiologically normal glycemic conditions. In turn, this model will then be used to investigate the putative pathological effects of altered membrane cholesterol content on insulin-stimulated glucose uptake and its potential role in the etiology of insulin resistance in skeletal muscle as it relates to the development of metabolic syndrome and the onset of Type 2 diabetes. Furthermore, this model will be used to selectively enrich specific membrane systems within these cultured myotubes (i.e. either the sarcolemma/T-tubule or sarcoplasmic reticulum membrane systems) in order to further investigate whether differential membrane cholesterol content may be directly related to the impairment of GLUT4 translocation observed in insulin resistant skeletal muscle of hypercholesterolemic individuals.

Research Objectives

1. **Develop a reproducible tissue culture model of insulin-stimulated glucose uptake in skeletal muscle differentiated myotubes derived from the C2C12 myocyte cell line utilizing a non-metabolizable, fluorescent analog of glucose (2-BNDG) to quantify glucose uptake response in this cell type.**

2. **Using a combination of a cholesterol/methyl-β-cyclodextrin (MβC) complex and a fluorescent analog of cholesterol to confirm spatial localization, define a set of pulse/chase tissue culture conditions capable of selectively modulating the cholesterol content of both the external SL and internal SR membranes in cultured differentiated myotubes.**
3. **Characterize the effects of selectively modulating the cholesterol content of either SL or SR membranes on insulin-stimulated glucose uptake in cultured differentiated myotubes.**

Research Hypothesis

Experiment 1:

Hypothesis 1: C2C12 myocytes can be induced to form multi-cellular myotube structures in culture which exhibit sub-cellular organization and express differentiation markers similar to those observed in skeletal myofibers *in vivo*.

Hypothesis 2: Differentiated C2C12 myotubes will exhibit a dose-dependent, insulin-stimulated glucose uptake response when grown under appropriate normoglycemic (80mg/dL) tissue culture conditions.

Experiment 2:

Hypothesis 3: Increasing the membrane cholesterol content of differentiated C2C12 myotubes by exposing them to a cholesterol/MβC complex in culture will result in the inhibition of insulin-stimulated glucose uptake compared to control conditions.

Hypothesis 4: Selective cholesterol enrichment of either the external SL membranes or the internal SR membranes of differentiated C2C12 myotubes can

be achieved using a cholesterol/MβC complex combined with a set of defined pulse/chase culture conditions.

Experiment 3:

Hypothesis 5: Selective cholesterol enrichment of the external SL membrane of differentiated C2C12 will be achived using a short-term exposure to cholesterol/MβC complex resulting in the inhibition of insulin-stimulated glucose uptake compared to control conditions.

Hypothesis 6: Selective cholesterol enrichment of the internal SR membrane of differentiated C2C12 myotubes will be achieved using a defined pulse/chase exposure to cholesterol/MβC complex resulting in the inhibition of insulin-stimulated glucose uptake compared to control conditions.

Hypothesis 7: Similar levels of cholesterol enrichment of both the SL and SR membranes of differentiated C2C12 myotubes using a combination of both acute and pulse/chase exposure to cholesterol/MβC complex will not inhibit insulin-stimulated glucose uptake compared to control conditions.

Outline

An overview of this proposal is presented which summarizes the details used in establishing cholesterol's effects on insulin-stimulated glucose uptake in cultured myotubes.

Chapter 1 (introduction) introduces the subject and summarizes the basis and importance for developing the proposed model and conducting the proposed experiments.

Chapter 2 (Literature Review) presents background information behind the main topics covered. First, we provide an overview of the importance of normal insulin-stimulated glucose uptake and the consequences of an impaired insulin response. Next, the biochemical signaling pathways involved in normal insulin signaling and the function of cholesterol within membranes. Then, a discussion on how altered cholesterol affects insulin signaling. Finally, an overview of possible cell culture models that can be used to study the effect of altered membrane cholesterol content on insulin-stimulated glucose uptake and the experimental challenges that must be accounted for in developing such a model.

Contributions to the Field

Insulin resistance and Diabetes Mellitus 2 are chronic diseases that plaque American society. Also, hypercholesterolemia has been strongly correlated both with insulin resistance and diabetes mellitus 2, as well as increased sarcolemma/T-tubule cholesterol content and impaired GLUT4 translocation. The existing literature provides support for the concept that diet-induced hypercholesterolemia may ultimately lead to insulin resistance in skeletal muscle by altering the cholesterol content of skeletal muscle membranes leading to the disruption of a key membrane-mediated event, namely GLUT4 translocation. This study aims to demonstrate that insulin-stimulated glucose uptake is inhibited by increased cholesterol membrane content, and that the inhibition is specifically related to differential cholesterol enrichment of internal sarcoplasmic

reticulum membranes rather than just the external sarcolemma/T-tubule membrane. These will add to the literature by providing a highly reproducible tissue culture model of skeletal muscle myofibers in which to investigate a range of physiologically and pathologically skeletal muscle responses, demonstrate a direct link between muscle membrane cholesterol content and insulin resistance, and provide valuable information in understanding the cellular mechanisms involved in the etiology and onset of insulin resistance and diabetes mellitus 2.

Definition of Important Terms and Abbreviations:

SL: Sarcolemma/T-tubule membrane

SR: Sarcoplasmic Reticulum membrane

IR: Insulin receptor

HDL: High Density Lipoprotein

LDL: Low density lipoprotein

GLUT1: Glucose Transporter 1

GLUT4: Glucose Transporter 4

MβC: Methyl Beta Cyclodextrin

WSC: Water Soluble Cholesterol (i.e. Cholesterol/ Methyl Beta Cyclodextrin Complex)

2-NBDG: 2-(*N*-(7-Nitrobenz-2-oxa-1,3-diazol-4-yl)Amino)-2-Deoxyglucose

MHC: Myosin Heavy Chain

DHP: Dihydropyridine

Chapter 2 – Review of Literature

Skeletal Muscle and Glucose Homeostasis

Skeletal muscle is responsible not only for the generation of force required for musculoskeletal movement but is also one of the most metabolically active tissues in the body. Representing up to 40% of total body mass in humans, skeletal muscle is a primary consumer of circulating glucose and important regulator of whole body glucose homeostasis. Over and above the levels required to maintain basal cellular function, glucose uptake into skeletal muscle is stimulated by exercise in order to meet the energy needs of contractile activity, or by insulin and its signaling pathway in response to increased blood-glucose concentrations. Impairments in the insulin signaling pathway resulting in insulin resistance or glucose tolerance are caused by and/or associated with obesity, chronic inactivity, diet, and hypercholesterolemia, and can lead to serious adverse health conditions including diabetes mellitus 2 (Type 2 diabetes), gout, blindness, and increased risk of cancer. [10, 32, 51-59].

Under normal conditions, high concentrations of glucose in circulation induce production of insulin by pancreatic beta cells in order to stimulate glucose deposition out of the blood [60, 61]. The primary targets of insulin stimulation and glucose deposition include adipocytes, cardiac muscle, and the largest insulin-sensitive organ in the body: skeletal muscle. Very low concentrations of glucose in circulation stimulation production of glucagon by pancreatic alpha cells in order to stimulation gluconeogenesis, or the production of carbohydrates from lipids or proteins, by the liver. The actions of both insulin and glucagon aim to keep concentrations of glucose in the blood at safe levels,

typically between 3.9mM and 5.6mM [62]. Very low concentrations of glucose can lead an individual to lose consciousness, while chronic high concentration of glucose in circulation contributes to a process called glycosylation, where a carbohydrate forms a covalent bond with a protein. Many proteins require this process, but when concentrations of glucose are too high glycosylation can occur for proteins not meant to be glycosylated, which diminishes the function of the protein. For example, glucose reacts with the the NH2 terminal of the hemoglobin beta chain to form hemoglobin Acl, which is associated with, and used a common measurement to test for diabetes and control of glucose homeostasis [63].

In healthy individuals, circulating levels of glucose are normally maintained within a physiological concentration range of approximately 60–100mg/deciliter in the fasted state. Food intake results in a rapid increase in the circulating levels of glucose to as much as ~200mg/dL within 1hr. This postprandial hyperglycemia induces the release of insulin into the circulation in order to bring glucose concentrations in circulation down to a safe level. As might be expected, disruption of insulin's ability to stimulate glucose uptake by its target tissues, especially skeletal muscle, can and does result in significant negative outcomes associated with the onset of either acute or chronic hyperglycemia.

Glucose Uptake in Skeletal Muscle

Glucose Transporters

Skeletal muscle is the largest insulin-sensitive tissue in the body and is the primary target for insulin-stimulated glucose uptake. Glucose must pass through specific Glucose Transporters (GLUT) in the membrane in order to enter the cell to be

metabolized. There are 12 known GLUT molecules (GLUT1 through GLUT12) that facilitate active transport of carbohydrates through the cell membrane into the cytoplasm. Some have affinities for carbohydrates such as fructose or sucrose, while others are specific to glucose [15]. There are two major GLUT molecules in skeletal myofibers, namely Glucose Transporter 1 (GLUT1), and Glucose Transporter 4 (GLUT4) [64]. GLUT1 is responsible for glucose uptake required to satisfy basal metabolic activity and is constitutively expressed in the plasma membrane of all cell types and the specifically the sarcolemma of skeletal muscle myofibers [11].

GLUT1 expression is upregulated by chronic activity of light to moderate intensity [65], as well as stimulation of the PI3K/Akt pathway as demonstrated using PI3K inhibitor wortmannin [66], the importance of which is discussed in detail later in this chapter. Exercise affects GLUT1 expression through exercise-induced activation of AMPK [67, 68].

The total amount of GLUT1 proteins present in the membrane of skeletal muscle does not change significantly in response to a single bout of exercise, nor acute stimulation by insulin [69]. In the case of chronic physical activity myofibers undergo significant protein turnover and remodeling, and as a result GLUT1 expression and localization in the myofiber sarcolemma membrane increases to meet the average basal metabolic need for glucose associated with myofiber hypertrophy. Skeletal muscle however, must be able to response to acute metabolic stimuli such as moderate to intense exercise, or, insulin stimulation when glucose concentrations in the circulation are high, by increasing the amount of glucose taken up by the myofiber. In response to acute stimulation of either type, skeletal muscle myofibers rely on a second related type of

transmembrane glucose transporter, GLUT4, which is stored in internl membrane vesicles called GLUT4 Storage Vesicles (GSVs) and rapidly translocated to the myofiber sarcolemma membrane in response to such stimuli.

Figure 1: GLUT4 Translocation

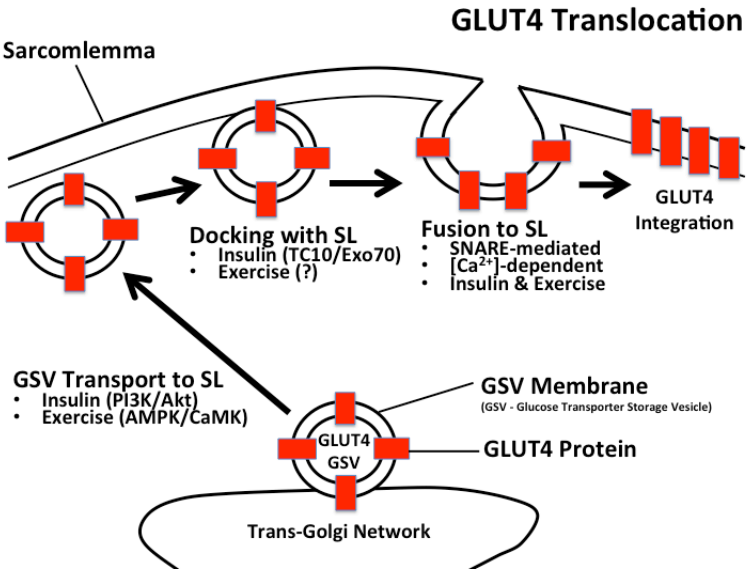

GLUT4 is expressed predominately in skeletal muscle, cardiac muscle, and adipocytes, and localized to internal membrane stores until stimulated to translocate [15]. In response to contractile activity (exercise) or insulin stimulation, large stores of GLUT4 transport vesicles translocate from internal membranes to the sarcolemma for a fast and substantial increase in glucose uptake by the myofiber [15]. Insulin-stimulated glucose uptake mediated via GLUT4 translocation is responsible for 70-80% of postprandial glucose deposition out of the circulation into skeletal muscle, making it critical for maintaining normal blood-glucose concentrations in circulation [70, 71]. Insulin plays a critical role in GLUT4 translocation by not one but two distinct signaling pathways, leading to both translocation and membrane fusion of GLUT4 transport vesicles with the sarcolemma.

GLUT4 is responsive to both insulin stimulation and exercise, through multiple biochemical signaling pathways, leading to translocation and tethering of GLUT4 Storage Vesicles (GSVs) to the myofiber membrane. Translocation involves the process

of bringing GSVs containing GLUT4 from their budding site on the Trans-Golgi Network to the sarcolemma of the myofiber membrane, while tethering is the process of anchoring the GSVs to the membrane for fusion and ultimate integration of GLUT4 into the sarcolemma. Exercise induces translocation of GLUT4 Storage Vesicles (GSVs) through a Ca^{2+}/CaMK dependent pathway, while insulin stimulates both translocation and tethering of GSVs through the PI3K/Akt and CAP/TC10 signaling pathways, respectively.

Figure 2: GLUT4-Dependent Glucose Uptake

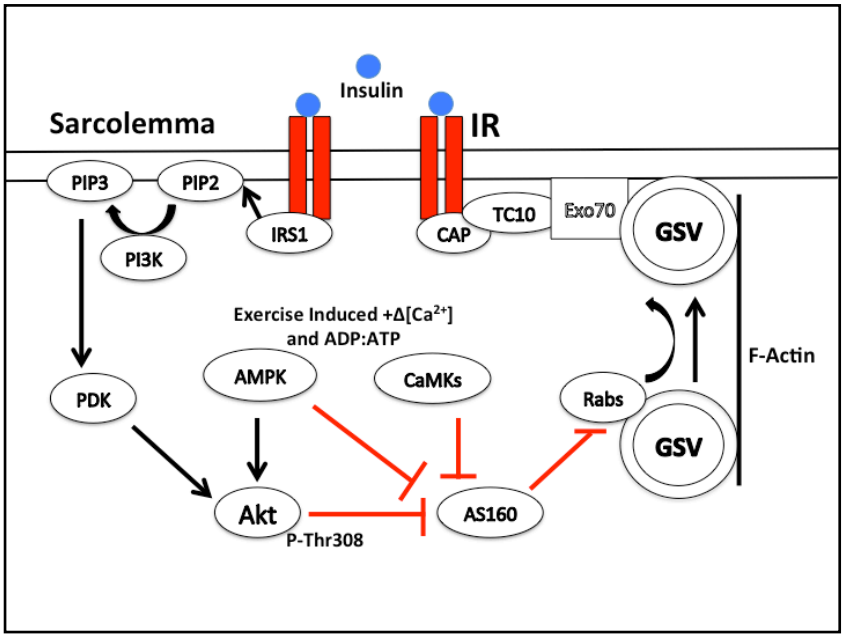

Insulin-Stimulated GLUT4 Translocation

The insulin receptor is comprised of 4 individual proteins: two alpha subunits present on the cell surface, and two beta subunits that extend through the membrane. The alpha subunits bind with insulin from circulation resulting in a conformational change and autophosphorylation of the beta subunits, where one subunit phosphorylates the other. These phosphate ions are then cleaved and bound to Insulin Receptor Substrate 1 (IRS1) [13, 18, 72]. Once IRS1 is phosphorylated it activates the critical Phosphoinnositol-3 Kinase (PI3K) / Protein Kinase B (Akt) pathway, which is involved

in a number of cellular phenotypes including myofiber size [73], and glucose uptake [18, 74]. The role of PI3K in GLUT4 translocation has been confirmed through chemical inhibition by wortmannin and LY294002, expression of dominant negative mutants, and PI3K antibodies which all inhibit GLUT4 translocation and glucose uptake [18, 74].

Akt has a complex role in insulin signaling, contributing through at least two isoforms of the Akt protein: Akt1 and Akt2 [18]. In response to IRS1 activation, the p85 regulatory subunit of Phospho-inositol 3 Kinase (PI3K) catalyzes the phosphorylation of PIP2 to form PIP3 [74]..The phosphate ion on PIP3 is then passed to and activates both protein kinase B (Akt) and 3' phosphoinositol-dependent kinase-1 (PDK-1), which in turn activates both Akt and atypical protein kinase C (PKC). Akt2 regulates GLUT4 translocation through phosphorylation-inhibition of a negative regulator of exocytosis vesicle trafficking. Akt2 is phosphorylated at two binding sites; its Thr308 and Ser473 domains, both activated by insulin. Akt's Thr308 residue is phosphorylated by PDK-1, while Ser473 is phosphorylated by mTORC2. Ser473 and mTORC2 are part of a feedback loop where mTORC2 is activated by mTORC1, which in turn is activated by phosphorylation of Akt's Thr308 residue. It has been demonstrated that it is specifically phosphorylation at the Thr308 residue that leads to GLUT4 translocation [75]. Akt activation in response to insulin stimulation results in the phosphorylation of Akt Substrate 160kd (AS160) at five distinct phosphorylation sites, inhibiting its activity in GSV retention [76-80]. AS160 regulates GLUT4 trafficking through its GTPase Activating Protein (GAP) domains that bind to Rab proteins 6,8,10 and 14. Rab proteins function by holding the GLUT4 storage vesicles (GSVs) along actin filaments as the GSVs are trafficked towards the sarcolemma membrane. In short, insulin stimulated Akt

activation inhibits AS160, allowing Rab proteins to facilitate GLUT4 translocation [14, 76, 81-83].

Insulin-Stimulated GSV Docking

From a separate pool of insulin receptors originates a separate pathway independent of PI3K/Akt and also residing in caveolae. In response to insulin receptor autophosphorylation, a caveolae membrane-bound adaptor protein with Pleckstrin and Src homology domains (APS) catalyses the phosphorylation of Cbl Associated Protein (CAP). CAP then recruits, phosphorylates, and binds Cbl to the caveolae membrane. Activated Cbl provides docking sites for and recruits the CrkII/C3G complex. This complex binding to Cbl is what determines the GSVs site of fusion into the membrane. Once bound, the C3G subunit reveals active phosphorylation sites for TC10, a small GTPase protein. TC10 activation initiates the assembly of GLUT4 exocytosis complex (Exo) consisting of Exo70, Sec6 and Sec8 subunits, and is dependent on being localized to caveolae [18, 26-30, 57]. This step is responsible for catalyzing the final tethering step in GLUT4 translocation and fusion to the myofiber membrane. This process is essentially an exocytosis mechanism in same way a cell excretes waste products, where the vesicle becomes part of the out membrane and the vesicle contents are expelled. However GSVs have GLUT4 imbedded in membrane of the vesicle, adding GLUT4 to the myofiber sarcolemma membrane as GSV membranes fuse with the outer membrane.

Exercise Induced GLUT4 Translocation and Fusion

Exercise-induced GLUT4 translocation is a multifactorial process and includes signaling pathway intermediates such as calcium dependent calmodulin protein kinases (CaMKK and CaMKII), AS160, AMPK, and Kv1.3. [84-87]. AMPK is responsive to changes in the intracellular ATP:ADP ratio which shifts during exercise. In response to a decrease in the AP:ADP ratio associated with contractile activity,. AMPK is converted to an active form which in turn inhibits activation of Akt which is responsible for carrying out GLUT4 translocation via insulin [84]. The AMP analog AICAR has been used to demonstrate that activation of AMPK significantly increases glucose uptake [88], however AMPK inhibition or attenuation has little effect [84].

While exercise induced activation of AMPK has been shown to be the key factor in the initiation of exercise-induce GLUT4 translocation, calcium also appears to be critical for this process to occur. Calcium (Ca^{2+}) is also a major contributor to exercise induced GLUT4 translocation through its intermittent fluctuations in cytoplasmic concentrations during physical activity. A contraction-stimulating action potential is delivered to the sarcomeres of a myofiber through the Traverse Tubule (T-Tubule) membrane system which is an intracellular extension of the external sarcolemma membrane. The T-Tubule system carries post-synaptic action potentials to the Dihydropyridine (DHP) receptor, an ion-gated channel located in the T-Tubule membrane juxtaposed to the Ryanadine (RyR) channels located in the terminal cisternae of the internal SR membrane which together form the Triad region of the myofiber T-Tubule/SR membrane system. The RyR channel is a voltage sensing Calcium channel that when stimulated by the DHP receptor in response to an action potention, releases Ca^{2+} into the sarcoplasm of the myofiber causing a muscle contraction. Ca^{2+} release from

the SR causes a muscle contraction by uncovering the myosin heavy chain binding sites on troponin along the actin filament, a process collectively known as excitation-cotraction (EC) coupling. Sustained physical activity can increase [Ca^{2+}] by 100-fold [89], which contributes to GSV fusion and GLUT4 translocation to the sarcolemma.

The precise mechanism of calcium-induced GSV translocation is currently unclear, but there are several molecules known to be involved that are activated by exercise-induced release of calcium within the sarcoplasm of the myofiber. Several studies have shown Ca+ /calmodulin dependent kinases (CaMK) to be critical for the process. Wright et al. used the calmodulin inhibitor KN-93 to block activation of CaMKs and GSV translocation, demonstrating the necessity for Ca+/calmodulin dependent activation of CaMKs. Witczak also demonstrated the role of CaMKK by using viral vectors transfected into mouse muscle inducing an overexpression of CaMKK and a 2.5 fold increase in insulin-stimulated glucose uptake. Angin et al. demonstrated this same effect in cardiomyocytes [87].

Both Wright and Witczak et al also demonstrated this effect is independent of AMPK by using CaMKK inhibitor STO-609 coupled with electrical stimulation-induced contraction [90, 91], while Nui et al. demonstrated that contraction induced AMPK activation induced GLUT4 translocation independent of CaMKII [92]. Not all data demonstrates CaMKK and AMPK to be separate pathways however; Jensen et al. used the same CaMKK inhibitor STO-609 and found a decrease in muscle glucose uptake through an AMPK-dependent pathway [93].

Both AMPK and calmodulin are thought to interact with Akt Substrate of 160kd (AS160). Kramer et al. demonstrated that both AMPK activation and contraction

stimulated glucose uptake [79], and also found that mutations in AMPKs binding sites render AS160 unresponsive to AMPK [79]. AS160 also has calmodulin binding domains, mutations of which inhibit contraction induced glucose uptake [79].

Aside from CaMKK, AMPK and AS160, a voltage-gated potassium channel (Kv1.3) and SNARE-dependent exocytosis have also been identified as calcium-dependent mediator of GLUT4 translocation to the sarcolemma [85]. Li et al found that blocking the release of calcium from the SR in adipocytes allowed Kv1.3 to in turn block GLUT4 translocation. This demonstrates Kv1.3 as a negative regulator of GLUT4 translocation that is inhibited by calcium release from the SR.

Soluble N-ethylamaleimaide-sensitive factor attachment protein receptors (SNAREs) play a critical role in exocytosis [94], including GSV docking and fusion with the sarcolemma. GSV fusion is facilitated by soluble C2-domain factor Doc2b; Yu et al. demonstrated in a reconstituted proteoliposome fusion system that calcium is required for Doc2b to facilitate the fusion of GSVs to SNARE protein complex SNAP23 through two active calcium binding sites on its C2A and C2B domains [95]. Further, Yu et al. demonstrated that Doc2b significantly bends the membrane inward during SNARE dependent exocytosis. These studies demonstrate exercise-dependent calcium release to be a powerful mediator of GLUT4 translocation.

Disregulation of Glucose Homeostasis and Insulin Resistance

In normal conditions increased blood-glucose concentrations initiate the production of insulin by the pancreas. The increased production of insulin stimulates glucose uptake in skeletal muscle bringing blood-glucose concentrations back to normal and safe levels. Impairments in insulin signaling, referred to as insulin resistance, render an individual unable to respond to increased glucose or insulin in circulation, which can result in chronic and dangerously high concentrations of glucose in the circulation and potential pathological levels of protein glycosylation. Insulin resistance can be induced by diet [1, 2], prolonged spaceflight [7] and chronic physical inactivity [3-6, 10], and is the root cause of diabetes mellitus II, while significantly ncreasing the risk of developing gout, blindness and many types of cancer.

Figure 3: Insulin Resistance

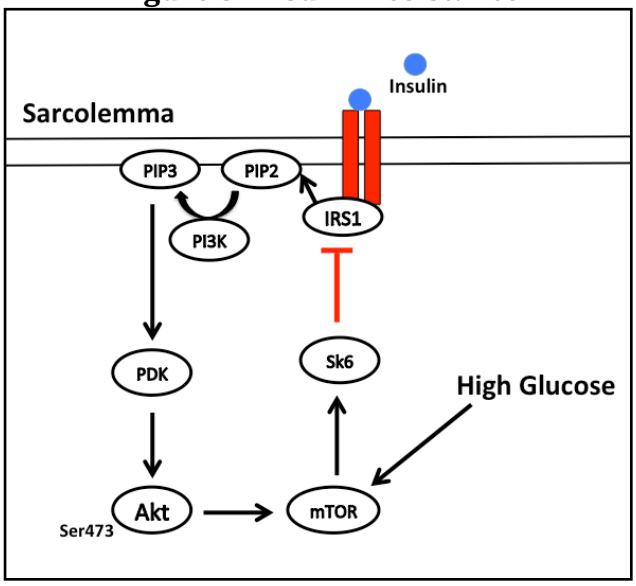

Insulin signaling can be directly impaired through several molecular mechanisms. Chronic high concentrations of circulating glucose, or hyperglycemia, can cause insulin resistance through a negative feedback loop involving downstream targets of PI3K/Akt: mTORC1 and SK6. High glucose concentrations over-stimulate mTORC1, in turn over-stimulating SK6, which directly inhibits phosphorylation of IRS1 by insulin receptors [31]. Chronic high concentrations of insulin, or hyperinsulinemia, cause insulin resistance through the same negative feedback loop that inhibits IRS1 activation, but through over-stimulation of IRS and the PI3K/Akt pathway leading to overstimulation of mTORC1[31].

Hypercholesterolemia, and increased membrane cholesterol content has also been implicated in insulin resistance through its association with the disease in human models [32], as well as animal models [1].

Cholesterol and Myofiber Membrane Composition

Our basic understanding of biological membranes is based on the concept of a lipid bilayer made up primarily of phospholipids in which a variey of other lipids and proteins are embedded. This prototypical model is collectively called the fluid mosaic model of membrane structure [96]. Though our understanding of membrane structure has evolved considerably since the fluid mosaic model was originally conceived, one critical aspect of the model remains, namely that biological membranes possess both fluid and gel properties resulting in regions of the membrane exhibiting local rigidity while remaining essentially fluid in its overall structure. Mammalian cellular membranes consist of a phospholipid bilayer composed mostly of glycophospholipids with hydrophilic glycogen heads and hydrophobic unsaturated fatty acid chain tails. The amphipathic nature of these phospholipids creates a stable membrane structure where the hydrophyllic heads form the extracellular and intracellular sides of the membrane, while the hydrophobic tails form the inner region of the membrane bilayer. This also means that transmembrane signaling and transport through this bilayer must occur through highly regulated mechanisms, and specialized transmembrane proteins with both hydrophilic and hydrophobic regions that allow them to reside within and pass through these hydrophobic and hydrophilic regions, respectively. One critical component of mammalian cell membranes is cholesterol, where the density of cholesterol within the

membrane can alter both membrane fluidity and rigidity [25, 97] while providing structural support to the phospholipids bilayer. Because of its amphipathic nature, cholesterol is also capable of forming a molecular sheath around predominantly hydrophilic transmembrane proteins, such as the insulin receptor (IR) or GLUT channels, allowing the hydrophilic transmembrane proteins to span the hydrophobic regions of the lipid bilayer. Further, in cholesterol-enriched membrane microdomains such as caveolae, increased packing of cholesterol within the bilayer region locally increases membrane order and membrane rigidity, while decreasing membrane permeability [24]. Transmembrane signaling and membrane fusion, such as that required for GLUT4 translocation in skeletal myofibers is also dependent on cholesterol-rich microdomains. For example, caveolae located in the sarcolemma membrane are also the docking site for internal membrane GLUT4 trafficking vesicles [13, 18] suggesting that the cholesterol content of these membrane microdomains may also play a role in modulating GLUT4 translocation

Cholesterol Biosynthesis

Cholesterol is incorporated into membrane by exogenous sources, either synthesized with in the cell or taken from circulation. Synthesis with in the cell occurs in the endoplasmic reticulum of the cell and is initiated by Sterol Regulatory Element Binding Protein (SREBP) when membrane cholesterol content is low. SREBP is a transcription factor inducing the transcription of the genes responsible for the synthesis of cholesterol [98]. SREBP is also activated in response to exercise induced activation of AMPK [99]. Among the 40+ membrane bound proteins expressed and involved in the

process, the enzymatic activity of 3-hydroxy-3methylglutaryl-CoA reductase (HMG CoAR) is most critical as it is a rate limiting step in the production of the cholesterol precursor mevalonate [100]. Although myofibers do synthesize cholesterol, they predominately rely on endogenous LDL as their rate of synthesis is of the slowest in the body [101-103].

LDL Uptake and HDL Excretion

Endogenous cholesterol production is inhibited when adequate amounts are obtained from diet sources. Cholesterol, triglycerides and phospholipids are hydrophobic and require carrier molecules to enter the circulation. After ingestion, cholesterol is packaged with other lipids into structures called "micelles" allowing cholesterol to pass through the walls of the small intestine. Once in the circulation, cholesterol and other lipids are re-packaged with a protein exterior, which forms a low-density lipoprotein (LDL). LDL receptors are located in specialized compartments within the sarcolemma called clathrin-coated pits, where LDL is consumed by the cell through a process called receptor mediated endocytosis. After binding, both LDL and the LDL receptor cross the cell membrane, while afterwards the receptor is detached and reincorporated back into the sarcolemma [104]. Excess cholesterol is either esterified within the sarcoplasmic reticulum by sterol o-acyltransferase for storage, or expelled out of the cell by ATP-binding cassette transporters (ABCs) ABCA1 and ABCG1, which aid in both translocation to the membrane and packaging of free cholesterol into lipoproteins. Cholesterol leaves the cell packaged as a water-soluble, high-density lipoprotein (HDL) [105].

Cholesterol Trafficking to Internal Membranes

Once inside the cell the LDL molecule is hydrolyzed to form free cholesterol esters that are cycled through the sarcolemma and internal membranes [104]. Due to the higher cholesterol content of cellular membranes compared to the cytoplasm, the transport and induction of cholesterol into membranes occurs along a step gradient, and requires active transport. An exact mechanism of intracellular cholesterol trafficking is currently unknown, however there is evidence for both vesicular and non-vesicular transport mechanisms [106].

Caveolae Composition, Structure, and Cellular Location

Figure 4: Membrane Composition

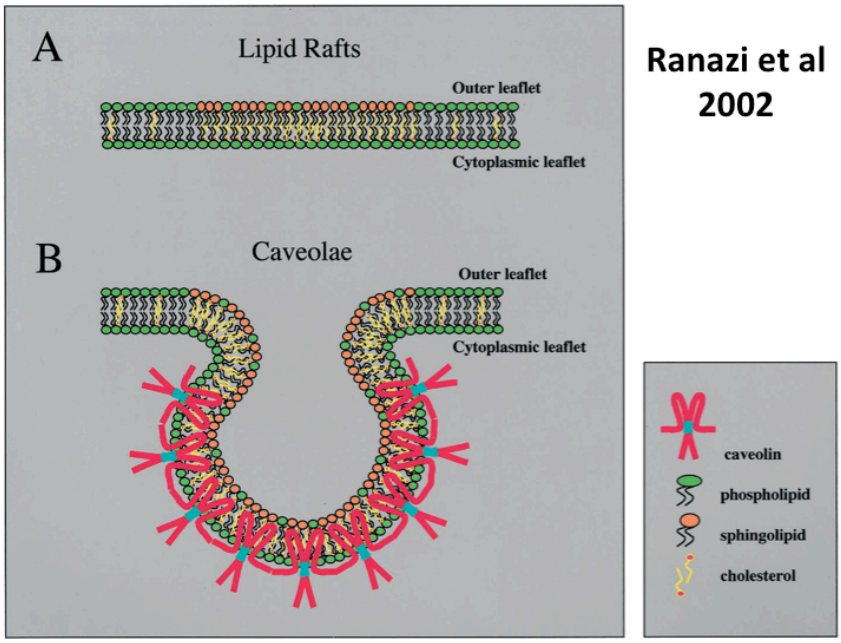

Ranazi et al 2002

In eukaryotic cells cholesterol-rich microdomains host the majority of receptors and membrane-bound components of growth signaling pathways, like that of insulin, and FGF [19]. Cholesterol exists within these domains among the fatty acid chain tails of the phospholipids, or the hydrophobic region of the membrane [19], and serves to provide

structural support for membranes [107], decrease membrane fluidity [24], and increase membrane ordering among transmembrane or membrane-bound proteins [108].

These cholesterol-rich microdomains are categorized as either lipid rafts or caveolae. Lipid rafts are flat domains, while caveolae are small invaginations structurally dependent on the cholesterol-binding protein caveolin [19]. In skeletal muscle the isoform caveolin-3 is critically important for maintaining caveolae structure, as caveolin-3 knockout models show an absence of caveolae [109, 110], T-Tubule dysfunction, altered distribution of the dystrophin glycoprotein complex [109, 111], and muscle degeneration [111].

These cholesterol-rich microdomains exist within the sarcolemma as well as internal organelle membranes such as the sarcolamic reticulum membrane system. Evidence demonstrates that reduced membrane cholesterol within sarcolemma microdomains weakens the myofiber membrane and decreases membrane order [97], while increased cholesterol decreases membrane fluidity but leaves it rigid and susceptible to exercise-induced damage [25, 97]. These fluid and rigid states are termed either gel or liquid ‘phases’, and depend on the type of phospholipid, the saturation of the phospholipid fatty acid chain tail, and the amount of cholesterol with the membrane [97]. These biophysical properties can be measured quantitatively through determining a Young’s Modulus value, or specific to cell membranes, the elastic modulus. Multiple normal cell functions have been linked to these modulus values, including phagocytosis in macrophages [112] and ABCA1-mediated cholesterol efflux in hamster kidney cell [113].

The composition of caveolae includes cholesterol, and glycerine- and ceramide-based phospholipids. Glycerophospholipids are unsaturated fatty acids with double bonds between the carbons along their fatty acid chain [97, 114]. These double bonds create 'kinks', or bends in the fatty acid chain tails of phospholipids that take up more space with the phospholipid bilayer, thereby decreasing membrane density, rigidity, and increasing fluidity. Glycerine based phospholipids include phosphotitidylcholine (PC), phosphotitylethanolamine (PE), and phosphatidylserine (PS), and phosphotityleinositol (PI). Phosphotitylcholine is the most abundant phospholipid in most biological membrane systems, representing roughly 50% of all phospholipids within most membrane systems [115]. However, lipid rafts and caveolae have a particularly low concentration of glycerophospholipids compared to the rest of the membrane, while ceramide based phospholipids are more concentrated in these microdomains [19]. These microdomains host a myriad of cell regulatory signaling molecules and therefore require a highly ordered, stable, but fluid membrane. Ceramide-based sphingolipids provide this stability because of the biochemical structure of their fatty acid chain tails.

Cholesterol preferentially associates with the ceramide-based phospholipid sphingomyelin [97, 114, 116], which are long chained saturated fatty acids with an absence of double bonds along their carbon chains. The absence of double bonds means there are no 'kinks' in the fatty acid chain, the molecule itself is more evenly cylindrical, and they can therefore be packaged much more tightly within the membrane. Tight packaging of sphingomyelin increases membrane order within these domains, but decreases membrane fluidity, keeping the membrane region in a solid 'gel' phase. The addition of cholesterol between the fatty acid chains of sphingolipids serves to fluidize

solid phase membrane regions into a 'liquid-ordered' state by keeping fatty acid chain tails of phospholipids ordered, but also allowing lateral diffusion of membrane components [97, 114].

Caveolae are particularly concentrated within the Travers-Tubule (T-Tubule) system of the myofiber, however cholesterol and caveolin-3 anchored microdomains are also found in the SR membrane of skeletal muscle fibers, independent of the RYRY and DHPR [85, 117], and have been shown to primarily exist within these internal membrane structures of skeletal muscles in both humans and rodents [117]. The SR membrane harbors the sarcoendoplasmic reticulum calcium ATPase (SERCA) pumps responsible for pumping calcium back into the SR membrane system after a muscle contraction. The function of SERCA pumps in the SR membrane directly affects GLUT4 translocation through regulation of Ca+ in rodent myocardium [118, 119] and cardiomyocytes [120].

Cholesterol and GSV Membrane Fusion

Vesicle membrane fusion to the sarcolemma is dependent on SNARE proteins, a class of membrane proteins responsible for cellular membrane-membrane fusion events discussed previously in this chapter. IN the specific case of skeletal muscle, SNARE proteins are responsible for opening the initial fusion pore and connecting the membranes of the sarcolemma and the GSV [121], while cholesterol has been observed to directly affect this process [122-129]. Cholesterol has been shown to lower the activation energy of SNARE-mediated pore formation [128]. A second way in which cholesterol has been observed to affect fusion is through altering the orientation of the SNARE protein motifs within the membrane. Tong et al demonstrated that the synaptobrevin TM domain was

tilted when reconstituted membranes lacked cholesterol, and became perpendicular after the addition of cholesterol, which coincided with increased membrane fusion [129] suggesting that membrane cholesterol content has a direct impact on the efficiency of GSV tethering and fusion with the sarcolemma membrane during GLUT4 translocation due to steric influences on SNARE proteins embedded in the membrane.

Cholesterol and Insulin Resistance

While cellular mechanisms involved in the etiology of hyperglycemia- and hyperinsulinemia-induced insulin resistance have been described, increases in either SL or SR membrane cholesterol may also contribute. Evidence to support this contention comes from a strong association between hypercholesterolemia/ hypertriglyceridemia and insulin resistance, an association between hypercholesterolemia and increased sarcolemma cholesterol content, and an association between membrane cholesterol and insulin resistance. However it has never been specifically demonstrated that increased membrane cholesterol content in skeletal muscle fibers inhibits insulin-stimulated glucose uptake.

Bonora et al. demonstrated the prevalence of insulin resistance in various metabolic disorders and found insulin resistance to be present in 53% of all hypercholerolemia patients, 84.2% of hypertriglyceridemia patients, and 88% of subjects with low HDL [32]. The prevalence of insulin resistance in subjects with low HDL is important to note given how cholesterol is processed; cholesterol is first packaged as LDL, absorbed and used by the cell, then expelled as HDL. Therefore, low HDL means

that cholesterol is not being expelled from the cell, and potentially accumulating in the membranes.

As discussed earlier in this chapter, Ca^{2+} has a distinct role in GSV translocation, docking and fusion through CaMK, AMPK, AS160, Kv1.3, SVII, and SNARE proteins [78, 79, 85, 87, 95], while cholesterol has been demonstrated to affect Ca^{2+} mediated vesicle fusion and reuptake of calcium back into the SR during E-C coupling [87]. The precise mechanism of cholesterol-induced changes in sarcoplasmic [Ca^{2+}] is currently unclear, but due to the sensitivity of GSV fusion to changes in [Ca^{2+}], and the role of Ca^{2+} in translocation and docking, cholesterol may also affect GSV translocation through a Ca^{2+} dependent mechanism as well.

Cholesterol and Membrane-Membrane Fusion

Membrane fusion between GSVs and cell membranes is inhibited in insulin resistant human adipose cells, despite insulin-stimulated GSV clustering at the plasma membrane of the adipocyte [130, 131]. While increased cholesterol membrane content may impact myofber glucose uptake by inhibiting the overall insulin signaling pathway at a variety of potential sites and through a variety of molecular signals, based on this observation it seems more likely that the primary site of disruption involves GLUT4 translocation, specifically GSV docking and fusion with the sarcolemma, One possible explanation for this disruption may be that a differential cholesterol content between the GSV membrane and the site of GSV fusion in the sarcolemma, leads to inhibition of this specific step in insulin-stimulated glucose uptake. For example, Garvey et al. provided evidence that in insulin resistant and diabetic individuals, GLUT4 was packed into more

dense membrane vesicles, and that GLUT4 translocation was inhibited in these individuals [132]. Breisblatt et al. found that the addition of cholesterol (33% by weight) to artificial bilayer membranes inhibited fusion between membranes, as well as altered optimal fusion temperatures [133]. Further, Koga et al. found that either removing cholesterol of mouse liver cells using methyl-β-cyclodextrin *in vitro*, or increasing membrane cholesterol by high-fat diet *in vivo,* suppressed autophagic vesicular fusion by as much as 70% [134]. While it is unclear whether overall increased membrane cholesterol content *per se*, or specifically differential cholesterol content between the two fusing membranes results in this inhibition, there is no doubt that cholesterol content is an important modulator of membrane-membrane fusion events in general.

Membrane Cholesterol and Insulin-Stimulated Glucose Uptake

Animal Models

Altering membrane cholesterol can be done *in vivo* through high fat diet [1, 2, 25], which coincides with insulin resistance [1, 2]. Lianos et al. demonstrated this increased membrane cholesterol to be found specifically in the T-tubule of mice fed a high fat diet [2]. Habegger et al. found the same intervention in mice to cause a loss of F-actin and dysfunction in GLUT4 vesicle transport [1]. Knoblauch et al. found that an increase in membrane cholesterol in hypercholesteremic mice coincided with increased sarcolemma damage following exercise [25], suggesting that the membrane-membrane fusion process essential for repair of exercise-induced membrane damage is inhibited in these animals. Conversely, it has also been demonstrated that lowering membrane

cholesterol using methyl-β-cyclodextrin (MβC) increases GLUT4-dependent glucose uptake and reduces insulin resistance in obese mice [2].

Cholesterol is most abundant in skeletal muscle tissue with in the membrane of the SR [117] and can independently affect GSV translocation intermediates. Increased cholesterol content in the SR membrane has been shown to physically inhibit SERCA rotational mobility in rabbit skeletal muscle, in turn affecting cytoplasmic [Ca^{2+}] [135]. However, it has never been directly observed in animal models that increased myofiber SL or SR membrane cholesterol content directly affects insulin signaling or glucose uptake. The major limitation with *in vivo* models of hypercholesterolemia, altered membrane cholesterol, and insulin resistance is the difficulty in proving causality.

Cellular Models

The effect of altered sarcolemma membrane cholesterol content on insulin stimulation has been studied extensively in 3T3-L1 adipocytes. Cholesterol depletion has been shown to inhibit IR autophophorylation, IRS-1 phosphorylation, glucose uptake, and activation of the PKB/Akt pathway [33-36]. These studies demonstrate the importance of cholesterol regarding insulin-stimulated glucose uptake, however decreased but not depleted cholesterol content via chromium has been shown to increase insulin-stimulated GLUT4 translocation and glucose uptake [37]. For internal membranes, cholesterol enrichment increases $[Ca+]_I$ while cholesterol depletion diminished [Ca+], a commonality among several cell lines [136]. The effect of altered cholesterol content in the SR membrane on insulin-stimulated glucose uptake however, has never been observed.

It is important to remember that the major recipient of insulin's effects *in vivo* is skeletal muscle while the majority of research on insulin-stimulated GLUT4 translocation and glucose uptake *in vitro* has been in adipocytes [13, 18, 19]. Further, caveolae membrane components can be cell and species specific [19] and therefore studying such signaling pathways in adipocytes may not accurately represent normal *in vivo* responses to hypercholesterolemia in general, or in skeletal muscle specifically. Considering skeletal muscle is the organ most responsible for glucose deposition out of circulation, an *in vitro* model that most closely resembles a functional skeletal muscle fiber would be better suited for investigating molecular mechanisms of insulin-stimulated glucose uptake.

Experimental Challenges

3T3-L1 adipocytes have also been used extensively to characterize insulin-stimulated GLUT4 translocation, glucose uptake, and altered membrane cholesterol content [13, 18, 19]. However, since skeletal muscle is the predominant tissue for glucose utilization an optimal cellular model of insulin-stimulated glucose uptake in skeletal muscle is critical for understanding whole body glucose homeostasis and our ability to treat its deregulation. The mouse C2C12 and rat L6 skeletal muscle-derived cell lines have been used previously for this purpose [12, 38-45, 137, 138]. The L6 cell line has been successfully used in the past to investigate insulin-stimulated GLUT4 translocation and glucose uptake [46], however L6 myotubes lack sarcomere formation and the potential for contractile activity [47, 48]. The C2C12 cell line has had mixed results regarding insulin-stimulated GLUT4 translocation and glucose uptake. Some researchers

have found little to no glucose uptake response to insulin-stimulation [12, 44, 50, 139], while few have described successful protocols for insulin stimulated glucose uptake [43] and GLUT4 translocation [39]. The C2C12 cell line however does effectively forms sarcomeres and develops contractile potential [47, 49]. Considering the complicated interweaving network of insulin- and contraction-induced signaling pathways mediating GLUT4 translocation, a detailed and reproducible cellular model of insulin-stimulated glucose uptake in a C2C12 myotube culture would provide significant opportunities to more fully investigate the underlying cellular mechanisms involved in normal insulin-stimulated skeletal muscle glucose uptake and the etiology of various environmental conditions leading to pathologies such as insuline resistance and Type II diabetes.

Interestingly, much of the literature investigating insulin stimulated glucose uptake includes only high-glucose medium conditions up until the glucose uptake measurements are performed, or does not list the glucose concentrations in which these cells were cultured at all [12, 38, 50, 139]. The concentration of standard high glucose tissue culture medium is 25mM (450mg/dL), far greater than the low-glucose variety at 5.5mM (99mg/dL), which approaches the normal circulating levels of blood glucose at 70-100mg/dL in healthy individuals. A few researchers have demonstrated that incubation in high-glucose culture medium causes insulin resistance [31, 43]. Leonitieva et al. demonstrated impaired insulin-stimulated Akt phosphorylation in C2C12 myoblasts and impaired glucose uptake in retinal pigment epithelial (RPE) cells when using high glucose tissue culture medium, while 42-44h in low glucose tissue culture medium restored insulin sensitivity [31]. Nedachi et al. observed that high glucose content impaired insulin-stimulated 2-deoxy glucose (2DG) uptake within only 5 minutes of

exposure [43]. Therefore, it is quite possible that currently much of the literature may be describing tissue cultures models that reflect hyperglycemia-induced insulin resistance rather than normal glucose uptake, especially considering the lack of an insulin response found by many researchers in a range of cell types. As such, when developing an appropriate tissue culture model for investigating insulin-stimulated glucose uptake in skeletal muscle tissue not only is the choice of cell type and degree of cell differentiation going to be important, but so too will be the impact of culture conditions, especially selection of glucose medium concentrations.

Summary

Hypercholesterolemia from diet or physical inactivity may contribute to insulin resistance by increasing membrane cholesterol content in skeletal muscle fibers. Altered cholesterol content in the outer membrane has been shown to affect GLUT4 translocation-mediating pathways *in vitro* using adipocytes, while animal and human models suggest a strong association between hypercholesterolemia, increased membrane cholesterol, and insulin resistance. The direct effect of increased membrane cholesterol content on insulin-stimulated glucose uptake has yet to be fully investigated using a reproducible and consistent model of skeletal muscle. Further, much of the literature regarding insulin-stimulated glucose uptake in tissue culture models describe utilizing high concentrations of glucose in the culture media, conditions that may unknowingly be causing insulin-resistance in these cultured cells. Therefore the aim of this study is to develop a reliable model to study insulin-stimulated glucose uptake under physiologically normal glycemic conditions in differentiated C2C12 myotubes, and use this model to

investigate the effect of altered membrane cholesterol content on insulin-stimulated glucose uptake.

Chapter 3 – Materials and Methods

Materials

Cell Lines:

The mouse C2C12 myocyte cell line was obtained from Sigma Aldrich (St. Louis, MO). Cells were initially expanded in tissue culture for three passages in culture to create a common pool of C2C12 myocyte cells (passage 3). This stock culture of C2C12 myocytes was resuspended in 10% (v/v) fetal bovine serum (FBS) containing 10% dimethylsulphoxide (DMSO), aliquoted into cryovials and stored under liquid nitrogen. All subsequent experiments investigating glucose uptake in C2C12 myotubes utilized C2C12 myocytes from this stock culture that were passage 8 or below.

Tissue Culture Medium Preparations:

Basal C2C12 tissue culture media consisted of Dulbecco's Modified Eagle's Media (DMEM) containing either 4.5g/L (25mM, 450mg/dL) (i.e. high glucose) or 1g/L (5.5mM, 100mg/dL) (i.e. low glucose) of glucose, Glutamax™ supplement, 25mM 4-(2-Hydroxyethyl)-1-piperazine ethanesulfonic acid (HEPES), 1mM pyruvate (Thermofisher, Waltham MA), and 4mM L-Glutamine. Both high glucose basal tissue culture medium (HG-DMEM) and low glucose basal tissue culture medium (LG-DMEM) contained 100 mM of both penicillin and streptomycin (Thermofisher, Waltham MA).

C2C12 growth medium consisted of HG-DMEM containing 10% (v/v) fetal bovine serum (FBS) (10%FBS.HG-DMEM). FBS was obtained from Thermofisher (certified US origin, Waltham, MA).

C2C12 differentiation medium consisted of either HG-DMEM containing 2% (v/v) heat inactivated horse serum (HS) (2%HS.HG-DMEM) or LG-DMEM containing 2% (v/v) HS (2%HS.LG-DMEM). Heat inactivated HS was obtained from Thermofisher (certified US origin, Waltham, MA).

C2C12 Serum Starvation medium consisted of LG-DMEM (Thermofisher, Waltham MA) containing 1% (w/v) filter sterilized, purified bovine serum albumin (BSA) (Thermofisher, Waltham MA) and 100mM penicillin and streptomycin (1%BSA.LG-DMEM).

Glucose uptake assay media consisted of glucose-free Dulbecco's Modified Eagle's Media (DMEM).

Tissue Culture Plates:

Standard T75 cell culture flasks (VWR, Radnor, PA) were used to expand C2C12 myocytes in tissue culture for use in subsequent experiments. 6-well tissue culture treated plates (VWR, Radnor, PA) were used for all experiments involving subsequent imaging, while 96-well tissue culture-treated plates optimized for fluorometric assays were used for glucose uptake, total protein and total cholesterol measurements (VWR, Radnor, PA).

Tissue Culture Reagents:

Dulbecco's Modified Phosphate buffered saline (DPBS-) (Sigma Aldrich, St. Louis MO, St. Louis MO), or DPBS+ containing 1mM calcium and 1mM magnesium (DPBS+)

(Thermofisher, Waltham MA) and 0.05% (w/v) trypsin EDTA solution (Sigma Aldrich, St. Louis, MO) were used for subculture of C2C12 cells. Porcine gel solution (used for coating of tissue culture plates in which C2C12 myoblasts were differentiated into myotubes) consisted of a sterilized aqueous solution made up of deionized water containing 1% (w/v) porcine gel (Sigma Aldrich, St. Louis MO).

Cell Labeling Reagents:

2-(*N*-(7-Nitrobenz-2-oxa-1,3-diazol-4-yl)Amino)-2-Deoxyglucose, a fluorescent, analog of glucose (2-NBDG) (Molecular Probes), was used to quantify either basal or insulin-stimulated glucose uptake into differentiated C2C12 myotubes.

Purified insulin from bovine pancreas (Sigma Aldrich, St. Louis MO, St. Louis MO) was used to stimulate insulin-stimulated glucose uptake into differentiated C2C12 myotubes.

A fluorescently labeled analog of cholesterol, 23-(dipyrromethene boron difluoride)-24-norcholesterol (Fluorescent Cholesterol Analog – FCA) (Avanti Lipids, Alabaster Al), was used to determine the initial experimental time course required to selectively enrich either the external or internal membranes of differentiated C2C12 myotubes with native cholesterol in culture.

Water-soluble cholesterol (WSC) (Sigma Aldrich, St. Louis MO, St. Louis MO) consisting of a cholesterol/methyl-β-cyclodextrin complex dissolved in tissue culture medium was used to selectively enrich either the external or internal membranes of

differentiated C2C12 myotubes with native cholesterol in culture prior to determining glucose uptake using 2-NBDG. Methyl-β-cyclodextrin (MβC) alone, dissolved in tissue culture medium, was used to selectively deplete native cholesterol from the membranes of differentiated C2C12 myotubes in culture prior to determining glucose uptake using 2-NBDG.

Immunohistochemical Reagents:

A skeletal muscle sarcomeric myosin heavy chain (MHC) mouse monoclonal IgG antibody was obtained from the Developmental Studies Hybridoma Bank (Iowa City, Iowa). A biotinylated anti-mouse peroxidase ABC detection kit was obtained from ABCAM (Cambridge United Kingdom). A dihydropyridine (DHP) receptor channel mouse monoclonal IgG1 primary antibody was obtained from (Thermo Scientific, Waltham Ma), and used in conjunction with a goat anti-mouse IgG1 AlexaFluor™ 647 obtained from Life Technologies (Carlsbad, CA). Heat-inactivated goat serum (HIGS), ammonium chloride and Triton X-100 (TX-100) were obtained from Sigma-Aldrich (St. Louis, MO). Dulbecco's Phosphate Buffered Saline (D-PBS) was obtained from Fisher Scientific (Hampton, NH). D-PBS was used either without calcium and magnesium (D-PBS-) or with 1mM calcium and magnesium (D-PBS+).

Methods

C2C12 Myoblast Culture:

Stock cultures of C2C12 myoblasts were removed from storage under liquid nitrogen and grown in T75 cell culture flasks using 10%FBS.HG-DMEM growth media

at an initial density of 2000 cells/cm^2. C2C12 myoblasts were cultured in a humidified, tissue culture incubator at 37^{o}C, in a 5% (v/v) CO_2 atmosphere. Once myoblasts reached approximately 60% confluence by visual inspection they were sub-cultured into a new T75 flask for further myocyte expansion, with a sub-set of cells being plated into either 6 or 96-well tissue culture plates for differentiation and subsequent experimentation. The remaining C2C12 myocytes were resuspended in FBS containing 10% dimethylsulphoxide (DMSO), aliquoted into cryovials and stored under liquid nitrogen to replenish C2C12 stock culture stores.

To subculture C2C12 myoblasts, growth media was removed from the cell monolayer and washed with two changes of sterile DPBS- for a total of two minutes. DPBS was removed and cells were incubated with 15mL of 0.05% trypsin/EDTA solution at 37^{o}C until the cells had detached from the flask. The cell suspension was then mixed 1:1 with growth media containing FBS in order to neutralize the trypsin. The cell suspension was then decanted from the tissue culture flask into sterile, 50 ml centrifuge tubes and centrifuged for 5 minutes at 100*xg*. The cell pellet was then resuspended into a single cell suspension by titurating the cell pellet in 5 ml of standard growth medium using a sterile 1ml pipette tip. The number of cells in the cell suspension was counted using a hemocytometer and then diluted to the desired cell density with fresh standard growth medium for subsequent sub-culture and/or experimentation.

Coating Cell Culture Plates in Porcine Gel for Subsequent Myotube Formation

C2C12 myotubes cultures were grown and differentiated in tissue culture-treated, non-pyrogenic 6-well or 96-well polystyrene plates. To provide additional adherence to

the culture surface, culture plates were coated with a porcine gel solution prior to cell seeding. Culture plates were first incubated for 1 hour at 37^{o}C in the porcine gel coating solution, followed by 3 washes with sterile deionized water and one wash with sterile DPBS-. Each well was aspirated to dryness prior to being seeded with C2C12 myoblasts at a known cell density.

C2C12 Myotube Differentiation:

Preliminary observations indicated that continuous culture and expansion of C2C12 myocytes beyond passage 10 in high glucose DMEM growth medium appeared to reduce the rate and subsequent degree of myotube differentiation that could be achieved in culture. As such, all experiments utilizing differentiated C2C12 myotube cultures were derived from C2C12 myocytes cultured for no more than 8 passages beyond the original myocyte cell line obtained from Sigma Aldrich (St. Louis, MO).

C2C12 myoblasts (below passage 8) were suspended in 10%FBS.HG-DMEM and seeded into either 6- or 96-well porcine gel-coated culture plates at a density of 10,000 cells/cm^2 of culture surface. Cells were grown for three days until the wells of each plate appeared by visual observation to be approximately ≥90% confluent. Once the cultures had reached ≥90% confluence, 10%FBS.HG-DMEM growth medium was replaced with 2%HS.LG-DMEM differentiation medium. 2%HS.LG-DMEM differentiation medium was exchanged for fresh differentiation medium every other day for 6 days. Formation of C2C12 myotubes was determined both visually, as determined by the formation of three dimensional myotubes structures in the culture, as well as subsequent verification of myotube differentiation by detection of myosin heavy chain (MHC) expression and

dihydropyridine (DHP) receptor expression using immunohistochemistry (IHC), both markers of terminal differentiation in skeletal muscle myofibers *in vivo* [140-144].

Skeletal Muscle Myosin Heavy Chain (MHC) Peroxidase Immunohistochemistry

C2C12 myotubes grown in 6-well tissue plates were first washed with two changes of D-PBS+, fixed and permeabilized in ice-cold methanol for 2 minutes, and washed again with two changes of DPBS+. The fixed myotubes were then incubated in 4% heat-inactivated goat serum in DPBS+ for 1 hour to block non-specific protein interactions prior to sarcomeric MHC primary antibody exposure. Samples were incubated overnight at 4^{o}C with a mouse polyclonal IgG primary hybridoma antibody specific to sarcomeric myosin heavy chain (MHC) at a concentration of 10ug/mL in DPBS+, supplemented with 1% HIGS to inhibit non-specific protein interaction. The following day myotube samples were washed a total of four times over 20 minutes using DPBS+, followed by detection of MHC primary antibody binding using a biotinylated goat-anti-mouse IgG secondary antibody coupled to horse-radish peroxidase (Abcam, Cambridge UK) as per the manufacturer's instructions. Skeletal muscle sarcomeric MHC peroxidase staining of myotubes was imaged under bright-field conditions using a light microscope (Olympus, Tokyo, Japan). To determine non-specific secondary antibody binding, parallel myotube cultures were subjected to the same immunocytochemistry protocol in the absence of the primary antibody.

Dihydropyridine (DHP) Receptor Fluorescent Immunohistochemistry

Myotubes in 6-welled plates were first fixed in 1% paraformaldehyde for 5 minutes then washed 3 times with DPBS+. Myotubes were then permeabilized using D-PBS+ containing 1% (v/v) TX-100 for 5 minutes and washed three times with DPBS+. Samples were then incubated for 30 minutes in D-PBS+ containing 50mM ammonium chloride to inhibit non-specific fluorescent signal followed by another three washes in DBPS+. Samples were incubated for 1 hour in D-PBS+ containing 4% HIGS to inhibit non-specific protein interactions followed by overnight incubation with a primary mouse anti-DHP IgG1 antibody diluted to 1:400 with D-PBS+ containing 1% (v/v) HIGS at 4ºC. The samples were washed using 5 changes of D-PBS+ and then incubated for 2 hours at room temperature with secondary antibody consisting of an Alexa Fluor™ 647-conjugated goat anti-mouse IgG1 secondary antibody (10mg/ml) diluted in D-PBS+ containing 1% (v/v) HIGS. Samples grown in 6-well plates were then washed three changes of DBPS+ over 5 min, aspirated to dryness, mounted in Fluoromount G, cover-slipped and then sealed. Mounted and sealed samples were excised from the plate with a blowtorch-heated scalpel as described in further detail later in this section in preparation for confocal microscopy analysis. Samples were imaged using excitation and emission wave-lengths of 647nm and 720nm, respectively. Since the emission wavelength of the Alexa™ 647nm fluorophore is beyond the visible light spectrum, fluorescent signal associated with secondary antibody binding was assigned a light blue color using the imaging software.

Basal and Insulin-Stimulated Glucose Uptake Measurements in C2C12 Myotubes

A fluorescent glucose analog, 2-(*N*-(7-Nitrobenz-2-oxa-1,3-diazol-4-yl)Amino)-2-Deoxyglucose (2-NBDG), a non-metabolizeable form of glucose, was used to determine glucose uptake under basal and insulin-stimulated conditions in differentiated C2C12 myotube cultures. A concentrated, stock 2-NBDG solution was prepared by dissolving 1mG of 2-NBDG powder in 1mL of serum-free, glucose-free DMEM medium which was then aliquoted and stored at -20^{o}C for future experiments.

Previous studies have suggested that differentiated C2C12 myotubes cultured in high glucose medium appear to exhibit insulin insensitivity and reduced insulin-stimulated uptake of glucose as compared to myotubes cultured in low glucose medium [31, 43]. In order to test whether or not high glucose culture conditions induced insulin insensitivity in the C2C12 myotubes utilized in this study, the effects of culturing differentiated C2C12 myotubes in high or low glucose differentiation medium for a period of two days prior to measuring glucose uptake was tested. As can be seen in **Table 1**, high glucose differentiation culture conditions did not have any discernible effect on the basal (i.e. GLUT1-mediated) uptake of glucose in differentiated C2C12 myotubes. However, exposure of C2C12 myotubes to low glucose culture conditions for a period of 48 hours prior to stimulation of the C2C12 myotubes with insulin caused a reproducible though not statistically significant increase in the amount of insulin-stimulated (i.e. GLUT4-mediated) glucose uptake.

Based on these initial experimental observations, to ensure maximum insulin sensitivity all subsequent experiments investigating glucose uptake utilized differentiated C2C12 myotubes incubated in low glucose differentiation medium for 48 hours prior to

testing. In addition, in order to negate the effects of insulin and other insulin-like growth factors that may be constitutively present in the serum fraction of the low glucose differentiation medium, 16 hours prior to testing C2C12 myotubes were washed with warm D-PBS+ to remove any serum components and then cultured in low glucose differentiation medium containing 1% (w/v) purified BSA as a serum substitute. The experimental tissue culture protocol and timeline for generating differentiated C2C12 myotube cultures used in subsequent glucose uptake experiments is depicted graphically below in **Figure 5**.

Figure 5: **Experimental Time Course for Differentiation and Subsequent Testing of Glucose Uptake In C2C12 Myotubes**

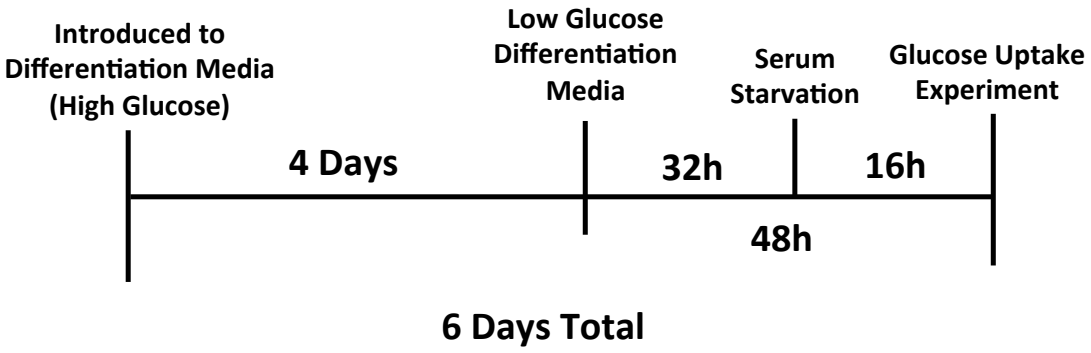

In order to determine basal (i.e. GLUT1-mediated) or insulin stimulated (i.e. GLUT4-mediated) glucose uptake, differentiated C2C12 myotube cultures in either 6-well or 96-well plates were first washed with warm D-PBS+ and then incubated for 30 minutes in a reaction buffer consisting of warm, glucose-free, serum-free DMEM containing 400μM 2-NBDG and either 0nm (basal uptake conditions), 10nM, 25nM, 50nM or 100nM insulin, respectively. The glucose uptake assay was carried out in the

dark at 37^{o}C in a tissue culture incubator. Labelled C2C12 myotubes were then washed with ice-cold DPBS^{+} and aspirated to dryness to remove any free 2-NBDG remaining in each well.

Labeled C2C12 myotubes in 6-welled plates were mounted in Fluormount G (Electronic Microscopy Sciences), cover-slipped and then immediately imaged under an epifluorescent microscope (Olympus) to visualize the uptake of the fluorescent glucose analog (2-NBDG) into myotubes (**Figure 3**). Alternatively, C2C12 myotubes assayed for glucose uptake in 96-well plates were immediately lysed in 100 microliters of ice-cold lysis buffer containing 0.1M potassium phosphate and 1% (v/v) Triton X-100 adjusted to pH 10 to release the fluorescent glucose analog (2-NBDG) taken up by the myotubes. The amount of 2-NBDG taken up by C2C12 myotube cultures in each well was quantified using a fluorometric plate reader (Thermofisher, Waltham MA) using an excitation wavelength of 468 nm and an emission wavelength of 540 nm. After measuring the fluorescent signal in the lysate of each well, a portion (10 microliters) of the lysate removed from each C2C12 myotube culture was analyzed for total protein content using a BCA protein assay kit (Thermofisher, Waltham MA). Glucose analog (2-NBDG) uptake (in fluorescent units - FU) per C2C12 myotube culture was reported as FU/mg total protein in order to normalize for any differences in the number of C2C12 myotubes present in each culture. In those experiments designed to investigate the effects of selective enrichment or depletion of C2C12 myotube membranes with cholesterol on glucose uptake, a separate portion of the lysate (10 microliters) was also analyzed for cholesterol content using a total cholesterol assay kit (Pointe Scientific, Canton, MI).

Cholesterol Localization in C2C12 Myotubes Under Different Pulse-Chase Labelling Conditions

In order to achieve selective enrichment of internal and external C2C12 myotube membranes with cholesterol, the time course for cholesterol trafficking in tissue culture under specific ***pulse-chase*** enrichment conditions was investigated. The time course of cholesterol trafficking between the tissue culture medium and its subsequent localization in specific myotube membrane structures was initially determined using a fluorescent analog of cholesterol, 23-(dipyrrometheneboron difluoride)-24-norcholesterol. While slightly larger than native cholesterol, when introduced to serum-containing tissue culture medium this fluorescent analog has previously been shown to be taken up and subsequently distributed within tissue cultured cell membranes in a similar manner to native cholesterol [145, 146].

Cholesterol and fluorescent cholesterol analogs are normally insoluble under aqueous conditions. In biological systems, cholesterol is transported in the blood or interstitial fluid complexed to carrier proteins such as low density lipoproteins (LDL). These carrier proteins transport the cholesterol to the external cell membranes where the cholesterol is taken up into the cell via the LDL receptor. As such, in order to introduce the hydrophobic fluorescent cholesterol analog molecule to C2C12 myotubes in culture, it must first be fully dissolved in pure ethanol prior to being subsequently diluted in serum-containing tissue culture medium.

23-(dipyrrometheneboron difluoride)-24-norcholesterol (fluorescent cholesterol analog) was initially reconstituted at a concentration of 2g/mL in pure ethanol, sonicated to ensure efficient mixing, aliquoted into smaller amounts and stored in the dark at 4^{o}C

for future experiments. Immediately prior to being added to serum-containing tissue culture medium, the stock analog solution was centrifuged at 10,000*xg* to remove any remaining undissolved material. Differentiated C2C12 myotubes growing in 6-well plates were cultured for 4 hours in standard differentiation medium containing different amounts of fluorescent cholesterol analog. After a defined period of exposure to the analog in culture, referred to as the initial "***pulse***" period, the C2C12 myotubes were washed with three changes of warm D-PBS+ and then fixed using D-PBS+ containing 1% (v/v) paraformaldehyde (Electron Microscopy Sciences) for 10 minutes at room temperature. Fixative solution was removed from the sample by washing with D-PBS+, mounted in Fluoromount G (Electron Microscopy Sciences), cover-slipped with a 24mm X 24mm square coverslip and then sealed with sealant. Fluorescent laser scanning confocal microscopy (Leica Scanning Confocal Microscope) was used for subcellular membrane visualization of the fluorescent cholesterol analog. For optimal image acquisition, the mounted and sealed sample was excised from the base of 6-well plate as described later in this section. The fluorescent cholesterol analog was imaged using excitation and emission wavelengths of 468nm and 540nm, respectively.

The optimal concentration and the minimum "***pulse***" labeling times required to enrich specific C2C12 membranes with fluorescent cholesterol analog was initially determined using confocal microscopy. These experiments indicated that a 4 hour "***pulse***" labelling period at a final working concentration of 50 μM of fluorescent cholesterol analog resulted in the selective enrichment of the external sarcolemma and contiguous T-tubule membranes that could be clearly discerned by confocal microscopy (**Figure 14**). In addition, using a 4hr "***pulse***" label followed by a subsequent 16 hour

"***chase***" period in standard differentiation medium absent the analog resulted in trafficking of the fluorescent cholesterol analog from the external sarcolemma/T-tubule membranes into the internal sarcoplasmic reticulum (SR) membrane system (**Figure 14E and F**). Furthermore, a 4hr "***pulse***" label and a 16 hour "***chase***" followed by an additional 4 hour "***pulse***" label resulted in significant enrichment of both external and internal membrane systems with the fluorescent cholesterol analog (**Figure 14G and H**). Data gained from these experiments were used to define the "***pulse***"/"***chase***" labeling conditions used to selectively enrich or deplete the external and internal membranes of C2C12 myotubes with native cholesterol in culture.

Enrichment and Depletion of Cholesterol in C2C12 Myotube Membranes

The cholesterol content in differentiated C2C12 myotube membranes was selectively altered using methyl- β -cyclodextrin (M β C), a cholesterol depletion approach previously used both in *in vitro* and *in vivo* studies [147]. Differentiated myotubes were enriched with native cholesterol in culture using a cholesterol / M β C complex known as Water-Soluble Cholesterol (WSC), or selectively depleted (external membranes) using M β C alone. As described above, a fluorescent cholesterol analog was used to experimentally define the "***pulse***"/"***chase***" labeling culture conditions subsequently used to selectively enrich or deplete the external and internal membranes of C2C12 myotubes with native cholesterol. As such, the sarcolemma/T-tubule membranes of differentiated C2C12 myotubes were selectively enriched with native cholesterol using a 4 hour "***pulse***" in serum-free differentiation medium (1%BSA.LG-DMEM) containing WSC at a final concentration of 200 μM cholesterol (the cholesterol / M β C complex is

prepared at a 1:23 ratio of cholesterol to MβC). Selective enrichment of the sarcoplasmic reticulum (SR) membranes of differentiated C2C12 myotubes with native cholesterol was achieved using a 4 hour "***pulse***" in medium containing WSC followed by a 16 "***chase***" in serum-free differentiation medium (1%BSA.LG-DMEM) alone. In addition, the sarcolemma/T-tubule membranes of differentiated C2C12 myotubes were selectively depleted of native cholesterol using a 4 hour incubation in serum-free differentiation medium (1%BSA.LG-DMEM) containing MβC alone at a final concentration of 4.6 mM, equivalent to the amount of MβC present in the 200 μM cholesterol/WSC complex. Enrichment and depletion of C2C12 myotube cultures, using WSC or MβC respectively, was chemically validated using a total cholesterol assay kit (Pointe Scientific, Canton, MI) after lysis of the treated myotubes cultures in lysis buffer containing 0.1M potassium phosphate and 1% (v/v) Triton X-100 adjusted to pH 10, the same lysis buffer utilized in glucose uptake assays.

Laser-Scanning Confocal Microscopy

All C2C12 myotube samples analyzed using fluorescent scanning confocal microscopy were imaged using a Leica Scanning Confocal Microscope (Imaging Core Facility, University of Houston). In order to allow subsequent confocal microscopy imaging of C2C12 myotube samples grown and processed in 6-well tissue culture plates, the myotubes in each well were first mounted, cover-slipped and sealed and then excised from the base of the 6-well tissue culture plates using a blowtorch-heated scalpel as demonstrated in **Figure 2.** Samples analyzed to determine the subcellular localization of the fluorescent cholesterol analog, 23-(dipyrrometheneboron difluoride)-24-

norcholesterol within C2C12 myotubes were imaged using excitation/emission wavelengths of 488 nm and 540 nm, respectively. In the case of samples analyzed to determine the subcellular localization of the dihydropyridine (DHP) receptor within C2C12 myotubes, the excitation/emission wavelengths used were 647 nm and 720 nm, respectively. Images were collected using arrange of magnifications (i.e. 20X dry lens, 63X oil lens and 100X oil lens) and scale bars provide final dimensions in microns. Where noted, images were collected under identical imaging conditions to allow comparison of the fluorescent signal observed between experimental labelling conditions.

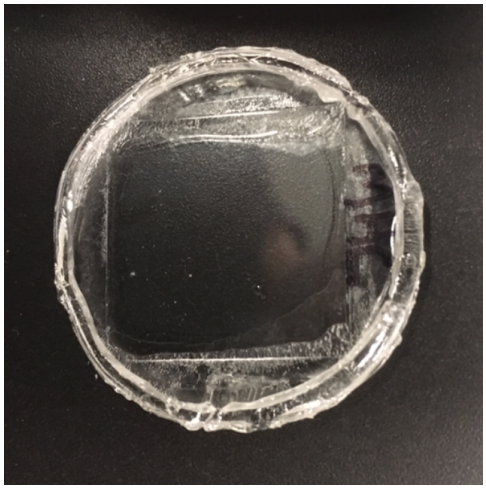

Figure 6: Micrograph of a coverslip-mounted C2C12 myotube sample excised from the culture surface of a 6-well tissue culture plate. Coverslip-mounted C2C12 myotube cultures grown on the culture surface of 6-well tissue culture plates were excised using a blowtorch-heated surgical scalpel in order for the sample to psychically fit the dimensions of the confocal microscope stage and allow the use of oil-based, optical lenses for ultra-high power magnification imaging.

Image Processing and Analysis

In order to obtain optimal spatial resolution of fluorescent cholesterol analog labelling of intracellular membrane components, or, specific fluorescent DHP antibody staining of T-tubule membranes, within individual C2C12 myotubes additional image

magnification and processing was performed. After initial confocal microscopy images of labelled C2C12 myotubes were acquired using a 100X magnification oil lens, specific regions of these images were electronically magnified by a factor of 300% using the Leica Confocal Microscopy Imaging Software. These electronically magnified images were then optimized using Huygens Deconvolution Software (Scientific Volume Imaging, Netherlands) to provide optimal spatial resolution of individual labelled membrane structures within the C2C12 myotube.

Statistical Analysis

An initial 5x6-way (enrichment condition x insulin concentration) ANOVA assessed any between enrichment conditions. One-way ANOVAs were used to assess each enrichment group across all insulin concentrations, as well as the differences between enrichment conditions for each insulin concentration. One-way ANOVAs were also used to examine differences in total cholesterol and basal glucose uptake between enrichment conditions. Bonferroni post-hoc analyses were conducted in the event of any statistical significance being identified between conditions. Statistical significance was set at an alpha value of $p = 0.05$.

Chapter 4: Results

The major cellular component of skeletal muscle tissue involved in glucose utilization *in vivo* is the myofiber. This project set out to develop and characterize a reproducible tissue culture model of skeletal muscle myofibers *in vivo* in which to mechanistically investigate the cellular mechanisms involved in insulin-stimulated glucose uptake quantified using a fluorescent analog of glucose, 2-NBDG. In turn, this differentiated C2C12 myotube model was then be used to investigate the potential effects of selective cholesterol enrichment of specific membrane structures on insulin signaling and insulin-stimulated glucose uptake.

Characterization of C2C12 Myotube Differentiation

Differentiation of C2C12 myocytes seeded at a specific cell density and grown under defined tissue culture conditions for a set period of time was initially assessed based on the visual appearance of large, multinucleated fusiform cells in culture. The degree of myotube differentiation under these defined culture conditions was subsequently confirmed using immunohistochemical detection of myosin heavy chain (MHC) and dihydropiridine (DHP) receptor protein expression by these myotubes, both terminal differentiation markers of skeletal muscle myofibers *in vivo* [140]. The myotube differentiation process initiated under these defined culture conditions involves the appearance of numerous, large, multinucleated fusiform cells when the culture is exposed to heat-inactivated horse serum over a 6 day period. Formation and maturation of these myotubes can be observed in C2C12 myotube cultures at day 1, 4 and 6 of differentiation (**Figure 7**).

Figure 7: Representative Phase Contrast Micrographs of C2C12 Myotube Differentiation over The Course of 6 Days in Culture. **Panel A** illustrates the initial alignment and fusion of C2C12 myocytes into myotubes after 24hr in high glucose differentiation medium. **Panel B** illustrates the initial formation of large, morphologically distinct C2C12 myotubes after 96 hours in high glucose differentiation medium. **Panel C** illustrates fully differentiated C2C12 myotube cultures after 144 hours of differentiation (96 hours in high glucose differentiation media followed by 48 hours of differentiation in low glucose medium).

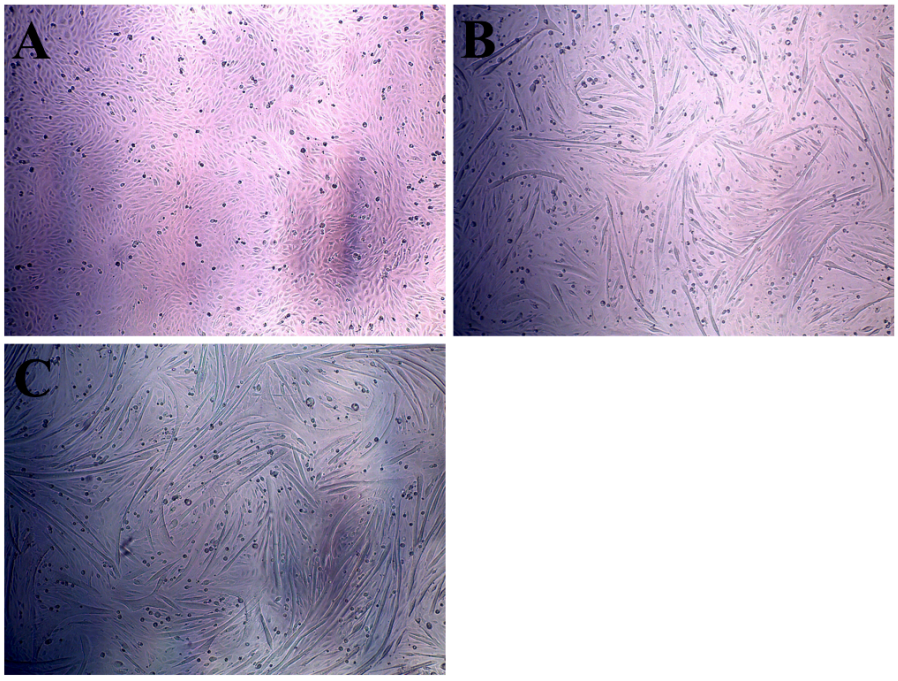

MHC protein expression by C2C12 myotubes after 6 days of differentiation in culture was confirmed using immunohistochemical staining using a mouse anti-myosin heavy chain (MHC) primary antibody followed by disclosure of primary antibody binding using an ABC immunoperoxidase staining kit and light microscopy (**Figure 8).**

Figure 8: Representative Micrographs of Sarcomeric Myosin Heavy Chain (MHC) Protein in Differentiated C2C12 Myotubes. C2C12 myotubes were differentiated for a total of six days, fixed in methanol and immunohistochemically stained for MHC protein disclosed using an immunoperoxidase secondary antibody kit. **Panel A** illustrates a low power light micrograph of MHC protein staining in large numbers of morphologically discrete, highly differentiated C2C12 myotubes in an individual myotube culture (Scale Bar – 200 µm). **Panel B** illustrates a high power light micrograph of MHC protein staining in an individual multi-nucleated, differentiated C2C12 myotube demonstrating the formation of myofibrils longitudinally orientated within the myotube (Scale Bar – 10 µm).

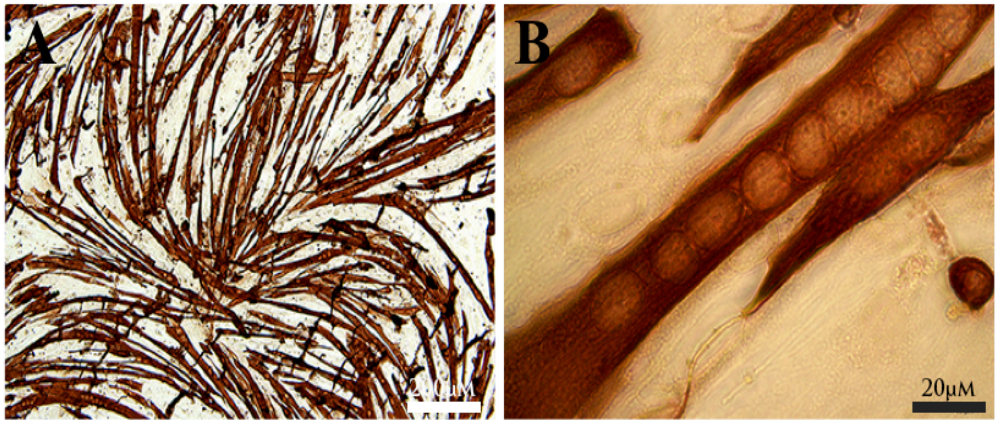

DHP receptor protein expression by C2C12 myotubes after 6 days of differentiation in culture was detected using a mouse anti-DHP primary antibody disclosed using a goat anti-mouse Alexa Fluor™ 647 fluorescent secondary antibody followed by confocal microscopy (**Figure 9).**

Figure 9: Representative Confocal Micrograph of Immunofluorescent DHP Receptor Staining In Differentiated C2C12 Myotubes. Image consists of a 1 μm thick optical section collected using a confocal microscope from a differentiated C2C12 myotube culture immunochemically stained for DHP receptor protein disclosed using an Alexa Fluor™ 647 fluorescent secondary antibody. (Scale Bar – 40 μm)

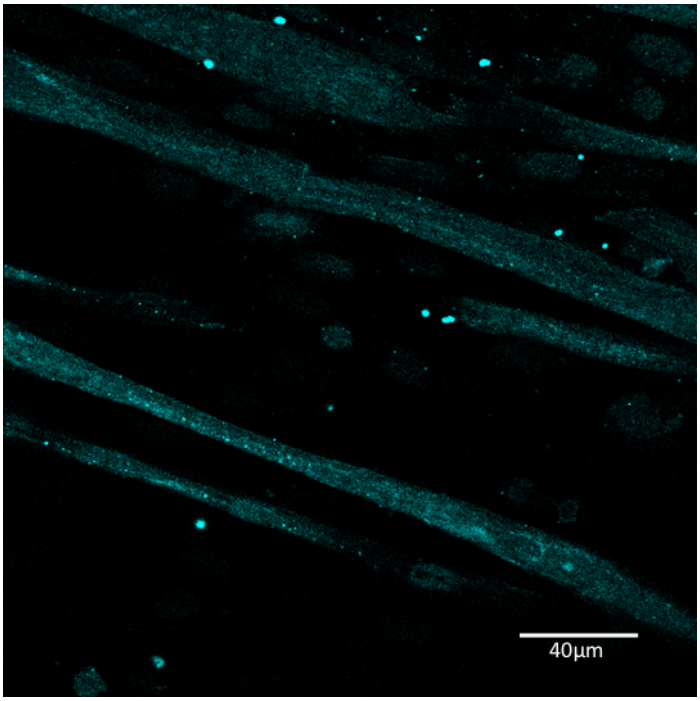

The temporally predictable appearance of large, three-dimensional, multi-nucleated myotubes coupled with the expression of both MHC and DHP receptor proteins demonstrate that the defined culture conditions developed in this study provide a highly reproducible means of generating large numbers of terminally-differentiated C2C12 myotubes in culture at will. Apart from studying the effects of selective cholesterol membrane enrichment on insulin-stimulated glucose uptake which is the focus of the present study, this well-characterized *in vitro* tissue culture model of skeletal myofibers may prove useful for investigating a variety of other physiologically and pathologically relevant mechanisms operating in skeletal muscle *in vivo*.

Characterization of Insulin Stimulated Glucose Uptake using 2-NBDG in C2C12 Myotubes.

In order to ensure that any glucose uptake detected and quantified in differentiated C2C12 cultures using the fluorescent glucose analog, 2-NBDG, truly reflected either basal or insulin-stimulated glucose uptake by myotubes, the cellular localization of 2-NBDG (Ex – 468nm, Em – 540nm) taken up by C2C12 myotube cultures was determined using epifluorescent microscopy. As can be seen in **Figure 10**, visual inspection of differentiated C2C12 myotube cultures exposed to 2-NBDG for 30 min in either the absence or the presence (i.e. 10nM insulin) using standard epifluorescent microscopy confirmed that the overwhelming majority of fluorescent 2-NBDG uptake was within the myotubes rather than by any unfused myocytes remaining in the culture (**Figure 10).**

Figure 10: Representative Fluorescent Micrographs of 2-NBDG Uptake in Differentiated C2C12 Myotube Cultures. **Panel A** illustrates basal 2-NBDG uptake while **Panel B** illustrates 2-NBDG uptake in the presence of 10nm insulin. These images demonstrate that the overwhelming amount of 2-NBDG taken up during a 30 minute exposure in the absence (i.e. basal glucose uptake) or presence of 10 nM insulin (i.e. insulin stimulated glucose uptake) is accounted for by myotubes rather than any unfused C2C12 myocytes remaining in the culture. (Scale Bar – 500 μm).

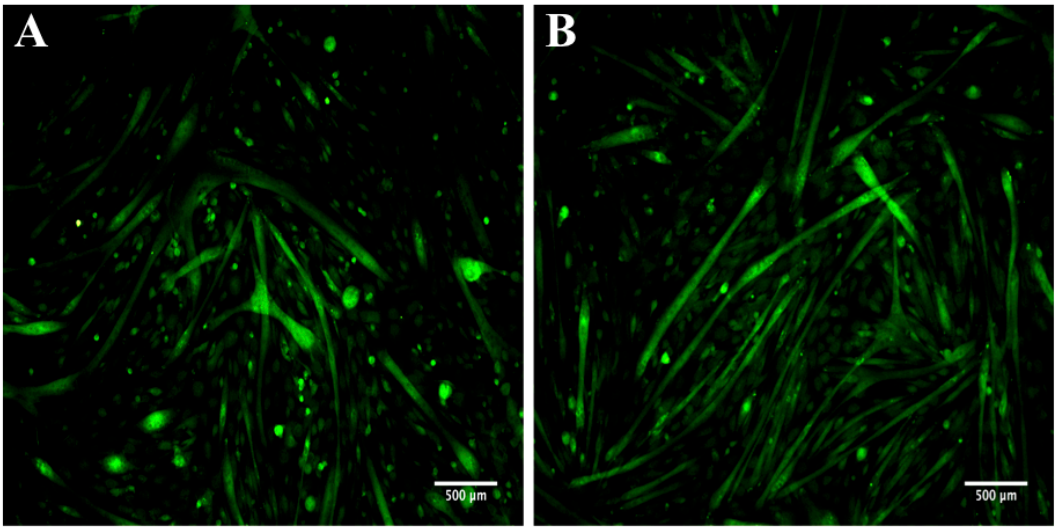

Initially, C2C12 myocytes and differentiated C2C12 myotubes where cultured in high glucose DMEM medium containing 25mM glucose, a concentration of glucose commonly used for culturing a variety of primary cells and established cell lines. However, physiologically speaking a circulating concentration of 25mM glucose (450mg/dL) is considered extremely hyperglycemic and potentially pathological if maintained over the long-term. Previous studies have demonstrated that even short-term incubation in tissue culture medium containing the high levels of glucose normally utilized in standard media preparations (25mM) appears to cause insulin resistance in a number of cultured cell types including skeletal muscle, with glucose uptake observed only after pre-incubation in low-glucose media (5.5mM or 100mg/dL glucose) [43].

In order to test the possibility that extended culture in high glucose conditions (i.e. 25mM glucose) might have resulted in a blunted insulin stimulated glucose uptake response in differentiated C2C12 myotubes generated under the culture conditions developed in this study, insulin stimulated glucose uptake in response to 10nM insulin was compared between: (1) C2C12 myotubes differentiated for 6 days under high glucose

conditions (i.e. 25 mM glucose) alone; and (2) C2C12 myotubes differentiated for 4 days under high glucose conditions (i.e. 25mM glucose) followed by an additional two days under low glucose conditions (i.e. 5.5mM glucose, 100mg/dL) (**Figure 11**).

Figure 11. The Effect of 48 Hours of Culture in Low Glucose Differentiation Media on Insulin Stimulated Glucose Uptake in C2C12 Myotubes. Insulin stimulation using 10nM insulin significantly increased glucose uptake in both conditions (* = $p < 0.05$). While culture in low glucose conditions increased insulin stimulated glucose uptake by approximately 20% compared to high glucose conditions, this increase was not found to be statistically significant. Glucose uptake per myotube culture was initially expressed as fluorescence units (FU)/(ug) of total protein and then normalized to the mean control value which was expressed as a value of one. Normalized values for glucose uptake for each condition were plotted as the mean +/- standard error. (N = 14 for each condition).

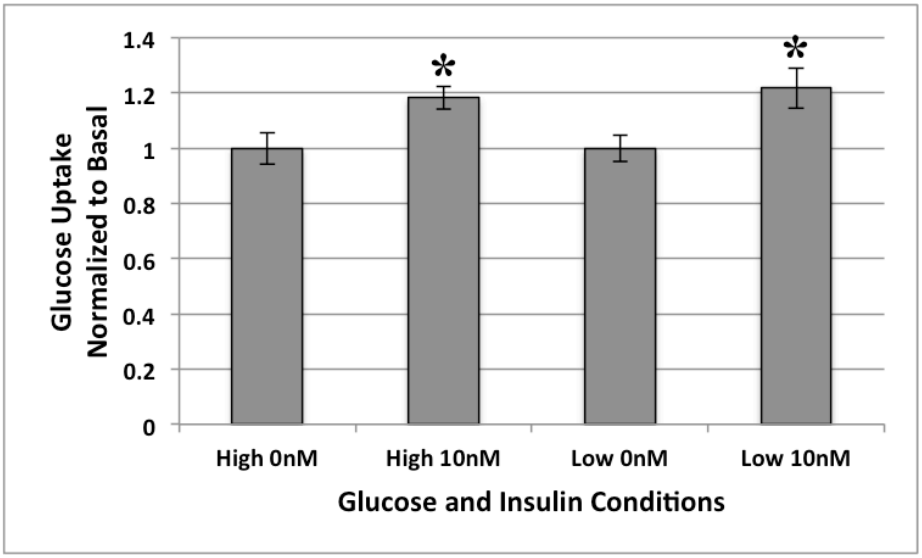

While there was no statistically significant difference in the amount of insulin stimulated glucose uptake detected between the two culture conditions described in **Figure 11,** glucose uptake under low glucose conditions (i.e. 5.5mM glucose, 100mg/dL) increased the amount of glucose uptake by approximately 20% as compared to glucose uptake in myotubes differentiated under high glucose conditions (i.e. 25mM glucose, 450mg/dL) alone (**Figure 11)**. As such, in order to ensure maximum possible sensitivity to insulin stimulation, all subsequent experiments in which glucose uptake was measured utilized C2C12 myotube cultures differentiated for 4 days under high glucose conditions followed by an additional 2 days of differentiation under low glucose conditions (**Figure 5**).

Subsequent to assessing the effects of differentiating C2C12 myotubes under high and low glucose conditions on insulin stimulated glucose uptake, the optimal concentration of insulin required to stimulate maximal glucose uptake in differentiated C2C12 myotubes was determined. Using differentiated C2C12 myotube cultures differentiated under the low glucose culture conditions described above, an insulin dose-response curve was constructed using insulin concentrations of 0nM, 2nM, 20nM, 200nM, 600nM and 1000nM, respectively.

Figure 12. The Effect of Insulin Stimulation on Glucose Uptake in C2C12 Myotubes. An initial ANOVA revealed a significant ($p < .05$) effect of increasing insulin concentration on insulin stimulated glucose uptake. Glucose uptake per myotube culture was initially expressed as fluorescence units (FU)/(ug) of total protein and then normalized to the mean control value which was expressed as a value of one. Normalized values for

glucose uptake for each insulin concentration were plotted as the mean +/- standard error. (N for each insulin concentration was as follows: 0nM N = 10, 2nM N = 13, 20nM N = 12, 200nM N = 14, 600nM N = 14, 1000nM N = 14).

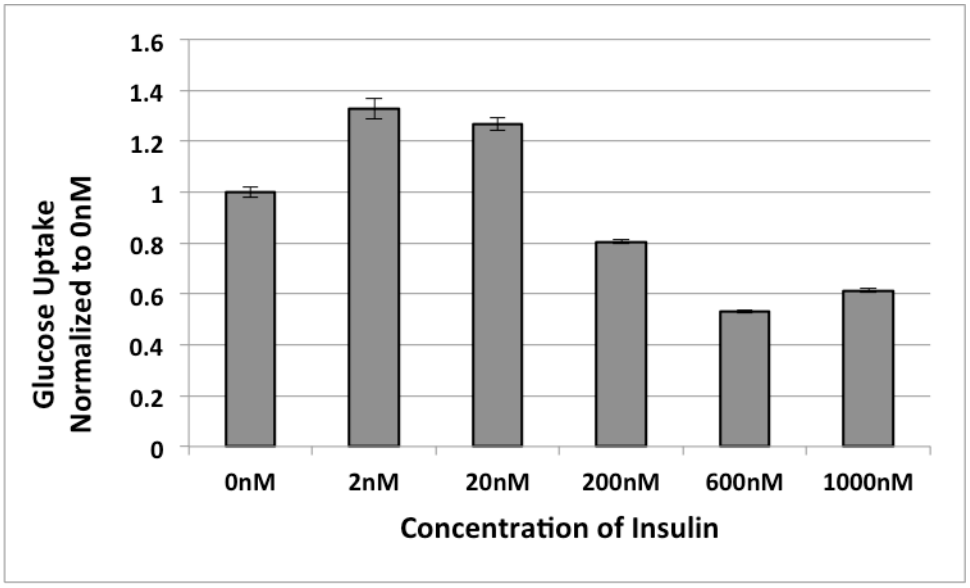

The data presented in **Figure 12** suggest that lower concentrations of insulin (i.e. 0 – 20nM) stimulate myotube glucose uptake, whereas higher concentrations of insulin (i.e. 200nM – 1000nM) resulted in what appeared to be active inhibition of glucose uptake over and above that seen control cultures (i.e. 0 nM insulin). In order to capture the maximum insulin stimulated glucose uptake response in C2C12 myotube cultures, while also accounting for the possibility that the concentration of insulin required to induce a maximum response may change depending on experimental conditions, all subsequent experiments in which the effects of selective cholesterol membrane modification on insulin stimulated glucose uptake were studied utilized an insulin dose response curve consisting of 0nM 10nM, 25nM, 50nM and 100nM insulin.

Using DHP Protein Expression to Spatially Resolve Sarcolemma/T-tubule Membranes in Differentiated C2C12 Myotubes

When C2C12 myotubes were immunohistochemically stained for DHP receptor protein followed by confocal microscopy analysis, DHP receptor staining allowed identification and spatial resolution of sarcolemma/T-tubule membranes within the myotubes (**Figure 13**). While DHP receptor labelling of sarcolemma/T-tubule membranes in C2C12 myotubes is not as robust as observed in adult skeletal muscle *in vivo* [117], the DHP receptor staining pattern observed in **Figure 13** clearly discloses specific regions of discrete membrane structures within the myotube histologically and spatially reminiscent of DHP receptor sarcolemma/T-tubule staining seen in whole myofibers *in vivo* [117].

Figure 13: Representative Fluorescent Confocal Micrographs of DHP Receptor Immunofluorescent Staining In Differentiated C2C12 Myotubes. **Panel A** illustrates DHP receptor protein staining in a single differentiated C2C12 myotube (Scale Bar – 10μm). **Panel B** illustrates a high powered image of the region indicated in Panel A demonstrating the spatial arrangement of the sarcolemma/T-tubule membrane system in which the DHP receptor resides (Scale Bar – 1μm).

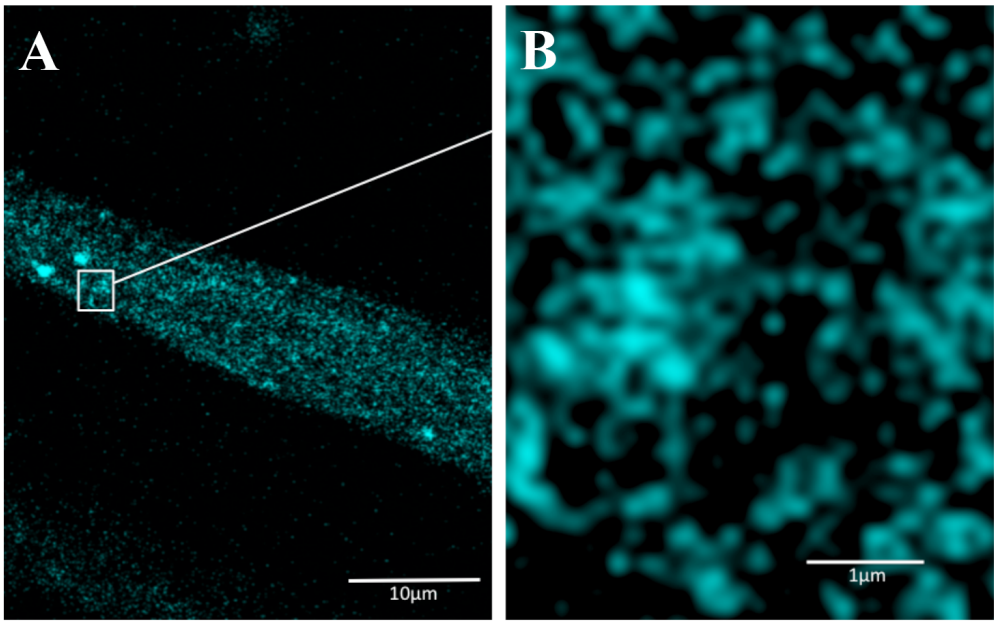

Determining Selective Membrane Cholesterol Enrichment Conditions Using a Fluorescent Cholesterol Analog

In order to achieve selective enrichment of internal and external C2C12 myotube membranes with cholesterol, the time course of cholesterol trafficking in myotubes cultured under specific exogenous cholesterol ***pulse-chase*** enrichment culture conditions was investigated. The time course of cholesterol trafficking between the tissue culture medium and its subsequent localization within specific myotube membrane structures was initially determined using a fluorescent analog of cholesterol, 23-(dipyrrometheneboron difluoride)-24-norcholesterol. While slightly larger than native cholesterol, this fluorescent analog when introduced to serum-containing tissue culture medium has previously been shown to be taken up and subsequently distributed within cell membranes in a similar manner to native cholesterol [145, 146]. Using defined pulse-chase labeling conditions and the fluorescent cholesterol analog, 23-(dipyrrometheneboron-difluoride)-24-norcholesterol in culture, followed by

morphological confocal microscopy analysis, we demonstrate that specific pulse-labeling conditions results in predictable, differential membrane cholesterol enrichment within differentiated C2C12 myotubes (**Figure 14)**. In addition, the fluorescent confocal microscopy images presented in **Figure 14 (Panels A, C, E, G and I)** were all acquired under identical imaging conditions allowing the relative amount of fluorescent cholesterol analog present within myotube membranes to be compared between different pulse-chase enrichment conditions.

Figure 14: Representative Fluorescent Confocal Micrographs Illustrating the Spatial Localization of the Fluorescent Cholesterol Analog (23-(Dipyrromethene**b**oron-Difluoride)-24-Norcholesterol) within Individual C2C12 Myotubes Induced by Specific Pulse-Chase Labeling Conditions. Images are single cross sections from within the myofiber to demonstrate the enrichment pattern throughout the myofiber following each pulse-chase labeling condition. **Panels A, C, E, G, I** and **K** are low power images, while **Panels B, D, F, H, J** and **L** are high power images of the specific regions indicated in their matching low power images. **Panels A** and **B** illustrate the enrichment of myotube membranes with fluorescent cholesterol analog induced by the 4hr Pulse labeling condition. **Panels C** and **D** illustrate the enrichment of myotube membranes with fluorescent cholesterol analog induced by the 4hr Pulse-4hr MβC labeling condition. **Panels E** and **F** illustrate the enrichment of myotube membranes with fluorescent cholesterol analog induced by the 4hr Pulse-16hr Chase labeling condition. **Panels G** and **H** illustrate the enrichment of myotube membranes with fluorescent cholesterol analog induced by the 4hr Pulse-16hr Chase-4hr Pulse labeling condition. **Panels I** and **J**

illustrate the enrichment of myotube membranes with fluorescent cholesterol analog induced by the 4hr Pulse-16hr Chase-4hr MβC labeling condition. **Panels A, C, E, G, I** and **K** were all acquired under identical imaging conditions allowing relative comparison of the amount of fluorescent cholesterol analog present within the membrane to be compared. **Panels B, D, F, H, I** and **J** were all acquired under identical imaging conditions and then processed using image deconvolution software. Dimensions are indicated on each image by scale bars.

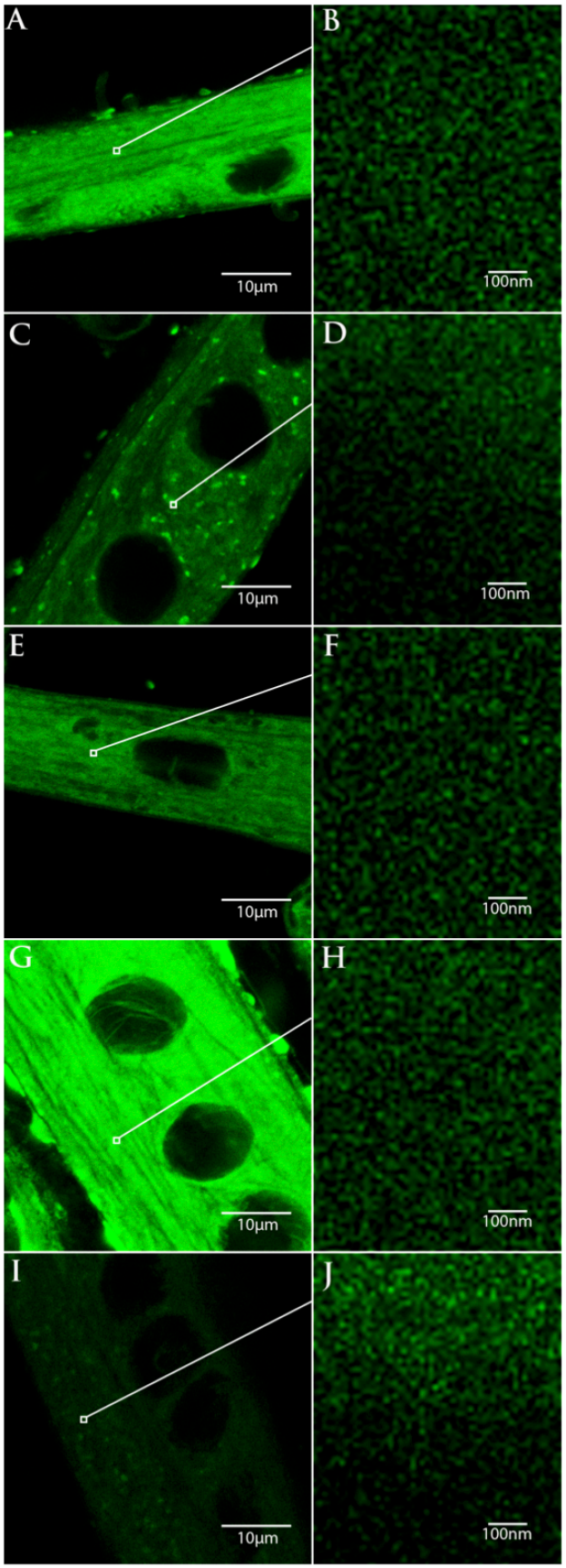
A
10µm
B
100nm
C
10µm
D
100nm
E
10µm
F
100nm
G
10µm
H
100nm
I
10µm
J
100nm

Identifying Which C2C12 Membranes Are Enriched under Different Pulse-Chase Labeling Conditions

In order to determine which membrane structures within C2C12 myotubes were enriched with the fluorescent cholesterol analog, confocal microscopy images of C2C12 myotube membranes labeled under defined pulse-chase labeling conditions were compared to similar confocal microscopy images of C2C12 myotubes immunohistochemically stained for membrane specific protein markers. The sarcolemma/T-tubule DHP receptor staining pattern observed in C2C12 myotubes (**Figure 13**) appears similar to the membrane labelling pattern observed in myotubes exposed to a 4hr Pulse label with the fluorescent cholesterol analog (**Figure 14, Panels A & B**), indicating that the 4hr Pulse label condition selectively enriched the sarcolemma/T-tubule membranes of C2C12 myotubes. When selective cholesterol enrichment conditions were combined with selective cholesterol depletion conditions using methyl-β-cyclcodextrin (MβC) to strip cholesterol from the membrane, various membrane components appear to be selectively enriched and/or depleted. For example, a 4h Pulse with the fluorescent cholesterol analog followed by a 4h exposure to MβC (**Figure 14, Panels C & D**) resulted in an overall reduction in the amount of fluorescent cholesterol analog remaining in the sarcolemma/T-tubule membrane compared to the 4hr Pulse condition alone, with exception of certain regions of the sarcolemma/T-tubule membrane which appeared to retain most if not all of the cholesterol accrued during the prior 4r Pulse labeling period. However, the fluorescent cholesterol analog labelling pattern observed after the 4hr Pulse-16hr Chase labeling (**Figure 14, Panels E & F**) appeared to be spatially different to that of the 4hr pulse labelling pattern, indicating that

the 4hr pulse-16hr chase labeling conditions did not selectively enrich the sarcolemma/T-tubule membranes but rather the internal sarcoplasmic reticulum (SR) membranes of the myotube. In addition, the 4h Pulse-16h Chase-4h Pulse labelling condition showed the greatest amount of relative cholesterol enrichment of any labeling condition, with enrichment of all myotube membranes being observed (**Figure 14, Panels G & H**). This result was in contrast to the 4h Pulse-16h Chase-4h MβC labeling condition (**Figure 14, Panels I & J**) which showed relatively lower levels of enrichment of the internal SR membrane compared to that observed in the 4hr Pulse-16hr Chase condition (**Figure 14, Panels E & F**), with exception of certain regions of the SR membrane which appeared to retain most if not all of the cholesterol accrued during the prior 4r Pulse-16hr Chase labeling period. The results observed from the 4hr Pulse-4hr MBC and 4hr Pulse-16hr Chase-4hr MBC labeling conditions may suggest the that the relatively large molecular size of the MβC molecule limits its access to all membrane components within the myotube resulting in it being unable to remove cholesterol from those physically inaccessible regions, or, that certain regions of the membrane are resistance to removal of cholesterol using MβC.

Enrichment of C2C12 Myotube Membranes with Native Cholesterol Using with a Water Soluble Cholesterol (WSC) Complex

Utilizing identical pulse–chase labeling conditions previously determined using the fluorescent cholesterol analog, C2C12 myotubes were enriched with native cholesterol using a cholesterol/methyl-β-cyclcodextrin (MβC) complex know as water-soluble cholesterol (WSC). Since the efficacy of the pulse-chase labeling protocols for

native cholesterol membrane enrichment in myotubes could not be monitored using confocal microscopy, the total membrane cholesterol content in each myotube culture after each defined pulse-chase labeling condition was monitored biochemically to ensure that cholesterol enrichment and/or depletion of myotubes with native cholesterol was in fact occurring (**Figure 15**). An initial ANOVA indicated greater total cholesterol content in C2C12 myotubes that had been enriched with WSC ($p < 0.01$). In addition, all cholesterol enrichment and/or depletion conditions were significantly ($p < 0.01$) different, with the exception of the 4h Pulse-4h MβC and 4h Pulse-16h Chase-4h MβC conditions which were not significantly different from each other (**Figure 15**).

Figure 15: The Effect of Defined Pulse-Chase Enrichment and Depletion Conditions on Total Native Cholesterol Content of C2C12 Myotubes. Total native cholesterol content in all cholesterol enrichment and/or depletion conditions was significantly (* = $p < 0.01$) different when compared to the control condition. Further, all conditions were found to be different from each other, with the exception of the 4h Pulse-4h MβC (green bar) condition and 4h Pulse-16h Chase-4h MβC (orange bar) condition which were not significantly different than each other. Individual myotube cultures were batch generated from different stock C2C12 myocyte cultures derived from a single parent C2C12 myocyte culture. The combined data presented below was obtained from a total of 368 individual myotube cultures generated in six individual 96 well plates. The N for each separate condition analyzed is as follows: Control N = 47, 4h Pulse N = 70, 4h Pulse-4h MβC N = 60, 4h Pulse-16h Chase N = 63, 4h Pulse-16h Chase-4h Pulse N = 60, 4h Pulse-16h Chase-4h MβC N = 68. Total cholesterol content per myotube culture was

initially expressed as (ng) of total cholesterol/(ug) of total protein and then normalized to the mean control value which was expressed as a value of one. Normalized values for total cholesterol for each condition were plotted as the mean +/- standard error.

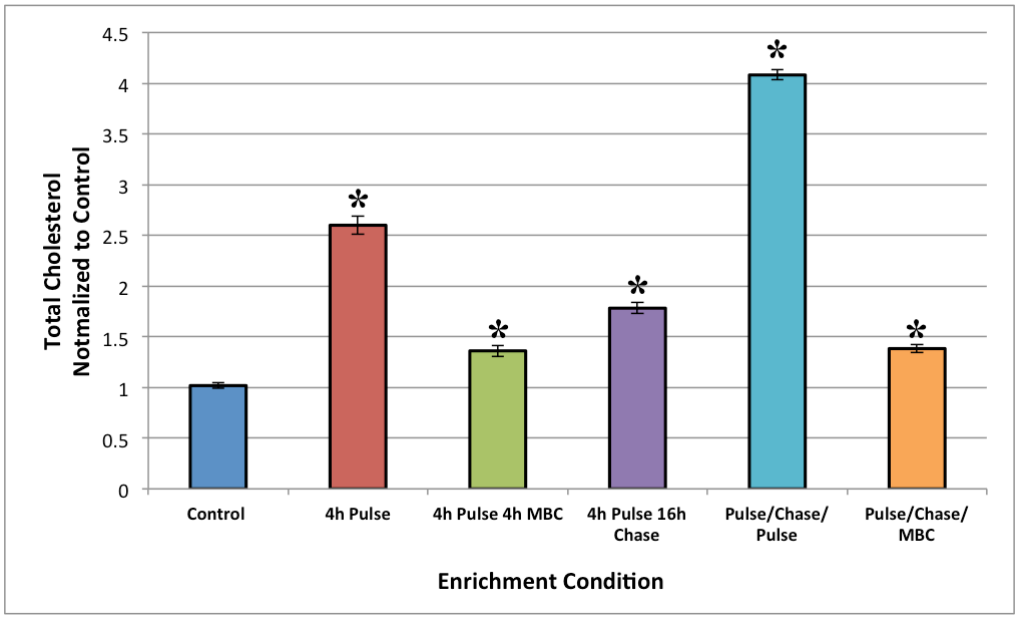

In conjunction with the spatial membrane localization information obtained from confocal microscopy analysis of C2C12 myotubes labeled with fluorescent cholesterol analog, these biochemically derived results demonstrate that using defined sequential combinations of exposure to WSC and/or MβC allow the native cholesterol content of specific membranes within C2C12 myotubes to be manipulated in a mechanistic and predictable fashion.

The Effects of Cholesterol on Basal Glucose Uptake in C2C12 Myotubes

While a non-significant ($p = 0.086$) decrease in non-insulin stimulated basal glucose uptake by myotubes was observed following native cholesterol enrichment of the sarcolemma/T-tubule membrane using the 4h Pulse labeling condition (**Figure 16)**, an

initial One-Way ANOVA did not reveal any significant effects on basal glucose uptake associated with any of the various native cholesterol enrichment or depletion conditions.

Figure 16. The Effect of Membrane Cholesterol Enrichment and Depletion on Non-Insulin Stimulated, Basal Glucose Uptake in C2C12 Myotubes. An initial one-way ANOVA revealed no overall effect ($p < 0.071$) of native cholesterol enrichment and/or depletion on basal, non-insulin stimulated glucose uptake. Individual myotube cultures were batch generated from different stock C2C12 myocyte cultures derived from a single parent C2C12 myocyte culture. The combined data presented below was obtained from a total of 238 individual myotube cultures grown in 96 well plates generated on four separate occasions. The N for each separate condition analyzed is as follows: Control N = 84, 4h Pulse N = 42, 4h Pulse-4h MβC N = 42, 4h Pulse-16h Chase N = 42, 4h Pulse-16h Chase-4h Pulse N = 14, 4h Pulse-16h Chase-4h MβC N = 14. Basal glucose uptake per myotube culture was expressed initially as fluorescence units (FU)/(ug) of total protein and then normalized to the mean control value which was expressed as a value of one. Normalized values for basal glucose uptake for each condition were plotted as the mean +/- standard error.

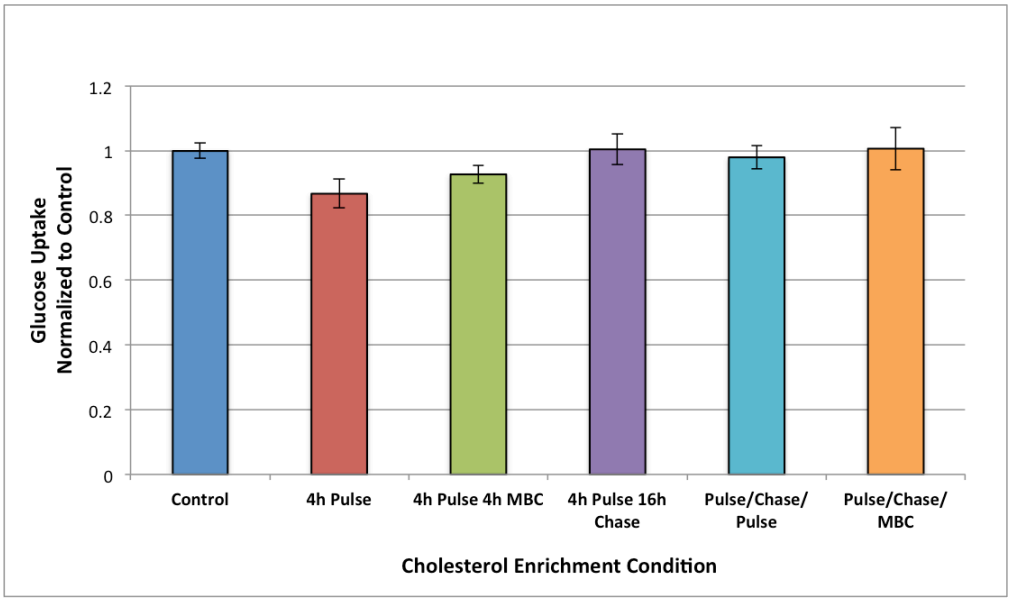

These data suggest that constitutive myotube basal glucose uptake mediated via GLUT1 transporters located in the sarcolemma/T-tubule membranes of myotubes remains unaffected by short-term enrichment or depletion of myotube membranes with cholesterol. However, the non-significant decrease observed in basal glucose uptake observed after sarcolemma/T-tubule cholesterol enrichment (i.e. 4hr Pulse) is intriguing. These preliminary data indicate that while basal, GLUT1 mediated glucose uptake is not directly impacted by the short-term changes in membrane cholesterol content described in this study, it is possible that basal non-insulin stimulated, GLUT1-mediated glucose uptake pathways may be altered under chronic hypercholesteremic conditions.

The Effects of Cholesterol Enrichment and/or Depletion Conditions on Insulin-Stimulated Glucose Uptake in C2C12 Myotubes

The effects on insulin stimulated glucose uptake of five separate enrichment/depletion conditions were compared to control conditions using a 5X6

ANOVA **(Table 1).** This analysis indicated that the Control, the 4hr Pulse and the 4hr Pulse-4hr MBC conditions were all significantly different from each other at all insulin concentrations tested (**Figure 17, Table 1**). Importantly, the significant inhibition of insulin stimulated glucose uptake observed after enrichment of the sarcolemma/T-tubule membrane with cholesterol using the 4hr Pulse condition was partially rescued in 4hr Pulse-4hr MBC condition when cholesterol was subsequently removed by stripping with MBC (**Figure 17**).

Figure 17. The Effect of Membrane Cholesterol Enrichment and/or Depletion on Insulin Stimulated Glucose Uptake in C2C12 Myotubes. Results of a 5X6-way ANOVA analysis (**Table 1**) indicated that insulin stimulated glucose uptake in the Control, the 4hr Pulse labeling condition, and the 4hr Pulse-4hr MBC labeling condition, labeling conditions were all significantly ($p < 0.01$) different from each other at all insulin concentrations tested. In addition, while the 4hr Pulse-16hr Chase labeling condition was not significantly different overall from the control condition, the concentration of insulin required to induce the maximal insulin stimulated glucose uptake response was significantly ($p < 0.01$) increased from 10nM to 50nM insulin. Individual myotube cultures were batch generated from different stock C2C12 myocyte cultures derived from a single parent C2C12 myocyte culture. The combined data presented below was obtained from a total of 882 individual myotube cultures grown in 96-well plates generated on 3 separate occasions. The N for each separate condition analyzed is as follows: Control N = 252 (0nM N = 84, for all other insulin concentrations N = 42) 4h

Pulse N = 210 (42 data points per insulin concentration), 4h Pulse-4h MβC N = 210 (42 data points per insulin concentration), 4h Pulse-16h Chase N = 210 (42 data points per insulin concentration). Glucose uptake per myotube culture was initially expressed as fluorescence units (FU)/(ug) of total protein and then normalized to the mean control value which was expressed as a value of one. Normalized values for glucose uptake for each condition and insulin concentration were plotted as the mean +/- standard error.

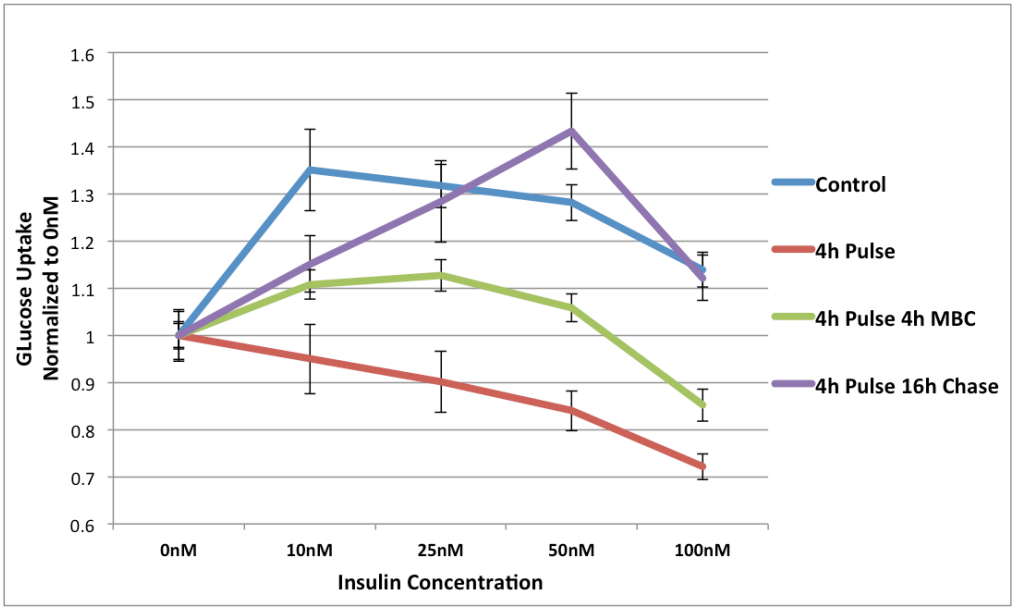

These data provide direct experimental evidence that increased membrane cholesterol content is causally related to the disruption of insulin stimulated glucose uptake in a highly differentiated *in vitro* model of skeletal myofibers. In addition, while overall insulin stimulated glucose uptake in the 4hr Pulse-16hr Chase enrichment condition was not significantly different from control levels, maximal glucose uptake occurred at approximately five times the insulin concentration required under control conditions (i.e. 50nM insulin as compared to 10nM insulin) (**Figure 17, Table 1**). These data provide direct experimental evidence that selective cholesterol enrichment of myotube sarcoplasmic reticulum (SR) membranes induces insulin insensitivity similar to

that seen in skeletal myofibers of individuals suffering from a range of pathological conditions, such as obesity, hypercholesterolemia and Type 2 diabetes.

The effects of selectively enriching both the sarcolemma/T-tubule and SR membranes with cholesterol (4hr Pulse-16hr Chase-4hr Pulse), or, selectively enriching the SR membrane while subsequently depleting the sarcolemma/T-tubule membrane (4hr Pulse-16hr Chase-4hr MβC) on insulin stimulated glucose uptake were also compared to that observed under control conditions (**Figure 18**).

Figure 18. The Effect of Sequential Cholesterol Enrichment and Depletion on Insulin Stimulated Glucose Uptake in C2C12 Myotubes. Results of a 5X6-way ANOVA analysis (**Table 1**) indicated that insulin stimulated glucose uptake induced by both the 4hr Pulse-16hr Chase-4hr Pulse labeling condition and the 4hr Pulse-16hr Chase-4hr MβC labeling condition were significantly different than that observed in the control condition ($p < 0.01$). Individual myotube cultures were batch generated from different stock C2C12 myocyte cultures derived from a single parent C2C12 myocyte culture. The combined data presented below was obtained from a total of 321 individual myotube cultures generated in 96 well plates on three separate occasions. The N for each separate condition analyzed is as follows: Control N = 252, 4hr Pulse-16hr Chase-4hr Pulse N = 69 (14 data points for all insulin concentrations except at 50nM insulin, with 13 data points) and 4hr Pulse-16hr Chase-4hr MβC N = 69 (14 data points for each insulin concentration except for 0nM insulin with 13 data points). Glucose uptake per myotube culture was initially expressed as fluorescence units (FU)/(ug) of total protein and then normalized to the

mean control value which was expressed as a value of one. Normalized values for glucose uptake for each condition were plotted as the mean +/- standard error.

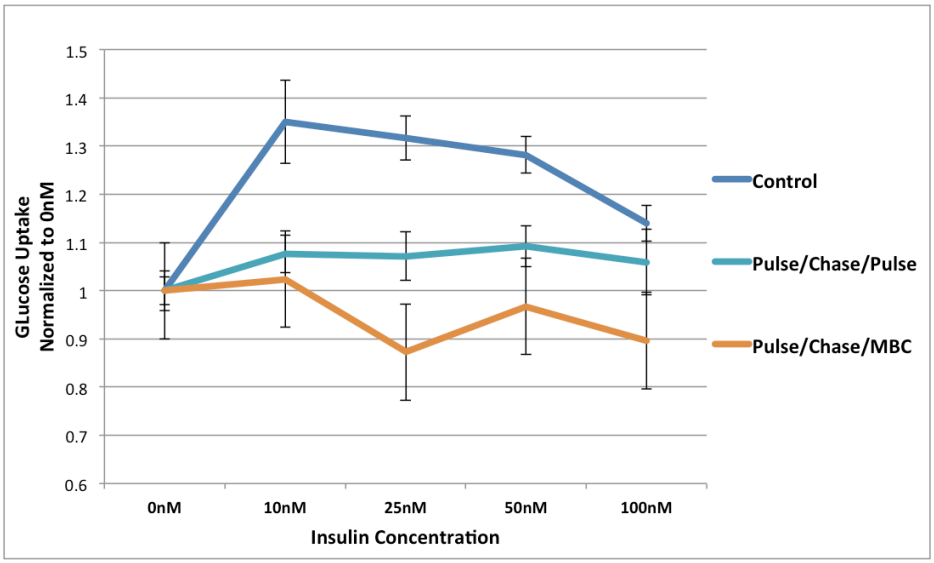

Both the 4hr Pulse-16hr Chase-4hr MβC and the 4hr Pulse-16hr Chase-4hr Pulse labeling conditions were significantly ($p < 0.01$) different from the control (**Figure 13, Table 1**), however not different from each other. Further, the 4hr Pulse-16hr Chase-4hr MβC labeling condition was different from the control condition at every insulin concentration tested ($p < 0.05$), whereas the 4hr Pulse-16hr Chase-4hr Pulse labeling condition was not different from the 4hr Pulse-16hr Chase-4hr MβC labeling condition at all insulin concentrations tested.

Table 1 Results from a 5X6 ANOVA Analysis on the Effects of Different Membrane Cholesterol Enrichment and/or Depletion Conditions on Insulin Stimulated Glucose Uptake. A 5x6-way ANOVA revealed that insulin stimulated glucose uptake in the 4h

Pulse, 4h Pulse-4h MβC, 4h Pulse-16h Chase-4hr Pulse and 4hr Pulse-16hr Chase-4hr MβC labeling conditions were all different from control conditions ($p < 0.01$). One-way ANOVAs within each enrichment conditions revealed significantly increased insulin stimulated glucose uptake responses overall in the control ($p < 0.01$), 4hr Pulse ($p < 0.01$), 4hr Pulse-16h Chase ($p < 0.01$), and 4hr Pulse-4hr MβC conditions ($p < 0.05$). Significance differences in glucose uptake between cholesterol enrichment/depletion conditions, within individual conditions across multiple insulin concentrations, or between conditions at the same insulin concentration are indicated in Table 1. (***** = different from control at $p < 0.05$, # = different from 0nM at $p < 0.05$, † = different from control at respective insulin concentration at $p < 0.05$).

	Membranes Enriched		**Insulin Concentration**				
Enrichment Condition	**SL**	**SR**	**0nM**	**10nM**	**25nM**	**50nM**	**100nM**
Control	NA	NA	1 ±.086 N=84	**1.35**# ±.086 N=42	**1.31**# ±.046 N=42	**1.28**# ±.038 N=42	1.14 ±.037 N=42
4h Pulse*	**+**	No Change	1 ±.055 N=42	**0.95**† ±.074 N=42	**0.9**† ±.065 N=42	**0.84**† ±.043 N=42	**0.72**#† ±.028 N=42
4h Pulse 4h MβC*	**+/-**	No Change	1 ±.026 N=42	1.11 ±.031 N=42	**1.13**# ±.033 N=42	**1.06**† ±.03 N=42	**0.85**#† ±.034 N=42
4h Pulse 16h Chase	No Change	**+**	1 ±.051 N=42	1.15 ±.06 N=42	**1.28**# ±.086 N=42	**1.43**# ±.081 N=42	1.12 ±.048 N=42
4h Pulse 16h Chase 4h Pulse*	**+**	**+**	1 ±.041 N=13	1.08 ±.039 N=14	1.07 ±.05 N=14	1.09 ±.043 N=14	1.06 ±.068 N=14
4h Pulse 16h Chase 4h MβC*	**-**	**+**	1 ±.029 N=14	**1.02**@ ±.053 N=14	**0.87**† ±.033 N=13	**0.97**† ±.032 N=14	**0.9**† ±.042 N=14

Chapter 5 – Discussion

Previous studies have demonstrated that there is a relationship between various environmental conditions, such as a high fat diet, physical inactivity and aging, and the development of a range of chronic pathological conditions such as obesity, hypercholesterolemia, metabolic syndrome, aged-related sarcopenia and Type 2 diabetes. Two common characteristics associated with these chronic pathological conditions are evidence of lipid metabolism dysregulation and a range of structural and metabolic adaptations observed in skeletal muscle prior to the onset or during the course of these diseases.

The overall purpose of this study was to investigate the potential causal relationship(s) between muscle membrane cholesterol content (previously shown to be impacted by a high fat diet, obesity, hypercholesterolemia and physical inactivity) and disrupted insulin receptor signaling and insulin stimulated glucose uptake in skeletal myofibers. In order to investigate this relationship, we first developed and characterized a well-defined *in vitro* tissue culture model consisting of highly differentiated C2C12 myotubes that exhibit both the morphological and biochemical markers of skeletal myofibers *in vivo* (**Figures 7, 8 and 9**). Access to this controlled and highly reproducible *in vitro* model, coupled with the development of novel approaches for selectively manipulating cholesterol content of specific myotube membranes *in vitro*, has allowed the mechanistic investigation of how increased membrane cholesterol content and its cellular location might be responsible for disrupted insulin signaling and insulin stimulated glucose uptake observed in skeletal myofibers *in vivo*.

Previous research has suggested that alterations in myofiber membrane cholesterol content are correlated with the onset and development of insulin insentivitiy and glucose tolerance *in vivo* [1]. In addition, a number of previous tissue culture studies have provided data supporting the concept that changing total membrane cholesterol content in cultured adipocytes modulates insulin signaling and insulin mediated glucose uptake in these cells [13, 18]. Building on these previous observations, the data presented in our current study provides direct experimental evidence that increased membrane cholesterol content, as well as the specific membrane component in which it is increased, is causally linked to disruptions in insulin signaling and insulin stimulated glucose uptake by skeletal muscle-derived myotubes in culture. As such, our results provide a mechanistic explanation of how increases in cholesterol membrane content can disrupt the underlying cellular mechanisms involved in insulin receptor signaling, insulin stimulated glucose uptake and GLUT4 translocation in skeletal muscle. These data also provide a mechanistic model capable of explaining the underlying relationship between conditions exhibiting abnormal regulation of lipid metabolism and increased circulating cholesterol levels, such as obesity and hypercholesterolemia, and the onset of insulin insensitivity and glucose tolerance in conditions such as metabolic syndrome and Type 2 diabetes.

Development of a Well-Defined, Highly Differentiated C2C12 Myotube Model

The present study set out to a develop a highly controlled and reproducible *in vitro* model of skeletal myofibers consisting of highly differentiated C2C12 myotubes exhibiting the morphological and biochemical markers of terminally differentiated

skeletal myofibers *in vivo*. This model was then used to investigate the effects of selective enrichment or depletion of membrane cholesterol upon insulin signaling and insulin stimulated glucose uptake. While C2C12 myotube cultures are a well-recognized *in vitro* model in which to study physiologically relevant events that occur in skeletal myofibers *in vivo* [12, 39, 43, 44, 47, 49, 50, 139], it is not always clear from the literature how these myotube cultures were generated experimentally, whether or not these myotubes exhibited the morphological and biochemical markers associated with terminal differentiation of skeletal myofibers *in vivo*, or, if myotube cultures generated over time remained consistent in their response to experimental stimuli.

The C2C12 myotube model reported here addressed many of these issues by controlling for tissue culture conditions and growth parameters already known to introduce variability into tissue culture models including: creating stock C2C12 myocyte cultures with a known passage number from which all subsequent myotube cultures were generated; utilizing media preparations that mimic physiologically relevant conditions *in vivo*; utilizing defined myocyte seeding densities and culture periods to ensure uniform myocyte growth and myotube differentiation in culture over time; and confirming myotube differentiation by both morphological criteria and biochemical expression of skeletal muscle terminal differentiation markers. In addition, to ensure maximum response to insulin stimulation, C2C12 myotube cultures were cultured and differentiated in tissue culture medium containing defined amounts of glucose mimicking physiological glucose concentrations *in vivo*. By defining and controlling such tissue culture parameters, we have developed a highly reproducible C2C12 myotube tissue culture model of skeletal myofibers *in vivo* that exhibit a high degree of terminal differentiation

as demonstrated by the temporally predictable generation of large, three dimensional, multi-nucleated fusiform myotubes that express both myosin heavy chain (MHC) and dihydropyridine (DHP) receptor (**Figure 8 and 9**), as well as a spatially organized, intra-myofiber T-tubule membrane system (**Figure 13)**.

Further, the use of 2-NBDG, a fluorescent analog of glucose, allowed fluorescent microscopy visualization of both basal and insulin stimulated glucose uptake at the individual cellular level. Direct microscopic analysis provided visual evidence that glucose uptake in these cultures was associated overwhelming with glucose uptake by myotubes rather than by any undifferentiated myocytes remaining in the culture (**Figure 10**). In addition, confirmation that the vast majority of the 2-NBDG was accounted for by myotube uptake allowed this *in vitro* model to be configured into a 96-well plate format, high-throughput assay designed to study the effects of membrane cholesterol on insulin signaling and insulin stimulated glucose uptake.

High Glucose and Insulin-Induced Insulin Resistance in Cultured Cells

Some authors have found little to no insulin-stimulated glucose uptake response in C2C12 myotube cultures [12, 38, 44, 50], while others demonstrate clear experimental responses to insulin [43]. Adding to this ambiguity, some researchers have shown that tissue culture under high glucose conditions induces insulin resistance and that exposure of these cells to low glucose conditions prior to insulin stimulation rescues the insulin response [31, 43]. For example, Nedechi et al reported a 19% increase in insulin-stimulated glucose uptake in C2C12 myotubes cultured in high glucose conditions as compared to a 42% increase in insulin-stimulated glucose uptake in myotubes grown in

high glucose and then exposed to low glucose media. Further, it was reported that high glucose media inhibited the insulin response after only 5 minutes of exposure [43].

Leontieva et al found similar results demonstrating high glucose-induced insulin resistance using RPE cells [31]. To gain insight into the mechanism by which this occurs, these researchers used rapamycin to inhibit mTOR activation in the presence of high glucose-induced insulin resistance resulting in the restoration of insulin stimulated glucose uptake in the presence of high glucose. Leontieva et al also used an SK6 inhibitor to gain further insight into the cellular mechanisms responsible for high glucose-induced insulin resistance. SK6, a serine/threonine kinase, is an inhibitor of insulin receptor autophosphorylation, while itself inhibited by mTOR. Leontieva et al found that SK6 inhibitors restored insulin sensitivity in the presence of high glucose-induced mTOR over activation, demonstrating the mechanism of a negative feedback loop that induces insulin resistance (displayed in **Figure 3**) [31].

This negative feedback loop was further explored using insulin to induce insulin resistance. Leontieva et al found that over stimulation with insulin using 1ug/mL (175nM) overnight inhibited any further stimulation as measured by Akt activation in RPE cells [31]. Although this effect was observed in RPE cells and not differentiated skeletal muscle myotubes, Leontieva et al demonstrated many common characteristics between RPE cells and C2C12 myotubes in regards to insulin stimulation and glucose metabolism, and therefore it could be argued the same negative feedback mechanisms may exist in C2C12 myotubes in vitro and by extension skeletal muscle myofibers *in vivo*.

While we did not detect any significant effect of culture in low glucose conditions on insulin stimulated glucose uptake (**Figure 11**), we did however observe a small increase (approximately 20%) in the sensitivity of differentiated C2C12 myotubes to insulin. Based on the possibility that C2C12 myotubes may develop high glucose-induced insulin insentivitiy, C2C12 myotube cultures utilized in this study were maintained in low glucose medium during the final two days of differentiation in order to ensure maximal sensitivity to subsequent insulin stimulation.

Glucose Uptake in Response to Various Insulin Concentrations

Review of the literature describing the use of C2C12 myotube cultures as a model in which to study insulin receptor signaling and insulin stimulated glucose uptake provides contradictory information on both the degree of C2C12 myotube sensitivity to insulin and the optimal amount of insulin required to induce maximal insulin stimulated glucose uptake. While it is possible that some of this ambiguity may have arisen because the myotubes utilized in previous studies were generated under different culture conditions or exhibited varied stages of differentiation, it is also possible that other cellular related mechanisms may be responsible.

In the current study, preliminary pilot experiments were carried out to investigate the appropriate concentration of insulin to induce maximal insulin stimulated glucose uptake in differentiated C2C12 myotubes. Initially, concentrations of 2nM, 20nM, 200nM, 600nM and 1000nM of insulin were used to induce insulin stimulated glucose uptake in differentiated C2C12 myotube cultures (**Figure 12)**. This broad dose-response range was utilized to capture the most commonly used insulin concentration (i.e. 100nM)

previously reported in the literature to induce insulin stimulated glucose uptake in C2C12 myotubes. In C2C12 myotubes cultured under controlled differentiation conditions, the maximal insulin-stimulated glucose uptake response (approximately 35% above basal glucose uptake levels) was observed somewhere below 20nM insulin, whereas insulin concentrations above 200nM resulted in inhibition of glucose uptake (**Figure 12**). Based on these initial results, all subsequent experiments investigating the effects of membrane cholesterol manipulation on insulin stimulated glucose uptake (**Figures 17 and 18**) utilized a range of insulin concentrations spanning the region of the insulin dose-response curve corresponding to the predicted maximal insulin stimulated glucose uptake response (i.e. 0nM, 10nM, 25nM, 50nM and 100nM insulin).

While there are many examples in the research literature of repeated agonist-mediated receptor activation leading to receptor inactivation or down-regulation of receptor protein expression, including the development of insulin insensitivity in hyperinsulinemic patients [148], the majority of such negative feedback loops on cell signaling events occur after prolonged, chronic elevations in agonist concentration. However, the inhibition of insulin stimulated glucose uptake in C2C12 myotubes observed with insulin concentrations above 100nM (**Figures 12, 17 and 18**) occurred within 30 minutes of exposure to insulin, rather than after a prolonged period of time.

Our experimental observations indicate that increased insulin concentrations (i.e. above 100nM insulin) rapidly induce inhibition of insulin stimulated glucose uptake in control C2C12 myotubes. Based on the time course of this inhibitory effect, these data suggest that the acute inhibition (i.e. within 30 min) in insulin stimulated glucose uptake is mediated by either inactivation of existing insulin receptors located in the external

sarcolemma/T-tubule membranes of the myotube, or, inhibition of subsequent intracellular elements of the insulin signaling pathway, while the rapid onset (i.e. 30 minutes) of this effect makes it highly unlikely that inhibition is due to receptor protein downregulation.

While the exact cellular mechanism(s) responsible for the acute inhibitory effect of large insulin concentrations on insulin stimulated glucose uptake in C2C12 myotubes remain unknown, one possible explanation comes from previous studies which demonstrated that over-activation of the insulin receptor rapidly induced a negative feedback loop on insulin receptor signaling through inhibition of the Akt-mTOR portion of the signaling pathway. Although these observations were made in cultured RPE cells, since the insulin receptor mediated Akt-mTOR signaling pathway is highly conserved across multiple cells types, our experimental data supports the contention that a similar negative feedback loop may operate in both C2C12 myotubes and skeletal muscle *in vivo*.

Interestingly, previous studies utilizing C2C12 myotubes in which to study insulin receptor signaling and insulin stimulated glucose uptake mechanisms routinely employ only a single insulin stimulation concentration of 100nM insulin with stimulation periods ranging from 20min to 16hr [12, 38, 43, 44, 50]. Using these experimental conditions, a number of studies have reported little or no response to insulin stimulation [12, 44, 50, 139]. While it is possible that the C2C12 myotubes utilized in these previous studies may not have been fully differentiated (e.g. leading to under-developed insulin receptor signaling pathways), our experimental data suggests that it may be more appropriate to employ a range of lower insulin concentrations in order to capture the maximal insulin

stimulated glucose uptake response and to prevention potential insulin receptor inactivation.

Pulse-Chase Labeling of Myotube Membranes Using a Fluorescent Cholesterol Analog

Pulse-chase labeling protocols designed to enrich specific C2C12 myotube membrane components were experimentally defined utilizing a fluorescent cholesterol analog introduced to the tissue culture medium. This approach allowed subsequent visualization and spatial resolution of the intracellular location of the fluorescent cholesterol analog within the membranes of differentiated C2C12 myotubes using confocal microscopy. Analysis of confocal images collected from each defined pulse-chase labeling condition demonstrated differential cholesterol enrichment and/or depletion of specific membranes within the myotube (**Figure 14**). By comparing confocal images of C2C12 myotubes immunostained for the DHP receptor, a specific spatial marker of sarcolemma/T-tubule membranes (**Figure 13**), the membrane location of the fluorescent cholesterol analog induced by each defined pulse-chase labeling condition could be deduced.

The spatial organization of the sarcolemma/T-tubule myotube membrane disclosed using DHP receptor immunostaining (**Figure 13**) visually resembles a "mesh-like" staining pattern with examples of "circular" membrane components. A similar, but much more morphologically distinct, circular "mesh-like" staining pattern organized around individual myofibrils has been previously described for the DHP receptor staining pattern in the sarcolemma/T-tubule system of skeletal myofibers *in vivo* [117]. Interestingly, the circular membrane components observed in C2C12 myotubes could

easily be imagined to be wrapped around the nascent myofibrils observed within differentiated C2C12 myotubes stained for MHC protein (**Figure 8**). A similar spatially organized, circular "mesh-like" fluorescent cholesterol analog labeling pattern was also observed in in confocal images of differentiated myotubes collected from the 4hr Pulse labeling condition (**Figure 14, Panels A and B**). Considering the requirement for the fluorescent cholesterol analog to first be incorporated into the external sarcolemma membrane of the myotube, the relatively short exposure time to the fluorescent cholesterol analog (i.e. 4hr), and the spatial similarities between the DHP receptor staining (**Figure 13**) and the fluorescent cholesterol analog membrane labeling patterns observed (**Figure 14, Panels A and B**), our results are highly consistent with the conclusion that the 4hr Pulse labeling condition results in selective cholesterol enrichment of the sarcolemma/T-tubule membranes of differentiated C2C12 myotubes. This conclusion was further supported by the fluorescent cholesterol analog membrane labeling pattern observed in the 4h Pulse-4h MβC labeling condition (**Figure 14, Panels C and D**) which clearly demonstrates the removal of the fluorescent cholesterol analog from the membranes in which it was initially deposited by a prior 4hr Pulse. Since there is no experimental evidence that MβC is either incorporated into cell membranes or actively transported into cells during 4hr of exposure, these data suggest that for MβC to have removed the fluorescent cholesterol analog previously deposited by the 4hr Pulse, MβC could only have removed fluorescent cholesterol analog from membranes in direct contact with the external tissue culture medium (i.e. the sarcolemma/T-tubule membrane).

When the fluorescent cholesterol analog membrane labeling induced by the 4hr Pulse-16hr Chase labeling condition (**Figure 14, Panels E and F**) was analyzed, subtle differences in the spatial labeling pattern were observed compared to the sarcolemma/T-tubule labeling observed in the 4hr Pulse labeling condition (**Figure 14, Panels A and B**), including a lack of complete circular "mesh-like" membrane labeling. These differences suggested that internal sarcoplasmic reticulum (SR) membranes rather than sarcolemma/T-tubule membranes had been selectively enriched in the 4hr Pulse-16hr Chase labeling condition. However, in the absence of comparative images of sarcoplasmic reticulum (SR) membranes identified using a protein marker similar to sarcolemma/T-tubule membrane DHP receptor staining, definitive identification of the SR membrane component in this study was impossible. However, since the high power confocal images of C2C12 myotubes labeled with fluorescent cholesterol analog (**Figure 14, Panels A, C, E, G and I**) were all collected under identical imaging conditions, evidence to support our conclusion that the 4hr Pulse-16hr Chase labeling condition selectively enriched the SR membrane with cholesterol, rather than the sarcolemma/T-tubule membrane, comes from visually comparison of the overall fluorescent labeling intensity observed in the 4hr Pulse labeling condition. The fluorescent intensity associated with sarcolemma/T-tubule membrane labeling observed in the 4hr Pulse labeling condition is greater than observed in the 4hr Pulse-16hr Chase labeling condition. These results indicate that either the fluorescent cholesterol analog initially deposited into the sarcolemma/T-tubule membranes during the 4hr Pulse had been redistributed into additional membrane components during the subsequent 16hr Chase (thereby reducing the fluorescent signal per unit volume of membrane in the image), or,

alternatively the fluorescent cholesterol analog may have been metabolized within the myotube during the 16hr Chase. Since the fluorescent cholesterol analog utilized in this study has been used to track cell lineage in Zebrafish from the embryo stage through the adult stage [149], it seems unlikely that the reduction in fluorescent signal observed in the 4hr Pulse-16hr Chase labeling condition as compared to the 4hr Pulse labeling condition would be as a result of the label being metabolized during the 16hr Chase period. As such, the most logical explanation for the reduction in fluorescent signal observed in the 4hr Pulse-16hr Chase is that the label had been distributed into additional membrane components within the myotube (i.e. SR membrane).

In contrast, the 4hr Pulse-16 Chase-4h Pulse labeling condition (**Figure 14, Panels G and H**) resulted in much greater labeling of both sarcolemma/T-tubule and SR membrane components in the C2C12 myotubes compared to all other labeling conditions (**Figure 14, Panels A, C, E, G and I**). These results provide additional supporting evidence that the 4hr Pulse-16hr Chase labeling condition selectively enriched the SR membrane rather than the sarcolemma/T-tubule membrane, as it would be predicted that the use of two sequential exposures to the fluorescent cholesterol analog separated by a 16hr Chase period would firstly enrich the SR membrane and then for a second time enrich the sarcolemma/T-tubule membrane. In addition, the membrane labeling pattern observed in the 4hr Pulse-16 Chase-4h Pulse (**Figure 14, Panels G and H**) appears to resemble a combination of both membrane labeling patterns seen in the 4hr Pulse (**Figure 14, Panels A and B**) and 4hr Pulse-16hr Chase (**Figure 14, Panels E and F**) labeling conditions, including the complete circular “mesh-like” membrane labeling seen only in the 4hr Pulse labeling condition.

Similarly, if the overall model of how cholesterol is enriched, depleted and trafficked within myotube membranes using the pulse-chase labeling techniques developed in this study is correct, then the 4hr Pulse-16hr Chase-4hr MBC labeling condition (**Figure 14, Panels I and J**) would be predicted not only to result in SR membrane enrichment but also the removal of any fluorescent cholesterol analog remaining in the sarcolemma/T-tubule from the initial 4hr Pulse. Confocal images collected from C2C12 myotubes labeled with the fluorescent cholesterol analog using the 4hr Pulse-16hr Chase-4hr MBC labeling condition confirmed that prediction.

Confocal analysis of C2C12 myotubes labeled with fluorescent cholesterol analog and then depleted using MβC revealed the existence of certain membrane regions within the myotubes which appear resistance to cholesterol depletion using MβC (**Figure 14, Panels C, D, I and J**). The molecular weight of MβC is approximately 23 times larger than either native cholesterol or the fluorescent cholesterol analog. Because the T-tubule membranes are contiguous invaginations of the sarcolemma membrane extending into the central region of the myotube, MβC may not have had physical access to the entire sarcolemma/T-tubule membrane surface leading to certain regions of the sarcolemma/T-tubule membrane that still contain regions that appear to be enriched with fluorescent cholesterol analog. A second possibility is that these remaining enriched membrane regions represent clusters of lipid rafts or caveolae in the sarcolemma/T-tubule membrane that are resistant to extraction of cholesterol via MβC, or, alternatively endocytic vesicles derived from labeled sarcolemma/T-tubule membrane components that have been internalized into the C2C12 myotube.

Pulse-Chase Labeling using Native Cholesterol Followed by Total Cholesterol Measurements

While the spatial localization of native cholesterol delivered to C2C12 myotubes using Water Soluble Cholesterol (WSC) cannot be visually confirmed using confocal microscopy, analysis of the total cholesterol content in C2C12 myotubes confirm that the overall amount of native cholesterol delivered to the myotubes using identical pulse-chase labeling (**Figure 15**) parallels that observed in the case of the fluorescent cholesterol analog (**Figure 14**). For example, 4hr Pulse labeling with WSC resulted in approximately a 2.5-fold increase in total myotube native cholesterol content, while 4hr Pulse-4h MβC labelling resulted in a 42% increase in total myotube native cholesterol content (**Figure 15**). These quantitative results are consistent with the relative amount of fluorescent cholesterol analog enrichment directly observed confocal microscopy under these labeling conditions using (**Figure 14, Panels A and C**). Similarly, 4hr Pulse-16hr Chase-4hr Pulse labeling with WSC resulted in approximately a 4-fold increase in total myotube native cholesterol content, a result consistent with the relative amount of fluorescent cholesterol analog enrichment directly observed using confocal microscopy in this labeling condition (**Figure 14, Panel G**).

In addition, whereas 4hr Pulse labeling with WSC resulted in a 2.5 fold increase in total membrane cholesterol, the 4hr Pulse-16hr Chase labeling with WSC resulted in approximately a 1.75-fold increase in total myotube native cholesterol content (**Figure 15**) suggesting that a portion of the native cholesterol delivered to the sarcolemma/T-tubule system in the initial 4hr Pulse may have been metabolized by the myotubes. Alternatively, the difference observed between these two conditions may be as a result of

small amounts of residual MβC (derived from the WSC complex original present in the initial 4hr Pulse reagent) removing native cholesterol from the sarcolemma/T-tubule membrane.

Taken together, the spatial membrane localization information obtained from confocal microscopy analysis of myotubes labeled with fluorescent cholesterol analog coupled with the results of total membrane cholesterol analysis after WSC labeling, demonstrate that using defined sequential combinations of exposure to WSC and/or MβC allow the cholesterol content of specific membranes within myotubes to be manipulated in a mechanistic and predictable fashion. These qualitative and quantitative results concerning myotube membrane cholesterol content and intracellular location after defined pulse-chase labeling provide further evidence and support for the overall model suggested in this study for how cholesterol is trafficked within myotube membranes.

Cholesterol Enrichment on Basal Glucose Uptake

An initial one-way ANOVA examining basal glucose uptake across all enrichment conditions showed no overall effect, nor any differences between control conditions and any experimental conditions (**Figure 16**). Given that selective membrane cholesterol enrichment has such significant effects on insulin-stimulated glucose uptake in C2C12 myotubes (**Figures 17 and 18, Table 1**), these experimental data suggest that translocation of the different glucose transporters GLUT1 and GLUT4 responsible for basal and insulin stimulated glucose uptake respectively, is differentially regulated within the C2C12 myotube.

Cholesterol Enrichment and Insulin Resistance in C2C12 Myotubes

The data presented here demonstrate that membrane cholesterol enrichment inhibits insulin stimulated glucose uptake across multiple insulin concentrations. This is most evident in the 4hr Pulse enrichment condition which inhibited insulin stimulated glucose uptake at every insulin concentration tested (**Figure 17 and Table 1)** and resulted in a 2.5-fold increase in total native cholesterol content (**Figure 15)**. These data support the overall hypothesis that increased cholesterol content of C2C12 myotube membranes inhibits insulin stimulated glucose uptake. In the case of the 4h Pulse-4h MβC enrichment condition, cholesterol was first delivered to the sarcolemma/T-tubule membrane and then removed using MβC. This sequence of events was demonstrated by both fluorescent cholesterol analog labeling (**Figure 14, Panels A and C**), and by comparison of the total cholesterol content in C2C12 myotubes enriched with native cholesterol using the 4hr Pulse condition compared to 4hr Pulse-4hr MβC condition (**Figure 15)**. The removal of cholesterol from the sarcolemma/T-tubule membrane following initial enrichment in the 4hr Pulse-4hr MβC condition partially rescued the complete inhibition of the insulin-stimulated glucose uptake response observed in the 4hr Pulse condition (**Figure 17 and Table 1)**. The data from this "rescue" experiment demonstrates that increased cholesterol within the sarcolemma/T-tubule membrane is causally related to the inhibition of insulin-stimulated glucose uptake by C2C12 myotubes observed in the 4h Pulse condition.

However, unlike the 4hr Pulse condition that resulted in selective enrichment of sarcolemma/T-tubule membranes, the 4hr Pulse-16hr Chase condition resulted in selective enrichment of sarcoplasmic reticulum membranes (**Figure 14, Panels E** and **F).**

Insulin stimulated glucose uptake in this enrichment condition was not found to be significantly different overall from control conditions (**Table 1**). However, the maximal insulin stimulated glucose uptake response in this enrichment condition was not at 10nM insulin as in control conditions, but rather at 50nM insulin. This rightward-shift of the insulin dose-response curve suggests that cholesterol enrichment of the sarcoplasmic reticulum membrane induces insulin resistance in C2C12 myotubes.

Increased membrane cholesterol in external plasma membranes has been demonstrated to inhibit SNARE-mediated fusion of intracellular vesicle membranes to the plasma membrane due to steric hindrance of SNARE proteins by cholesterol. Specifically, increased membrane cholesterol in sarcolemma/T-tubule membranes has been shown to alter the physical orientation of SNARE proteins located in caveolae, resulting in reduced docking of intracellular vesicles during fusion [129]. Such cholesterol-induced disruption of SNARE-mediated vesicle fusion may explain the inhibition of insulin stimulated glucose uptake observed after sarcolemma/T-tubule cholesterol enrichment reported in the present study. Since insulin stimulated glucose uptake in skeletal muscle is dependent on the translocation of GSV membranes containing GLUT4 to, and subsequent fusion with the sarcolemma/T-tubule membrane via SNARE-mediated proteins, cholesterol enrichment of the sarcolemma/T-tubule membrane as observed after a 4hr Pulse label would be predicted to result in reduced fusion of GLUT4-containing GSV and a decrease in insulin stimulated glucose uptake. It is also possible that other membrane-bound proteins involved in insulin signaling pathway, including the insulin receptor itself, are also sterically hindered by increased

sarcolemma/T-tubule cholesterol membrane content, although we are not aware of any experimental evidence in the literature to support this contention.

Another way cholesterol enrichment of muscle membranes may result in inhibition of insulin-stimulated glucose uptake also involves GSV fusion, but through a different mechanism than cholesterol-mediated steric hindrance of SNARE proteins located in the sarcolemma/T-tubule membrane. The basis of this potentially novel inhibitory mechanism derives from fundamental observations concerning the fusogenic capacity of lipid membrane vesicles which contain different amounts of cholesterol. Using isolated membrane vesicle preparations prepared with various combinations of phospholipids and cholesterol in the vesicle membrane, it has been demonstrated that phospholipid membrane vesicles with differing cholesterol membrane content fuse less efficiently or not at all compared to membranes that contain either no cholesterol or similar amounts of cholesterol [133]. This phenomenon has been attributed to the effects of cholesterol on membrane fluidity and rigidity, where the activation energy associated with initiating and driving membrane-membrane fusion is lowest when these biophysical properties are most similar between the two fusing membranes and highest when these membrane biophysical properties are most different between the two fusing membranes. To date however, no direct experimental evidence has been presented to suggest that such a cholesterol-related membrane fusion phenomenon either occurs or is physiologically relevant to membrane-membrane fusion events in living cells.

If this novel model predicting membrane fusion efficiency is extended to membrane-membrane fusion events known to occur in skeletal muscle, especially those involved in insulin-stimulated GLUT4 translocation and subsequent fusion of GLUT4-

containing GSV membranes with the sarcolemma/T-tubule membrane, several predictions can be made. The first is that any difference in relative cholesterol content between sarcolemma/T-Tubule and GLUT4-containing GSV vesicle membranes will result in inhibition of insulin stimulated glucose uptake. The second is that the greater the difference is in relative cholesterol content between sarcolemma/T-Tubule and GLUT4-containing GSV vesicle membranes, the greater the resulting inhibition of insulin stimulated glucose uptake. The third is that conditions which result in equal cholesterol enrichment of both the sarcoplasmic/T-tubule and the GSV membranes equally will result in less or potentially no inhibition of insulin stimulated glucose uptake compared to those conditions which result in differential membrane cholesterol enrichment.

If this putative model of physiologically relevant membrane-membrane fusion events is correct, then experimental evidence generated in the current study of insulin stimulated glucose uptake in C2C12 myotubes selectively enriched with cholesterol should support these predictions. Since GSV membranes consist of membrane components that bud off from the sarcoplasmic reticulum membrane, selective enrichment of the SR membrane will by extension result in increased GSV membrane cholesterol content. When the relative cholesterol content of sarcolemma/T-tubule membranes and sarcoplasmic reticulum/GSV membranes created using the various selective cholesterol enrichment conditions utilized in this study are examined the following observations can be made:

1) Insulin stimulated glucose uptake is inhibited in those enrichment conditions where there is a difference in the cholesterol content of sarcolemma/T-tubule

membranes and sarcoplasmic reticulum/GSV membranes relative to one another, namely the 4hr Pulse, 4hr Pulse-4hr MβC, the 4hr Pulse-16hr Chase-4hr MβC and the 4hr Pulse-16hr Chase conditions.

2) The enrichment condition exhibiting the greatest differential in membrane cholesterol content (i.e. 4hr Pulse) is the condition exhibiting the greatest inhibition of insulin stimulated glucose uptake (i.e. 4hr Pulse), while the enrichment condition exhibiting the next greatest differential membrane cholesterol content (i.e. 4hr Pulse-16hr Chase-4hr MβC) is the condition exhibiting the next greatest inhibition of insulin stimulated glucose uptake.

3) The enrichment condition exhibiting the greatest amount of membrane cholesterol overall but having the most equal membrane cholesterol content of the enrichment conditions (i.e. 4hr Pulse-16hr Chase-4hr Pulse) is not the condition exhibiting the greatest inhibition of insulin stimulated glucose uptake.

As such, the experimental observations listed above support the predictions of a novel model of membrane-membrane fusion events as it relates to insulin stimulated glucose uptake and cholesterol membrane enrichment in C2C12 myotubes. However, the 4hr Pulse-16h Chase enrichment condition does not appear to fit all aspects of this model. For example, the 4hr Pulse-16h Chase enrichment condition was shown to selectively enrich the sarcoplasmic membrane/GSV membrane but does appear to exhibit inhibition of insulin stimulated glucose uptake, rather it results in a rightward-shift in the insulin dose response curve. It remains unclear as to the exact cellular mechanism(s) that may explain

the development of myotube insensitivity to insulin under these cholesterol enrichment conditions, but it is possible that it may also be related to reduced GSV membrane fusion.

CONCLUSION

The present study has developed and characterized a reproducible tissue culture model of skeletal muscle myofibers *in vivo* consisting of terminally differentiated C2C12 myotubes in which to mechanistically investigate the cellular mechanisms involved in insulin-stimulated glucose uptake quantified using a fluorescent analog of glucose, 2-NBDG. In turn, this differentiated C2C12 myotube model was then be used to investigate the effects of selective cholesterol enrichment of specific myotube membranes on insulin signaling and insulin-stimulated glucose uptake.

Using this *in vitro* C2C12 myotube model, we show insulin stimulated glucose uptake across a range of different insulin concentrations and describe what appears to be the initiation of a rapid negative feedback loop on the insulin signaling pathway associated with acute exposure to high concentrations of insulin that results in inhibition of insulin stimulated glucose uptake. Further, we demonstrate that pulse-chase labeling protocols developed as part of this study can selectively enrich sarcolemma/T-tubule and sarcoplasmic reticulum membranes with cholesterol in a defined, mechanistic fashion. In turn we show that inhibition of insulin-stimulated glucose uptake in C2C12 myotubes is causally linked to increased membrane cholesterol content and suggest a novel model for how and why differential membrane cholesterol content negatively effects membrane-membrane fusion events required for GLUT4-containing GSV membrane fusion with the sarcolemma/T-tubule membrane during insulin stimulated glucose uptake. These data

provide strong evidence that increased cholesterol content located in specific membranes of skeletal muscle are not only associated with but directly contribute with the development of insulin resistance. Finally, this study also provides evidence to support a mechanistic model capable of explaining the underlying relationship between conditions exhibiting abnormal regulation of lipid metabolism and increased circulating cholesterol levels, such as obesity and hypercholesterolemia, and the onset of insulin insensitivity and glucose tolerance in conditions such as metabolic syndrome and Type 2 diabetes.

References

1. Habegger, K.M., et al., *Fat-induced membrane cholesterol accrual provokes cortical filamentous actin destabilisation and glucose transport dysfunction in skeletal muscle.* Diabetologia, 2012. **55**(2): p. 457-67.
2. Llanos, P., et al., *The cholesterol-lowering agent methyl-beta-cyclodextrin promotes glucose uptake via GLUT4 in adult muscle fibers and reduces insulin resistance in obese mice.* Am J Physiol Endocrinol Metab, 2015. **308**(4): p. E294-305.
3. Richter, E.A. and M. Hargreaves, *Exercise, GLUT4, and skeletal muscle glucose uptake.* Physiol Rev, 2013. **93**(3): p. 993-1017.
4. Blanc, S., et al., *Fuel homeostasis during physical inactivity induced by bed rest.* J Clin Endocrinol Metab, 2000. **85**(6): p. 2223-33.
5. Mondon, C.E., et al., *Alterations in glucose and protein metabolism in animals subjected to simulated microgravity.* Adv Space Res, 1992. **12**(2-3): p. 169-77.
6. O'Keefe, M.P., et al., *Enhanced insulin action on glucose transport and insulin signaling in 7-day unweighted rat soleus muscle.* J Appl Physiol (1985), 2004. **97**(1): p. 63-71.
7. Tobin, B.W., P.N. Uchakin, and S.K. Leeper-Woodford, *Insulin secretion and sensitivity in space flight: diabetogenic effects.* Nutrition, 2002. **18**(10): p. 842-8.
8. Edwardson, C.L., et al., *Association of sedentary behaviour with metabolic syndrome: a meta-analysis.* PLoS One, 2012. **7**(4): p. e34916.
9. Bergouignan, A., et al., *Physical inactivity as the culprit of metabolic inflexibility: evidence from bed-rest studies.* J Appl Physiol (1985), 2011. **111**(4): p. 1201-10.
10. Hamburg, N.M., et al., *Physical inactivity rapidly induces insulin resistance and microvascular dysfunction in healthy volunteers.* Arterioscler Thromb Vasc Biol, 2007. **27**(12): p. 2650-6.
11. Mueckler, M., *Facilitative glucose transporters.* Eur J Biochem, 1994. **219**(3): p. 713-25.
12. Sargeant, R.J. and M.R. Paquet, *Effect of insulin on the rates of synthesis and degradation of GLUT1 and GLUT4 glucose transporters in 3T3-L1 adipocytes.* Biochem J, 1993. **290 (Pt 3)**: p. 913-9.
13. Watson, R.T., M. Kanzaki, and J.E. Pessin, *Regulated membrane trafficking of the insulin-responsive glucose transporter 4 in adipocytes.* Endocr Rev, 2004. **25**(2): p. 177-204.
14. Watson, R.T. and J.E. Pessin, *GLUT4 translocation: the last 200 nanometers.* Cell Signal, 2007. **19**(11): p. 2209-17.
15. Watson, R.T. and J.E. Pessin, *Intracellular organization of insulin signaling and GLUT4 translocation.* Recent Prog Horm Res, 2001. **56**: p. 175-93.
16. DeFronzo, R.A., et al., *The effect of insulin on the disposal of intravenous glucose. Results from indirect calorimetry and hepatic and femoral venous catheterization.* Diabetes, 1981. **30**(12): p. 1000-7.

17. Minn, H., et al., *In vivo effects of insulin on tumor and skeletal muscle glucose metabolism in patients with lymphoma.* Cancer, 1994. **73**(5): p. 1490-8.
18. Khan, A.H. and J.E. Pessin, *Insulin regulation of glucose uptake: a complex interplay of intracellular signalling pathways.* Diabetologia, 2002. **45**(11): p. 1475-83.
19. Pike, L.J., *Lipid rafts: bringing order to chaos.* J Lipid Res, 2003. **44**(4): p. 655-67.
20. Watson, R.T., et al., *Lipid raft microdomain compartmentalization of TC10 is required for insulin signaling and GLUT4 translocation.* J Cell Biol, 2001. **154**(4): p. 829-40.
21. Bickel, P.E., *Lipid rafts and insulin signaling.* Am J Physiol Endocrinol Metab, 2002. **282**(1): p. E1-E10.
22. Michel, V. and M. Bakovic, *Lipid rafts in health and disease.* Biol Cell, 2007. **99**(3): p. 129-40.
23. Karlsson, M., et al., *Colocalization of insulin receptor and insulin receptor substrate-1 to caveolae in primary human adipocytes. Cholesterol depletion blocks insulin signalling for metabolic and mitogenic control.* Eur J Biochem, 2004. **271**(12): p. 2471-9.
24. Ohvo-Rekila, H., et al., *Cholesterol interactions with phospholipids in membranes.* Prog Lipid Res, 2002. **41**(1): p. 66-97.
25. Knoblauch, M.A., D.P. O'Connor, and M.S. Clarke, *Obese mice incur greater myofiber membrane disruption in response to mechanical load compared with lean mice.* Obesity (Silver Spring), 2013. **21**(1): p. 135-43.
26. Baumann, C.A., et al., *CAP defines a second signalling pathway required for insulin-stimulated glucose transport.* Nature, 2000. **407**(6801): p. 202-7.
27. Chiang, S.H., et al., *Insulin-stimulated GLUT4 translocation requires the CAP-dependent activation of TC10.* Nature, 2001. **410**(6831): p. 944-8.
28. Ahmed, Z., B.J. Smith, and T.S. Pillay, *The APS adapter protein couples the insulin receptor to the phosphorylation of c-Cbl and facilitates ligand-stimulated ubiquitination of the insulin receptor.* FEBS Lett, 2000. **475**(1): p. 31-4.
29. Inoue, M., et al., *The exocyst complex is required for targeting of Glut4 to the plasma membrane by insulin.* Nature, 2003. **422**(6932): p. 629-33.
30. Inoue, M., et al., *Compartmentalization of the exocyst complex in lipid rafts controls Glut4 vesicle tethering.* Mol Biol Cell, 2006. **17**(5): p. 2303-11.
31. Leontieva, O.V., Z.N. Demidenko, and M.V. Blagosklonny, *Rapamycin reverses insulin resistance (IR) in high-glucose medium without causing IR in normoglycemic medium.* Cell Death Dis, 2014. **5**: p. e1214.
32. Bonora, E., et al., *Prevalence of insulin resistance in metabolic disorders: the Bruneck Study.* Diabetes, 1998. **47**(10): p. 1643-9.
33. Gustavsson, J., et al., *Localization of the insulin receptor in caveolae of adipocyte plasma membrane.* FASEB J, 1999. **13**(14): p. 1961-71.
34. Vainio, S., et al., *Dynamic association of human insulin receptor with lipid rafts in cells lacking caveolae.* EMBO Rep, 2002. **3**(1): p. 95-100.
35. Parpal, S., et al., *Cholesterol depletion disrupts caveolae and insulin receptor signaling for metabolic control via insulin receptor substrate-1, but not for*

mitogen-activated protein kinase control. J Biol Chem, 2001. **276**(13): p. 9670-8.
36. Sanchez-Wandelmer, J., et al., *Inhibition of cholesterol biosynthesis disrupts lipid raft/caveolae and affects insulin receptor activation in 3T3-L1 preadipocytes.* Biochim Biophys Acta, 2009. **1788**(9): p. 1731-9.
37. Chen, G., et al., *Chromium activates glucose transporter 4 trafficking and enhances insulin-stimulated glucose transport in 3T3-L1 adipocytes via a cholesterol-dependent mechanism.* Mol Endocrinol, 2006. **20**(4): p. 857-70.
38. Hilder, T.L., et al., *Insulin-independent pathways mediating glucose uptake in hindlimb-suspended skeletal muscle.* J Appl Physiol (1985), 2005. **99**(6): p. 2181-8.
39. Ueyama, A., et al., *GLUT-4myc ectopic expression in L6 myoblasts generates a GLUT-4-specific pool conferring insulin sensitivity.* Am J Physiol, 1999. **277**(3 Pt 1): p. E572-8.
40. Mitsumoto, Y. and A. Klip, *Development regulation of the subcellular distribution and glycosylation of GLUT1 and GLUT4 glucose transporters during myogenesis of L6 muscle cells.* J Biol Chem, 1992. **267**(7): p. 4957-62.
41. Isakoff, S.J., et al., *The inability of phosphatidylinositol 3-kinase activation to stimulate GLUT4 translocation indicates additional signaling pathways are required for insulin-stimulated glucose uptake.* Proc Natl Acad Sci U S A, 1995. **92**(22): p. 10247-51.
42. Tortorella, L.L. and P.F. Pilch, *C2C12 myocytes lack an insulin-responsive vesicular compartment despite dexamethasone-induced GLUT4 expression.* Am J Physiol Endocrinol Metab, 2002. **283**(3): p. E514-24.
43. Nedachi, T. and M. Kanzaki, *Regulation of glucose transporters by insulin and extracellular glucose in C2C12 myotubes.* Am J Physiol Endocrinol Metab, 2006. **291**(4): p. E817-28.
44. Jung, D.W., et al., *Novel use of fluorescent glucose analogues to identify a new class of triazine-based insulin mimetics possessing useful secondary effects.* Mol Biosyst, 2011. **7**(2): p. 346-58.
45. Ariga, M., et al., *Functional role of sortilin in myogenesis and development of insulin-responsive glucose transport system in C2C12 myocytes.* J Biol Chem, 2008. **283**(15): p. 10208-20.
46. Rudich, A. and A. Klip, *Push/pull mechanisms of GLUT4 traffic in muscle cells.* Acta Physiol Scand, 2003. **178**(4): p. 297-308.
47. Lawson, M.A. and P.P. Purslow, *Differentiation of myoblasts in serum-free media: effects of modified media are cell line-specific.* Cells Tissues Organs, 2000. **167**(2-3): p. 130-7.
48. Cooper, S.T., et al., *C2C12 co-culture on a fibroblast substratum enables sustained survival of contractile, highly differentiated myotubes with peripheral nuclei and adult fast myosin expression.* Cell Motil Cytoskeleton, 2004. **58**(3): p. 200-11.
49. Engler, A.J., et al., *Myotubes differentiate optimally on substrates with tissue-like stiffness: pathological implications for soft or stiff microenvironments.* J Cell Biol, 2004. **166**(6): p. 877-87.

50. Kotliar, N. and P.F. Pilch, *Expression of the glucose transporter isoform GLUT 4 is insufficient to confer insulin-regulatable hexose uptake to cultured muscle cells.* Mol Endocrinol, 1992. **6**(3): p. 337-45.
51. Despres, J.P., *Abdominal obesity as important component of insulin-resistance syndrome.* Nutrition, 1993. **9**(5): p. 452-9.
52. Despres, J.P., *The insulin resistance-dyslipidemia syndrome: the most prevalent cause of coronary artery disease?* CMAJ, 1993. **148**(8): p. 1339-40.
53. Seidell, J.C., *Obesity, insulin resistance and diabetes--a worldwide epidemic.* Br J Nutr, 2000. **83 Suppl 1**: p. S5-8.
54. Amati, F., et al., *Physical inactivity and obesity underlie the insulin resistance of aging.* Diabetes Care, 2009. **32**(8): p. 1547-9.
55. Eckardt, K., A. Taube, and J. Eckel, *Obesity-associated insulin resistance in skeletal muscle: role of lipid accumulation and physical inactivity.* Rev Endocr Metab Disord, 2011. **12**(3): p. 163-72.
56. Venables, M.C. and A.E. Jeukendrup, *Physical inactivity and obesity: links with insulin resistance and type 2 diabetes mellitus.* Diabetes Metab Res Rev, 2009. **25 Suppl 1**: p. S18-23.
57. Takahashi, S., et al., *Increased visceral fat accumulation further aggravates the risks of insulin resistance in gout.* Metabolism, 2001. **50**(4): p. 393-8.
58. Reaven, G.M., *Pathophysiology of insulin resistance in human disease.* Physiol Rev, 1995. **75**(3): p. 473-86.
59. Petersen, K.F. and G.I. Shulman, *Etiology of insulin resistance.* Am J Med, 2006. **119**(5 Suppl 1): p. S10-6.
60. Aspinwall, C.A., J.R. Lakey, and R.T. Kennedy, *Insulin-stimulated insulin secretion in single pancreatic beta cells.* J Biol Chem, 1999. **274**(10): p. 6360-5.
61. Santerre, R.F., et al., *Insulin synthesis in a clonal cell line of simian virus 40-transformed hamster pancreatic beta cells.* Proc Natl Acad Sci U S A, 1981. **78**(7): p. 4339-43.
62. Emerging Risk Factors, C., et al., *Diabetes mellitus, fasting blood glucose concentration, and risk of vascular disease: a collaborative meta-analysis of 102 prospective studies.* Lancet, 2010. **375**(9733): p. 2215-22.
63. Bunn, H.F., K.H. Gabbay, and P.M. Gallop, *The glycosylation of hemoglobin: relevance to diabetes mellitus.* Science, 1978. **200**(4337): p. 21-7.
64. Mueckler, M., *Family of glucose-transporter genes. Implications for glucose homeostasis and diabetes.* Diabetes, 1990. **39**(1): p. 6-11.
65. McMillin, S.L., et al., *GLUT4 Is Not Necessary for Overload-Induced Glucose Uptake or Hypertrophic Growth in Mouse Skeletal Muscle.* Diabetes, 2017. **66**(6): p. 1491-1500.
66. Clarke, J.F., et al., *Inhibition of the translocation of GLUT1 and GLUT4 in 3T3-L1 cells by the phosphatidylinositol 3-kinase inhibitor, wortmannin.* Biochem J, 1994. **300 (Pt 3)**: p. 631-5.
67. Barnes, K., et al., *Activation of GLUT1 by metabolic and osmotic stress: potential involvement of AMP-activated protein kinase (AMPK).* J Cell Sci, 2002. **115**(Pt 11): p. 2433-42.

68. Wu, C.L., et al., *Role of AMPK in UVB-induced DNA damage repair and growth control.* Oncogene, 2013. **32**(21): p. 2682-9.
69. Goodyear, L.J. and B.B. Kahn, *Exercise, glucose transport, and insulin sensitivity.* Annu Rev Med, 1998. **49**: p. 235-61.
70. Defronzo, R.A., et al., *Insulin resistance: a universal finding in diabetic states.* Bull Schweiz Akad Med Wiss, 1981: p. 223-38.
71. Nuutila, P., et al., *Different alterations in the insulin-stimulated glucose uptake in the athlete's heart and skeletal muscle.* J Clin Invest, 1994. **93**(5): p. 2267-74.
72. Sesti, G., et al., *Defects of the insulin receptor substrate (IRS) system in human metabolic disorders.* FASEB J, 2001. **15**(12): p. 2099-111.
73. Sandri, M., et al., *Signalling pathways regulating muscle mass in ageing skeletal muscle: the role of the IGF1-Akt-mTOR-FoxO pathway.* Biogerontology, 2013. **14**(3): p. 303-23.
74. Fruman, D.A., R.E. Meyers, and L.C. Cantley, *Phosphoinositide kinases.* Annu Rev Biochem, 1998. **67**: p. 481-507.
75. Karlsson, H.K., et al., *Insulin-stimulated phosphorylation of the Akt substrate AS160 is impaired in skeletal muscle of type 2 diabetic subjects.* Diabetes, 2005. **54**(6): p. 1692-7.
76. Sano, H., et al., *Insulin-stimulated phosphorylation of a Rab GTPase-activating protein regulates GLUT4 translocation.* J Biol Chem, 2003. **278**(17): p. 14599-602.
77. Thong, F.S., P.J. Bilan, and A. Klip, *The Rab GTPase-activating protein AS160 integrates Akt, protein kinase C, and AMP-activated protein kinase signals regulating GLUT4 traffic.* Diabetes, 2007. **56**(2): p. 414-23.
78. Kramer, H.F., et al., *Distinct signals regulate AS160 phosphorylation in response to insulin, AICAR, and contraction in mouse skeletal muscle.* Diabetes, 2006. **55**(7): p. 2067-76.
79. Kramer, H.F., et al., *AS160 regulates insulin- and contraction-stimulated glucose uptake in mouse skeletal muscle.* J Biol Chem, 2006. **281**(42): p. 31478-85.
80. Eguez, L., et al., *Full intracellular retention of GLUT4 requires AS160 Rab GTPase activating protein.* Cell Metab, 2005. **2**(4): p. 263-72.
81. Roach, W.G., et al., *Substrate specificity and effect on GLUT4 translocation of the Rab GTPase-activating protein Tbc1d1.* Biochem J, 2007. **403**(2): p. 353-8.
82. Miinea, C.P., et al., *AS160, the Akt substrate regulating GLUT4 translocation, has a functional Rab GTPase-activating protein domain.* Biochem J, 2005. **391**(Pt 1): p. 87-93.
83. Ishikura, S., P.J. Bilan, and A. Klip, *Rabs 8A and 14 are targets of the insulin-regulated Rab-GAP AS160 regulating GLUT4 traffic in muscle cells.* Biochem Biophys Res Commun, 2007. **353**(4): p. 1074-9.
84. Rockl, K.S., C.A. Witczak, and L.J. Goodyear, *Signaling mechanisms in skeletal muscle: acute responses and chronic adaptations to exercise.* IUBMB Life, 2008. **60**(3): p. 145-53.

85. Li, Y., et al., *Regulation of insulin secretion and GLUT4 trafficking by the calcium sensor synaptotagmin VII.* Biochem Biophys Res Commun, 2007. **362**(3): p. 658-64.
86. Kane, S. and G.E. Lienhard, *Calmodulin binds to the Rab GTPase activating protein required for insulin-stimulated GLUT4 translocation.* Biochem Biophys Res Commun, 2005. **335**(1): p. 175-80.
87. Angin, Y., et al., *Calcium signaling recruits substrate transporters GLUT4 and CD36 to the sarcolemma without increasing cardiac substrate uptake.* Am J Physiol Endocrinol Metab, 2014. **307**(2): p. E225-36.
88. Merrill, G.F., et al., *AICA riboside increases AMP-activated protein kinase, fatty acid oxidation, and glucose uptake in rat muscle.* Am J Physiol, 1997. **273**(6 Pt 1): p. E1107-12.
89. Berchtold, M.W., H. Brinkmeier, and M. Muntener, *Calcium ion in skeletal muscle: its crucial role for muscle function, plasticity, and disease.* Physiol Rev, 2000. **80**(3): p. 1215-65.
90. Wright, D.C., et al., *Ca2+ and AMPK both mediate stimulation of glucose transport by muscle contractions.* Diabetes, 2004. **53**(2): p. 330-5.
91. Witczak, C.A., et al., *Ca2+/calmodulin-dependent protein kinase kinase-alpha regulates skeletal muscle glucose uptake independent of AMP-activated protein kinase and Akt activation.* Diabetes, 2007. **56**(5): p. 1403-9.
92. Niu, W., et al., *Contraction-related stimuli regulate GLUT4 traffic in C2C12-GLUT4myc skeletal muscle cells.* Am J Physiol Endocrinol Metab, 2010. **298**(5): p. E1058-71.
93. Jensen, T.E., et al., *Possible CaMKK-dependent regulation of AMPK phosphorylation and glucose uptake at the onset of mild tetanic skeletal muscle contraction.* Am J Physiol Endocrinol Metab, 2007. **292**(5): p. E1308-17.
94. Lang, T., et al., *SNAREs are concentrated in cholesterol-dependent clusters that define docking and fusion sites for exocytosis.* EMBO J, 2001. **20**(9): p. 2202-13.
95. Yu, H., et al., *Doc2b promotes GLUT4 exocytosis by activating the SNARE-mediated fusion reaction in a calcium- and membrane bending-dependent manner.* Mol Biol Cell, 2013. **24**(8): p. 1176-84.
96. Singer, S.J. and G.L. Nicolson, *The fluid mosaic model of the structure of cell membranes.* Science, 1972. **175**(4023): p. 720-31.
97. van Meer, G., D.R. Voelker, and G.W. Feigenson, *Membrane lipids: where they are and how they behave.* Nat Rev Mol Cell Biol, 2008. **9**(2): p. 112-24.
98. Ikonen, E., *Cellular cholesterol trafficking and compartmentalization.* Nat Rev Mol Cell Biol, 2008. **9**(2): p. 125-38.
99. Hardie, D.G., *AMP-activated protein kinase: an energy sensor that regulates all aspects of cell function.* Genes Dev, 2011. **25**(18): p. 1895-908.
100. Lange, Y., J. Ye, and T.L. Steck, *How cholesterol homeostasis is regulated by plasma membrane cholesterol in excess of phospholipids.* Proc Natl Acad Sci U S A, 2004. **101**(32): p. 11664-7.
101. Martonosi, A.N., *Animal electricity, Ca2+ and muscle contraction. A brief history of muscle research.* Acta Biochim Pol, 2000. **47**(3): p. 493-516.

102. Dietschy, J.M. and M.D. Siperstein, *Effect of cholesterol feeding and fasting on sterol synthesis in seventeen tissues of the rat.* J Lipid Res, 1967. **8**(2): p. 97-104.
103. Spady, D.K., D.W. Bilheimer, and J.M. Dietschy, *Rates of receptor-dependent and -independent low density lipoprotein uptake in the hamster.* Proc Natl Acad Sci U S A, 1983. **80**(11): p. 3499-503.
104. Simons, K. and E. Ikonen, *How cells handle cholesterol.* Science, 2000. **290**(5497): p. 1721-6.
105. Schmitz, G. and M. Grandl, *The molecular mechanisms of HDL and associated vesicular trafficking mechanisms to mediate cellular lipid homeostasis.* Arterioscler Thromb Vasc Biol, 2009. **29**(11): p. 1718-22.
106. Soccio, R.E. and J.L. Breslow, *Intracellular cholesterol transport.* Arterioscler Thromb Vasc Biol, 2004. **24**(7): p. 1150-60.
107. Roduit, C., et al., *Elastic membrane heterogeneity of living cells revealed by stiff nanoscale membrane domains.* Biophys J, 2008. **94**(4): p. 1521-32.
108. Lundbaek, J.A., et al., *Cholesterol-induced protein sorting: an analysis of energetic feasibility.* Biophys J, 2003. **84**(3): p. 2080-9.
109. Galbiati, F., et al., *Caveolin-3 null mice show a loss of caveolae, changes in the microdomain distribution of the dystrophin-glycoprotein complex, and t-tubule abnormalities.* J Biol Chem, 2001. **276**(24): p. 21425-33.
110. Park, D.S., et al., *Caveolin-1/3 double-knockout mice are viable, but lack both muscle and non-muscle caveolae, and develop a severe cardiomyopathic phenotype.* Am J Pathol, 2002. **160**(6): p. 2207-17.
111. Hagiwara, Y., et al., *Caveolin-3 deficiency causes muscle degeneration in mice.* Hum Mol Genet, 2000. **9**(20): p. 3047-54.
112. Pontes, B., et al., *Membrane elastic properties and cell function.* PLoS One, 2013. **8**(7): p. e67708.
113. Nandi, S., et al., *ABCA1-mediated cholesterol efflux generates microparticles in addition to HDL through processes governed by membrane rigidity.* J Lipid Res, 2009. **50**(3): p. 456-66.
114. Brown, D.A. and E. London, *Structure and function of sphingolipid- and cholesterol-rich membrane rafts.* J Biol Chem, 2000. **275**(23): p. 17221-4.
115. Fiehn, W., et al., *Lipids and fatty acids of sarcolemma, sarcoplasmic reticulum, and mitochondria from rat skeletal muscle.* J Biol Chem, 1971. **246**(18): p. 5617-20.
116. Harder, T. and K. Simons, *Caveolae, DIGs, and the dynamics of sphingolipid-cholesterol microdomains.* Curr Opin Cell Biol, 1997. **9**(4): p. 534-42.
117. Clarke, M.S., et al., *In situ localization of cholesterol in skeletal muscle by use of a monoclonal antibody.* J Appl Physiol (1985), 2000. **89**(2): p. 731-41.
118. Safwat, Y., et al., *Modulation of skeletal muscle performance and SERCA by exercise and adiponectin gene therapy in insulin-resistant rat.* DNA Cell Biol, 2013. **32**(7): p. 378-85.
119. Waller, A.P., et al., *Sarcoplasmic reticulum Ca2+ ATPase pump is a major regulator of glucose transport in the healthy and diabetic heart.* Biochim Biophys Acta, 2015. **1852**(5): p. 873-81.

120. Contreras-Ferrat, A., et al., *Calcium signaling in insulin action on striated muscle.* Cell Calcium, 2014. **56**(5): p. 390-6.
121. Yang, S.T., et al., *The role of cholesterol in membrane fusion.* Chem Phys Lipids, 2016. **199**: p. 136-143.
122. Ge, S., J.G. White, and C.L. Haynes, *Critical role of membrane cholesterol in exocytosis revealed by single platelet study.* ACS Chem Biol, 2010. **5**(9): p. 819-28.
123. Wang, N., et al., *Influence of cholesterol on catecholamine release from the fusion pore of large dense core chromaffin granules.* J Neurosci, 2010. **30**(11): p. 3904-11.
124. Koseoglu, S., S.A. Love, and C.L. Haynes, *Cholesterol effects on vesicle pools in chromaffin cells revealed by carbon-fiber microelectrode amperometry.* Anal Bioanal Chem, 2011. **400**(9): p. 2963-71.
125. Finkenstaedt-Quinn, S.A., S.M. Gruba, and C.L. Haynes, *Variations in Fusion Pore Formation in Cholesterol-Treated Platelets.* Biophys J, 2016. **110**(4): p. 922-9.
126. Kreutzberger, A.J., V. Kiessling, and L.K. Tamm, *High cholesterol obviates a prolonged hemifusion intermediate in fast SNARE-mediated membrane fusion.* Biophys J, 2015. **109**(2): p. 319-29.
127. Lee, D.E., M.G. Lew, and D.J. Woodbury, *Vesicle fusion to planar membranes is enhanced by cholesterol and low temperature.* Chem Phys Lipids, 2013. **166**: p. 45-54.
128. Stratton, B.S., et al., *Cholesterol Increases the Openness of SNARE-Mediated Flickering Fusion Pores.* Biophys J, 2016. **110**(7): p. 1538-50.
129. Tong, J., et al., *A scissors mechanism for stimulation of SNARE-mediated lipid mixing by cholesterol.* Proc Natl Acad Sci U S A, 2009. **106**(13): p. 5141-6.
130. Lizunov, V.A., et al., *Impaired tethering and fusion of GLUT4 vesicles in insulin-resistant human adipose cells.* Diabetes, 2013. **62**(9): p. 3114-9.
131. Lizunov, V.A., et al., *Insulin regulates Glut4 confinement in plasma membrane clusters in adipose cells.* PLoS One, 2013. **8**(3): p. e57559.
132. Garvey, W.T., et al., *Evidence for defects in the trafficking and translocation of GLUT4 glucose transporters in skeletal muscle as a cause of human insulin resistance.* J Clin Invest, 1998. **101**(11): p. 2377-86.
133. Breisblatt, W. and S. Ohki, *Fusion in phospholipid spherical membranes. II. Effect of cholesterol, divalent ions and pH.* J Membr Biol, 1976. **29**(1-2): p. 127-46.
134. Koga, H., S. Kaushik, and A.M. Cuervo, *Altered lipid content inhibits autophagic vesicular fusion.* FASEB J, 2010. **24**(8): p. 3052-65.
135. Squier, T.C., D.J. Bigelow, and D.D. Thomas, *Lipid fluidity directly modulates the overall protein rotational mobility of the Ca-ATPase in sarcoplasmic reticulum.* J Biol Chem, 1988. **263**(19): p. 9178-86.
136. Bastiaanse, E.M., K.M. Hold, and A. Van der Laarse, *The effect of membrane cholesterol content on ion transport processes in plasma membranes.* Cardiovasc Res, 1997. **33**(2): p. 272-83.

137. Mayor, P., L. Maianu, and W.T. Garvey, *Glucose and insulin chronically regulate insulin action via different mechanisms in BC3H1 myocytes. Effects on glucose transporter gene expression.* Diabetes, 1992. **41**(3): p. 274-85.
138. Mitsumoto, Y., et al., *Differential expression of the GLUT1 and GLUT4 glucose transporters during differentiation of L6 muscle cells.* Biochem Biophys Res Commun, 1991. **175**(2): p. 652-9.
139. Yamamoto, N., et al., *Measurement of Glucose Uptake in Cultured Cells.* Curr Protoc Pharmacol, 2015. **71**: p. 12 14 1-26.
140. Takekura, H., B.E. Flucher, and C. Franzini-Armstrong, *Sequential docking, molecular differentiation, and positioning of T-Tubule/SR junctions in developing mouse skeletal muscle.* Dev Biol, 2001. **239**(2): p. 204-14.
141. Whalen, R.G., et al., *Contractile protein isozymes in muscle development: identification of an embryonic form of myosin heavy chain.* Proc Natl Acad Sci U S A, 1979. **76**(10): p. 5197-201.
142. Agbulut, O., et al., *Myosin heavy chain isoforms in postnatal muscle development of mice.* Biol Cell, 2003. **95**(6): p. 399-406.
143. Weydert, A., et al., *Sequential accumulation of mRNAs encoding different myosin heavy chain isoforms during skeletal muscle development in vivo detected with a recombinant plasmid identified as coding for an adult fast myosin heavy chain from mouse skeletal muscle.* J Biol Chem, 1983. **258**(22): p. 13867-74.
144. Schiaffino, S., et al., *Embryonic myosin heavy chain as a differentiation marker of developing human skeletal muscle and rhabdomyosarcoma. A monoclonal antibody study.* Exp Cell Res, 1986. **163**(1): p. 211-20.
145. Ogawa, Y. and M. Tanaka, *A fluorescent cholesterol analogue for observation of free cholesterol in the plasma membrane of live cells.* Anal Biochem, 2016. **492**: p. 49-55.
146. Rituper, B., et al., *Cholesterol-mediated membrane surface area dynamics in neuroendocrine cells.* Biochim Biophys Acta, 2013. **1831**(7): p. 1228-38.
147. Zidovetzki, R. and I. Levitan, *Use of cyclodextrins to manipulate plasma membrane cholesterol content: evidence, misconceptions and control strategies.* Biochim Biophys Acta, 2007. **1768**(6): p. 1311-24.
148. Boden, G., et al., *Insulin receptor down-regulation and impaired antilipolytic action of insulin in diabetic patients after pancreas/kidney transplantation.* J Clin Endocrinol Metab, 1994. **78**(3): p. 657-63.
149. Holtta-Vuori, M., et al., *BODIPY-cholesterol: a new tool to visualize sterol trafficking in living cells and organisms.* Traffic, 2008. **9**(11): p. 1839-49.